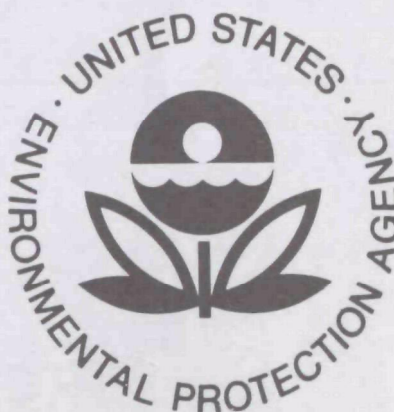


EPA-600/4-77-030
June 1977

Environmental Monitoring Series

A STUDY ON THE ACCURACY OF TYPE S PITOT TUBE



**Environmental Monitoring and Support Laboratory
Office of Research and Development
U.S. Environmental Protection Agency
Research Triangle Park, North Carolina 27711**

RESEARCH REPORTING SERIES

Research reports of the Office of Research and Development, U.S. Environmental Protection Agency, have been grouped into nine series. These nine broad categories were established to facilitate further development and application of environmental technology. Elimination of traditional grouping was consciously planned to foster technology transfer and a maximum interface in related fields. The nine series are:

1. Environmental Health Effects Research
2. Environmental Protection Technology
3. Ecological Research
4. Environmental Monitoring
5. Socioeconomic Environmental Studies
6. Scientific and Technical Assessment Reports (STAR)
7. Interagency Energy-Environment Research and Development
8. "Special" Reports
9. Miscellaneous Reports

This report has been assigned to the ENVIRONMENTAL MONITORING series. This series describes research conducted to develop new or improved methods and instrumentation for the identification and quantification of environmental pollutants at the lowest conceivably significant concentrations. It also includes studies to determine the ambient concentrations of pollutants in the environment and/or the variance of pollutants as a function of time or meteorological factors.

A STUDY ON THE ACCURACY OF TYPE-S PITOT TUBES

by

J. C. Williams, III

and

F. R. DeJarnette

Mechanical and Aerospace Engineering Department
North Carolina State University
Raleigh, North Carolina 27607

EPA Grant No. 803168

ROAP No. 26 AAG

Program Element No. 1 HA 327

Project Officer

William J. Mitchell

Quality Assurance Branch

Environmental Monitoring and Support Laboratory
Research Triangle Park, North Carolina 27711

Environmental Monitoring and Support Laboratory
Office of Research and Development
U. S. Environmental Protection Agency
Research Triangle Park, North Carolina 27711

DISCLAIMER

This report has been reviewed by the Environmental Monitoring and Support Laboratory, U. S. Environmental Protection Agency, and approved for publication. Mention of trade names or commercial products does not constitute endorsement or recommendation for use.

FOREWORD

In some testing the measurement of the velocity of the stack gas is usually obtained with the Staubscheibe ("S" type) pitot tube. The velocity measurement is one of the most critical measurements in source testing, because it is used to determine the rate at which gas is drawn into the sampling probe and is also used in calculating the volumetric flow rate. Since the Environmental Monitoring and Support Laboratory, Research Triangle Park, North Carolina has responsibility to establish the reliability of stationary source test methods, we funded the study reported herein. The objectives of this study were threefold: 1) to determine the behavior of a family of pitot tubes under the flow conditions normally encountered in source testing; 2) to determine the design parameters that affect the "S" type pitot calibration coefficient (C_p); and 3) to select the type "S" pitot tube that will be least sensitive to angular flow, to yaw, to pitch and to the presence of a sampling probe nozzle.

Overall, the results of this study determined that the distance between the two pressure ports of the "S" type pitot tube does not affect the calibration coefficient, C_p , under conditions of laminar flow. However, the calibration coefficient is C_p extremely sensitive to this port-to-port spacing under the conditions of yaw, pitch and angular flow. Increasing this distance seemed to make the C_p less sensitive to these parameters. But, unfortunately, the results of this study are not sufficient to design a pitot tube that is insensitive to the effect of yaw and pitch and yet will fit through most existing sampling ports. Obviously, further work is needed in this area.

One possibility that should be investigated further would be to insert the pitot tube approximately 3 cm further into the stack than the sampling probe. The results in this report indicate that under this condition most "S" type pitot tubes should give acceptable results.

Thomas R. Hauser, Ph.D.
Acting Director
Environmental Monitoring
and Support Laboratory

ABSTRACT

This research program was initiated with the overall objective of determining the effects of geometry, construction and use on the accuracy of S-type pitot tubes.

Fourteen different S-type pitot tube configurations were tested in the North Carolina State University subsonic wind tunnel at speeds from 4.52 m/s (15 ft/sec) to 30.48 m/s (100 ft/sec) to determine the effects of pitot tube geometry and speed on the pitot coefficient, C_p . In addition, certain of these S-type pitot tubes were tested in conjunction with sampling probes to assess the magnitude of the aerodynamic interference of the sampling probe on the pitot tube. Tests were conducted in which the S-type pitot tube was pitched from -20° to $+20^\circ$ or yawed from -30° to $+30^\circ$, in increments of 5° in each case, to determine the effects of misalignment on the pitot coefficient. Finally, the effect of swirl on the pitot coefficient was determined by testing a S-type pitot coefficient in a swirling flow field.

It was found that S-type pitot tube 3-04 could be yawed to $\pm 30^\circ$ or pitched from -14° to 20° and its pitot coefficient would change less than five percent of the accepted value of 0.85. This same pitot tube was also found to be the least sensitive to swirling flow, and therefore, it is recommended for future applications.

This report was submitted in fulfillment of Grant No. 803168 by the Department of Mechanical and Aerospace Engineering, North Carolina State University, under the sponsorship of the U. S. Environmental Protection Agency. This report covers the period June 1, 1974 to December 31, 1976, and work was completed as of December 31, 1976.

CONTENTS

Foreword	iii
Abstract	iv
Figures	vi
Symbols	ix
Acknowledgment	x
1. Introduction	1
2. Conclusions and Recommendations	3
3. Apparatus	5
4. Experimental Procedure	10
Calibration of S-Type Pitot Tubes and Determination of the Effects of Geometry	10
Interference Tests - Zero Sampling Rate	10
Interference Tests - 0.85 x Isokinetic Sampling Rate	11
Interference Tests - Isokinetic Sampling Rate	12
Pitch Tests	12
Yaw Tests	16
Swirl Tests	19
5. Data Reduction	20
6. Results and Discussion	22
Effect of Geometry on S-Type Pitot Tube Calibration	22
Interference Effects - Zero Sampling Rate	25
Interference Effects - Sampling at 0.85 x Isokinetic and Isokinetic Rates	30
Interference Effects - Misalignment of S-Type Pitot Tube, Sampling Probe Combination	30
Effect of Yaw and Pitch in the Absence of a Sampling Nozzle	35
Effect of Yaw with Interference	46
Effect of Pitch with Interference	46
Effect of Swirl	63
References	68
Appendix	
A. Velocity Profile of Wind Tunnel Test Section	69

FIGURES

<u>Number</u>		<u>Page</u>
1	Typical S-Type Pitot Tube and Nomenclature	6
2	Tunnel Set-Up of Assembly for an Interference Effects Test. Distance Between S-Type Pitot Tube and Sampling Probe, 10.188 inches	9
3a	Relative Positions of Sampling Probe and Pitot Tube with Sampling Probe 0.05 m Above Pitot Tube	13
3b	Relative Positions of Sampling Probe and Pitot Tube with Sampling Probe 0.05 m Below Pitot Tube	14
4	Relative Positions of Sampling Probe and Pitot Tube with Sampling Probe Port Slightly Ahead of Fore Port of Pitot Tube	15
5	Sign Convention	17
6	S-Type Pitot Tubes	18
7	Pitot Coefficient Versus Velocity for S-Type Pitot Number 3-01	23
8	Pitot Coefficient Versus Velocity for S-Type Pitot Number 3-02	23
9	Pitot Coefficient Versus Velocity for S-Type Pitot Number 3-03	24
10	Pitot Coefficient Versus Velocity for S-Type Pitot Number 3-04	24
11	Effects of Port-to-Port Spacing and Inter Tube Spacing on the Average Pitot Coefficient	26
12	Interference Effects on an S-Type Pitot Tube, Sampling Rate = 0, Spacing = 0	27
13	Interference Effects on an S-Type Pitot Tube, Sampling Rate = 0, Spacing = 0.01499 m	28

14	Interference Effects on an S-Type Pitot Tube, Sampling Rate = 0, Spacing = 0.03018 m	29
15	Interference Effects on an S-Type Pitot Tube, Sampling Rate = 0.85 x Isokinetic, Spacing = 0	31
16	Interference Effects on an S-Type Pitot Tube, Sampling Rate = 0.85 x Isokinetic, Spacing = 0.01499 m	32
17	Interference Effects on an S-Type Pitot Tube, Sampling Rate = Isokinetic, Spacing = 0	33
18	Effects of Misalignment of S-Type Pitot Tube - Sampling Probe Combination, Sampling Rate = Isokinetic, Spacing = 0	34
19	Effect of Yaw on S-Tube 4-10	36
20	Effect of Yaw on S-Tube 3-04	37
21	Effect of Yaw on S-Tube 3-01	39
22	Averaged Effect of Yaw	41
23	Effect of Pitch on S-Tube 4-10	42
24	Effect of Pitch on S-Tube 3-04	43
25	Effect of Pitch on S-Tube 3-01	44
26	Averaged Effect of Pitch	45
27	Effect of Yaw with Interference; Sampling Rate: 0.60 x Isokinetic Flow Rate	47
28	Effect of Yaw with Interference; Sampling Rate: 0.85 x Isokinetic Flow Rate	49
29	Effect of Yaw with Interference; Sampling Rate: 1.00 x Isokinetic Flow Rate	51
30	Effect of Yaw with Interference; Sampling Rate: 1.4 x Isokinetic Flow Rate	53
31	Averaged Effect of Yaw with Interference on S-Tube 4-10	54
32	Effect of Pitch with Interference; Sampling Rate: 0.60 x Isokinetic Flow Rate	55
33	Effect of Pitch with Interference; Sampling Rate: 0.60 x Isokinetic Flow Rate	56

34	Effect of Pitch with Interference; Sampling Rate: 0.85 x Isokinetic Flow Rate	57
35	Effect of Pitch with Interference; Sampling Rate: 0.85 x Isokinetic Flow Rate	58
36	Effect of Pitch with Interference; Sampling Rate: 1.00 x Isokinetic Flow Rate	59
37	Effect of Pitch with Interference; Sampling Rate: 1.00 x Isokinetic Flow Rate	60
38	Effect of Pitch Interference; Sampling Rate: 1.40 x Isokinetic Flow Rate	61
39	Averaged Effect of Pitch with Interference on S-Tube 4-10	62
40	Effects of Swirl on S-Tube 4-10	64
41	Effects of Swirl on S-Tube 3-04	65
42	Effects of Swirl on S-Tube 3-01	66

APPENDIX A

A1	Velocity Profile Across Test Section of NCSU Wind Tunnel	70
----	--	----

LIST OF SYMBOLS AND TERMS

C_p	pitot coefficient at a specific velocity
$\overline{C_p}$	average coefficient for the velocity range 4.5 to 30.5 m/sec
$\overline{C_{p_\infty}}$	average pitot coefficient for S-type pitot without the sampling probe attached
p	pressure
p_a	pressure measured in the aft facing leg of S-type pitot tube
p_f	pressure measured in the forward facing leg of S-type pitot tube
p_t	total (or stagnation) pressure
p_∞	pressure far ahead of pitot tube (static pressure)
R	gas constant
T	temperature
V	velocity of the gas
V_{CL}	velocity at centerline of test section
ρ	mass density of the gas
$C-C$	centerline to centerline spacing between sampling probe and pitot tube
S	distance between the two legs of the "S" type pitot tube (inter-tube distance)
W	outside diameter of pitot tube leg
D	offset distance on tube, see Figure 1
Pitch	rotation of the pitot tube about an axis which is normal to both the flow and the centerline of the S-type pitot tube, see Figure 5 and page 16.
Yaw	rotation of the pitot tube about the centerline of the tube, see Figure 5 and page 16.

ACKNOWLEDGMENTS

The authors wish to thank the U. S. Environmental Protection Agency for their financial support of this study. In addition, thanks are expressed to Dr. William J. Mitchell of the Quality Assurance Branch of the U. S. Environmental Protection Agency, Research Triangle Park, North Carolina, for his assistance in obtaining the equipment necessary for this study.

The authors also wish to thank Mr. Herbert E. Moretz, Ms. Ellen W. Terry and Mr. Benjamin F. Willis, graduate students in the Department of Mechanical and Aerospace Engineering at North Carolina State University, for their assistance in actually carrying out the tests reported herein and Mrs. Patricia T. Hummel for preparing the manuscript for this final report.

SECTION 1

INTRODUCTION

For an in-stack environment, high dust loadings that lead to solids build-up may result in erroneous pressure measurements when using a standard pitot-static tube. Consequently, the S-type (Stauscheibe or reverse type) pitot tube is employed in source sampling. The tube is used to determine the stack gas velocity and volumetric flow rate. Also in source sampling, the S-type pitot tube is used in conjunction with a sampling probe in order to measure the composition of pollutant emissions. The local sampling velocities should equal the actual local stack velocities when isokinetic sampling is required.

Normally, S-type pitot tubes are calibrated in terms of a pitot coefficient (C_p) which is defined as

$$C_p = \frac{V}{\sqrt{\frac{2(P_f - P_a)}{\rho}}} .$$

A pitot coefficient of 0.85 is the generally accepted value for S-type tubes. However, the S-type pitot tube is sometimes used in conjunction with a sampling probe. Consequently, it has been suggested [1] that each S-type pitot tube be calibrated with a sampling probe attached before use in sampling programs.

Unfortunately, there is very little data available to indicate how either design parameters or use of S-type pitot tubes affect the pitot coefficient. Gnyp, et al. [1] performed a detailed evaluation of a number of commercially available S-type pitot tubes. Beyond this, however, the information available in the literature seems to be scant and what data is available is not well documented. The distance between the upstream and downstream openings of the pitot tube, the angle of the pitot tube faces and the body of the tube, the angle between the pitot tube and the gas flow, and the range of gas velocities may affect the pressure readings of the S-type pitot tube and will therefore alter the pitot coefficient. In addition, when the S-type pitot tube is used in conjunction with a sampling probe to determine particulate or acid mist emissions, it is common practice to place the sampling probe close to the pitot tube. With the pitot tube and the sampling probe in close proximity to one another, the flow field about the sampling probe will alter the flow field about the pitot tube and vice versa. This aerodynamic interference may certainly alter the pressure indication of the pitot tube and lead to incorrect estimates of the flow velocity. Gnyp, et al. [1] have also evaluated this interference effect, but only for a number of commercially available S-type pitot tubes.

Finally, when S-type pitot tubes are used in actual source sampling, the flow in the source being sampled may be far from the ideal conditions of smooth and uniform flow. There may be varying degrees of swirl in the flow due to blowers, bends, and obstructions upstream of the sampling site. The effects of such swirling flow on the indications of S-type pitot tubes have apparently never been evaluated as a function of pitot tube design.

In view of the above, it was clear that there is a definite need for a definitive study of the effects of pitot tube design, construction and use to determine the accuracy with which measurements can be made using a S-type pitot tube. In 1974 the Department of Mechanical and Aerospace Engineering at North Carolina State University undertook such a study under the sponsorship of the Environmental Protection Agency. In particular an investigation was conducted to:

1. Calibrate a number of S-type pitot tubes.
2. Determine the effects of geometry changes, such as the upstream and downstream port to port distance, on the accuracy of S-type pitot tubes.
3. Determine the effects of misalignment of the S-type pitot tube with respect to the air stream (pitch and yaw).
4. Determine the aerodynamic interference effects due to the S-type pitot tube and the sampling probe being in close proximity to one another.
5. Determine the effect of swirling type flow and also sampling rate on the accuracy of S-type pitot tubes.

The present work reports on the results obtained in this study.

SECTION 2

CONCLUSIONS AND RECOMMENDATIONS

The data obtained from this investigation leads to the following conclusions:

1. The S-type pitot tubes, when tested independent of the sampling probe, exhibit pitot coefficients within three percent of the accepted value of 0.85 for speeds between 6.09 m/s (20 ft/sec) and 30.48 m/s (100 ft/sec). For speeds between 3.05 m/s (10 ft/sec) and 6.09 m/s (20 ft/sec), the variation of the pitot coefficient from 0.85 increases to five percent. Below 3.05 m/s (10 ft/sec), the measured pitot coefficient is unreliable. The pressure reading fluctuates as much as 50 percent for speeds lower than 3.05 m/s (10 ft/sec) and this fluctuation shows on the micromanometer. The fluctuation is so great that a "mean" pressure cannot be obtained.

2. In the range of flow speeds from 4.57 m/s (15 ft/sec) to 30.48 m/s (100 ft/sec) the pitot coefficient decreases slightly as the velocity increases, but this decrease is sufficiently small for the pitot coefficient to be represented by an average value in this range of velocities.

3. When an EPA type sampling probe is used in conjunction with an S-type pitot tube there may be an aerodynamic interference effect that will alter the average pitot coefficient of the S-type pitot tube. This interference is most noticeable when the centerline-to-centerline distance between the sampling probe and the S-type pitot tube is less than ten times the outside diameter of the pitot tube legs. The interference effects are greatest with large size sampling nozzles. However, sampling with the sampling probe tends to reduce the interference effects. The interference effects on the pitot tube were also reduced when the pitot tube was pushed 5 cm further into the wind tunnel than the sampling nozzle.

4. With regard to yaw, S-type pitot tube 3-04 gives the best results. This tube is capable of undergoing yaw angles from -30° to 30° while staying within five percent of the accepted value of 0.85 for the pitot coefficient. S-type pitot tube 3-01 requires a range from -25° to 25° in order to preserve this accuracy. In the case of S-type pitot tube 4-10, yaw angles from -9° to 9° are needed.

5. For the case of pitch, S-type pitot tube 3-04, again, proves to be superior. It may sustain pitch deflections as large as $\pm 20^{\circ}$

without exceeding the prescribed five percent tolerance of C_p . Similarly, as in the case of yaw, S-type pitot tube 3-01 gives intermediate results. A pitch range spanning from -14° to 20° will insure that the pitot coefficient is within five percent of the accepted value of 0.85. Pitch angles ranging from -6° to 20° are required to maintain a five percent tolerance for S-type pitot tube 4-10.

6. When interference effects from the sampling probe are coupled with yaw, S-type pitot tube 4-10 gives values for the pitot coefficient which are outside of the desired five percent tolerance for all angles of yaw between -30° and 30° . However, this error is not more than 12 percent.

7. When interference is present during pitch, S-type pitot tube 4-10 may be pitched from -15° to 2° and still maintain the five percent tolerance. If the tube is pitched as much as $\pm 20^\circ$ the errors encountered can be as large as ten percent.

8. While a swirling environment tends to increase the pitot coefficient for all the tubes studied, S-type pitot tube 3-04 experienced the smallest percent increase (2.7 percent).

SECTION 3

APPARATUS

All of the tests reported in the present work were conducted in the North Carolina State University Merrill Subsonic Wind Tunnel. This wind tunnel is a continuous flow, single return tunnel with a vented test section. The wind tunnel is capable of producing speeds from 0 to approximately 49.19 meters/sec (110 mph) in a test section 1.143 m (45 inches) wide, 0.8128 m (32 inches) high and 1.1684 m (46 inches) long (in the flow direction). The test section is fitted with large plexaglass windows, in the sidewalls, through which the test models may be observed, and a removable floor. Several test section floors were constructed and fitted with supports for the pitot tubes which were tested.

The actual velocity in the wind tunnel was measured in each test using an elliptical nose, standard, pitot-static tube manufactured by Airflow Developments Limited, High Wycombe, England. This elliptical nose pitot-static tube is regarded as the best available standard and is the only one recommended for use without individual calibration [1]. This standard probe has a pitot coefficient of unity. All S-type tubes were calibrated relative to this standard tube.

The S-type pitot tubes to be tested were supplied by the Environmental Protection Agency through the Grant Monitor. One tube (No. 4-10) was supplied completely assembled (with the two legs of the probe welded together). Five additional pairs of legs for S-type pitot tubes were supplied unassembled. Each of the legs supplied was bent at one end to an angle of 45° and the probe face was machined so that it was parallel to the main body of the tube. For each pair of legs the offset (dimension D in Figure 1) was different. A numbering system was devised to identify each pair of legs. In this numbering system the first digit indicates the length of the probe and the second and third digits indicate the particular probe within the series. Three inter-tube spacers were constructed at North Carolina State University. Each pair of legs could be assembled either with no spacer between the legs or with one of the constructed spacers between the legs. This combination of tube 4-10 plus five pairs of tube legs and four inter-tube spacings resulted in a total of 21 different S-type pitot tube configurations which could be tested. A total of 14 of these different configurations were tested. Table 1 lists the various tubes tested, together with the important geometrical dimensions of each tube.

Pressure indications at both the pitot and static ports of the standard pitot-static tube and at both the fore and aft ports of the S-type pitot tubes were measured on a micromanometer. With this instrument it is possible to

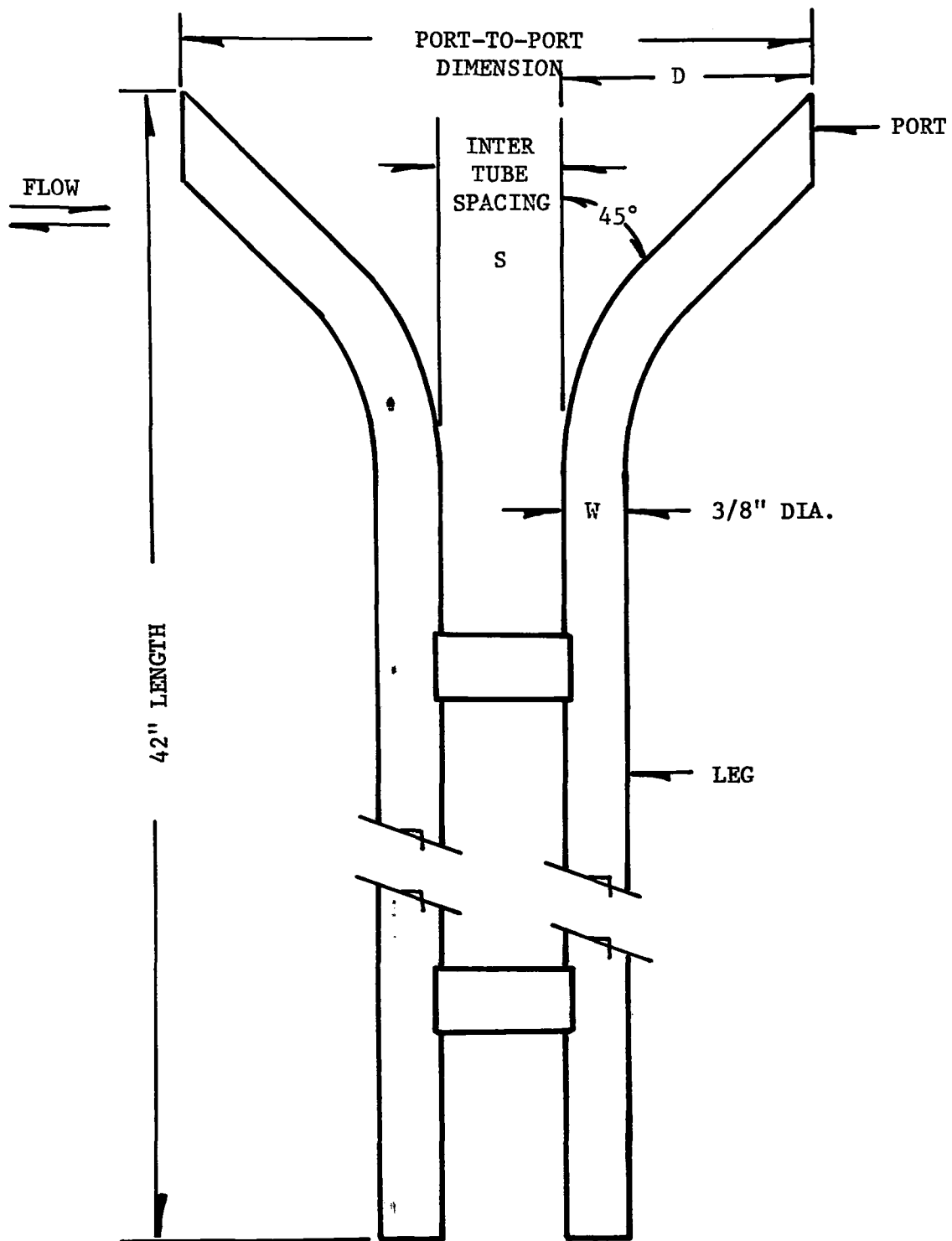


FIGURE 1. Typical S-Type Pitot Tube and Nomenclature

TABLE 1. Geometry of S-Type Pitot Tubes Tested.

Tube Number	Port to Port Dist. (P-P)	Inter Tube Spacing (S)	Offset Distance (D)	O.D. of pitot tube leg (W)
3-01	3.175	0.000	1.5875	0.9525
3-02	6.0325	0.000	2.9921	0.9525
3-03	8.2753	0.000	4.1148	0.9525
3-04	11.1176	0.000	5.588	0.9525
3-01	3.3909	0.254	1.5875	0.9525
3-02	6.2357	0.254	2.9921	0.9525
3-03	8.509	0.254	4.1148	0.9525
3-01	4.6888	1.5138	1.5875	0.9525
3-02	7.5463	1.5138	2.9921	0.9525
3-03	9.7892	1.5138	4.1148	0.9525
3-01	6.4567	3.0175	1.5875	0.9525
3-02	9.050	3.0175	2.9921	0.9525
3-20	3.9116	0.9144	1.4986	0.632
4-10	2.1742	0.000	1.0871	0.9525

- NOTES: 1. All dimensions are in cm.
2. Tube numbers are determined as follows:
- The leading digit indicates the approximate tube length in feet, rounded to the next smaller even footage.
 - The trailing two digits give the number of this tube in the given length series.
3. For some tubes $P-P \neq S + 2D$ due to distortions caused by the clamps.

measure pressure differences with an accuracy of ± 0.00254 cm (± 0.001 in) of water. All pressures were measured relative to atmospheric pressure. The atmospheric pressure was measured using a standard mercury filled barometer, which has an accuracy of ± 0.0127 cm (± 0.005 in) of mercury.

The gas temperature, used in calculating correction factors for the gas velocity, was measured using a standard chromel-alumel thermocouple, mounted inside the wind tunnel test section, in conjunction with a galvanometer read-out. Specific humidity of the atmospheric air was determined from the wet and dry bulb temperature measured using a sling-type psychrometer.

In the tests to determine the interference effects between the pitot tube and the sampling probe, three sampling probe nozzles with inside diameters of 0.635 cm (0.25 in), 0.953 cm (0.375 in), and 1.27 cm (0.500 in) were used. (The outside diameters of these three nozzles were 0.953 cm (0.375 in), 1.27 cm (0.500 in), and 1.59 cm (0.625 in), respectively.) Figure 2 shows the S-type pitot tube, the sampling probe and the standard pitot static tube in the wind tunnel test section. The sampling probe was connected to a commercially produced Staksamplr*. Tests were conducted with the Staksamplr turned off (zero sampling rate) and at various sampling rates through the nozzle-probe-Staksamplr system. The sampling probe, sampling-probe nozzles, and Staksamplr used in these tests were supplied by the Environmental Protection Agency through the Grant Monitor. Additional, specific details regarding each piece of equipment used in the present investigation are presented in References 2 and 3.

*Trademark

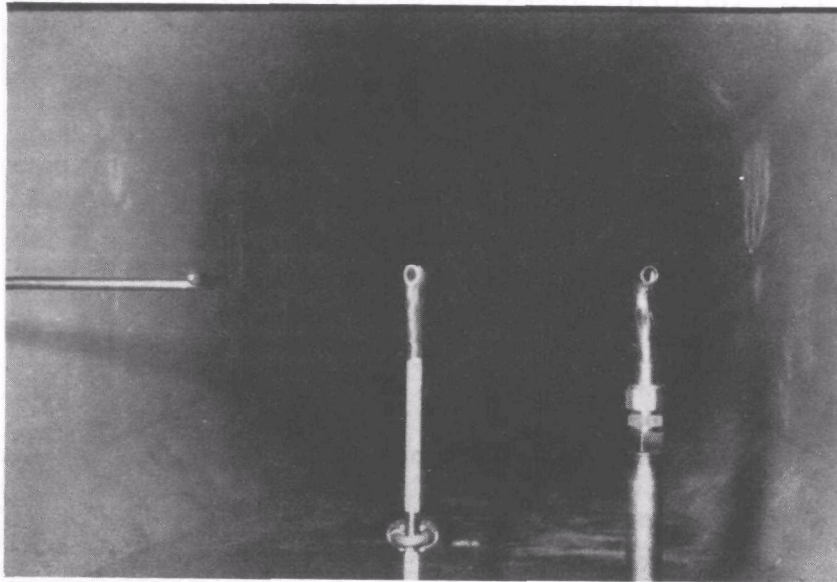


FIGURE 2. Tunnel Set-Up of Assembly for an Interference Effects Test. Distance Between S-Type Pitot Tube and Sampling Probe, 10.188 inches

SECTION 4

EXPERIMENTAL PROCEDURE

CALIBRATION OF S-TYPE PITOT TUBES AND DETERMINATION OF THE EFFECTS OF GEOMETRY

Each of the S-type pitot tubes used was calibrated against a standard elliptical nosed pitot-static tube. To accomplish this, the wind tunnel speed was first set at a given (approximate) velocity and the standard pitot-static tube was inserted into the wind tunnel so that the total pressure port was located at the center of the tunnel test section. Total and static pressures were then measured. The wind tunnel test section velocity is determined accurately from these measured pressures. The standard pitot-static tube was then withdrawn from the wind tunnel test section and the S-type pitot-tube immediately inserted at the same location in the wind tunnel (i.e. the upstream port of the S-type pitot tube was located at exactly the same location previously occupied by the ellipsoidal nose of the standard pitot-static tube). The pressures at the forward and aft ports of the S-type pitot tube were then measured. The S-type pitot tube was withdrawn from the tunnel. The test-section velocity was then increased and the above procedure was repeated at this new velocity. Initially this process was repeated in velocity increments of 1.52 m/s (5 ft/sec) for the velocity range from 1.52 m/s (5 ft/sec) to 30.48 m/s (100 ft/sec). Upon completion of this sequence of tests, the S-type pitot tube was rotated 180 degrees so that the pressure port which had been facing forward now faced aft and the pressure port which had been facing aft, now faced forward. The entire procedure outlined above was then repeated for the tube in this new orientation.

Preliminary testing showed that the measurements made at low velocities (below approximately 4.572 m/s) were inaccurate because it was difficult to accurately read the micromanometer at very low pressure differentials. For this reason, the measurements made at velocities below 4.522 m/s (15 ft/sec) were dropped and subsequent tests were made in the velocity range from 6.096 m/s (20 ft/sec) to 30.48 m/s (100 ft/sec) with increments of 3.048 m/s (10 ft/sec).

Since all the tubes were calibrated in this manner, the effects of varying geometry could be determined by comparing the calibrations of different pitot tubes.

INTERFERENCE TESTS - ZERO SAMPLING RATE

To determine the effects of aerodynamic interference of the sampling probe on the measurements of the S-type pitot tube, the sampling probe and

S-type pitot tube were tested together in the wind tunnel. To accomplish this the S-type pitot-tube and the sampling probe were mounted in the wind tunnel test section, through the tunnel floor, with a given centerline to centerline separation between the S-type tube and the sampling probe. The standard pitot static tube was inserted into the wind tunnel so that it was approximately 0.1524 m (6 in) from the S-type tube-sampling probe combination. (Figure 2 shows a view, looking downstream, of the S-type tube, the sampling probe and the standard pitot static tube in the wind tunnel.) The variation in velocity between the locating of the S-type pitot tube and the standard pitot tube was always less than two percent (See Appendix A).

With the combination of probes in position the wind tunnel speed was adjusted to approximately the desired value. The pitot and static pressures were measured, using the standard pitot-static tube, and then the standard pitot static tube was retracted to the tunnel wall. The pressures at each of the ports on the S-type tube were then measured for a number of different centerline to centerline spacings between the sampling probe and the S-type pitot tube. By moving the sampling probe the spacing between the S-type pitot tube and the sampling probe was varied from 0.03016 m (1 3/16 in) to 0.2588 m (10 3/16 in) in increments of 0.0254 m (1 in). With the clamping arrangement used in the present tests, 3.02 cm was the closest centerline to centerline distance at which the S-type pitot tube and the sampling probe could be mounted.

A spacing code was assigned to each of the centerline to centerline spacing in the following manner: The spacing 0.0316 m (1 3/16 in) was assigned the code number 0, the spacing 0.05556 m (2 3/16 in) was assigned the code number 1, the spacing 0.08096 m (3 3/16 in) was assigned the code number 2, etc. The highest code number used was 9, corresponding to a centerline to centerline spacing of 0.25877 m (10 3/16 in).

After some preliminary testing, it was found that the greatest variation in the pitot coefficient occurred at small centerline to centerline spacings. For later tests, therefore, measurements were only obtained at the spacings corresponding to code numbers 0, 1, 2, 4, and 9.

The entire procedure, outlined above, was repeated in the velocity range from 6.096 m/s (20 ft/sec) to 30.48 m/s (100 ft/sec) in increments of 6.096 m/s (20 ft/sec). These tests were conducted with S-type pitot tube number 3-01 with inter-tube spacings of zero, 0.0151 m and 0.03018 m, and with sampling probe nozzles of 0.00635 m (0.25 in), 0.009525 m (0.375 in), and 0.01275 m (0.5 in) diameter. For these tests the sampling rate was zero for the sampling probe.

INTERFERENCE TESTS - 0.85 x ISOKINETIC SAMPLING RATE

In cases where interference effects were determined with the sampling probe in operation, the standard pitot static measurements were made without the S-type pitot tube and the sampling probe in the tunnel. Instead, the standard pitot-static tube was inserted in the tunnel first so that the pitot pressure port was in the same location as in the zero sampling rate test. The pitot and static pressures were measured at a given tunnel setting. Once these pressures were measured, the standard pitot-static tube was retracted to the

wall of the tunnel and then the S-type pitot tube-sampling probe combination was inserted into the tunnel in the same location as was used in the zero sampling rate case. The Staksamplr was then turned on and adjusted so that the flow through the sampling probe was 85 percent of the isokinetic value. The pressures at the fore (upstream) and aft (downstream) ports of the S-type pitot tube were then measured as the centerline to centerline distance between the sampling probe and the S-type pitot tube was changed. Measurements were made for centerline to centerline spacings corresponding to code numbers 0, 1, 2, 4, and 9. Once these measurements were obtained, the Staksamplr was turned off. The S-type pitot tube-sampling probe combination was withdrawn from the tunnel and the standard pitot-static tube was once more inserted into the wind tunnel. The tunnel speed was adjusted to a new value and the above procedure was repeated. Tests were made at 4.572 m/s (15 ft/sec), and from 6.096 m/s (20 ft/sec) to 30.48 m/s (100 ft/sec) in increments of 6.096 m/s (20 ft/sec). These tests were conducted using pitot-tube number 3-01 with inter-tube spacings of zero, 0.0151 m (0.596 in) and 0.03018 m (1.188 in), and with sampling probe nozzle diameters of 0.00635 m (0.25 in), 0.009525 m (0.375 in), and 0.0127 m (0.5 in).

INTERFERENCE TESTS - ISOKINETIC SAMPLING RATE

Tests to determine the interference effects with the sampling probe sampling at the isokinetic flow rate were conducted in the same manner as the tests in which sampling was at 85 percent of the isokinetic rate. Again measurements were made at velocities of 4.572 m/s (15 ft/sec) and from 6.096 m/s (20 ft/sec) to 30.48 m/s (100 ft/sec) in increments of 6.096 m/s (20 ft/sec), with probes 3-01 and 3-02 with zero inter-tube spacing. Tests in this series were made at centerline to centerline distances corresponding to spacing code numbers 0, 1, and 9.

In addition, some of these tests were conducted with the sampling probe 0.05 m (2 in) beyond and 0.05 m (2 in) behind the S-type probe (Figure 3). Also several additional tests were conducted with the nozzle of the sampling probe extending slightly upstream of the upstream port of the S-type pitot tube, but with the tube axes in the same plane (Figure 4).

PITCH TESTS

A series of tests were conducted to determine the effects of pitch on the pitot coefficient for the S-type pitot tube. In these tests, and in subsequent tests to determine the effects of yaw and swirl, the standard pitot-static tube was not used to determine the speed at each test point. Instead, the wind tunnel speed was determined from the difference in two pressures measured by two wall pressure-taps in the wind tunnel and indicated on a micromanometer mounted on the outside of the wind tunnel. The wind tunnel speed was calibrated using the standard pitot static tube to relate the indications on the micromanometer to the pressure difference across the standard pitot static tube. Thereafter, the pressure indications on the micromanometer were used to determine the pressure difference which would exist across the standard pitot-static tube if it had been placed in the tunnel.

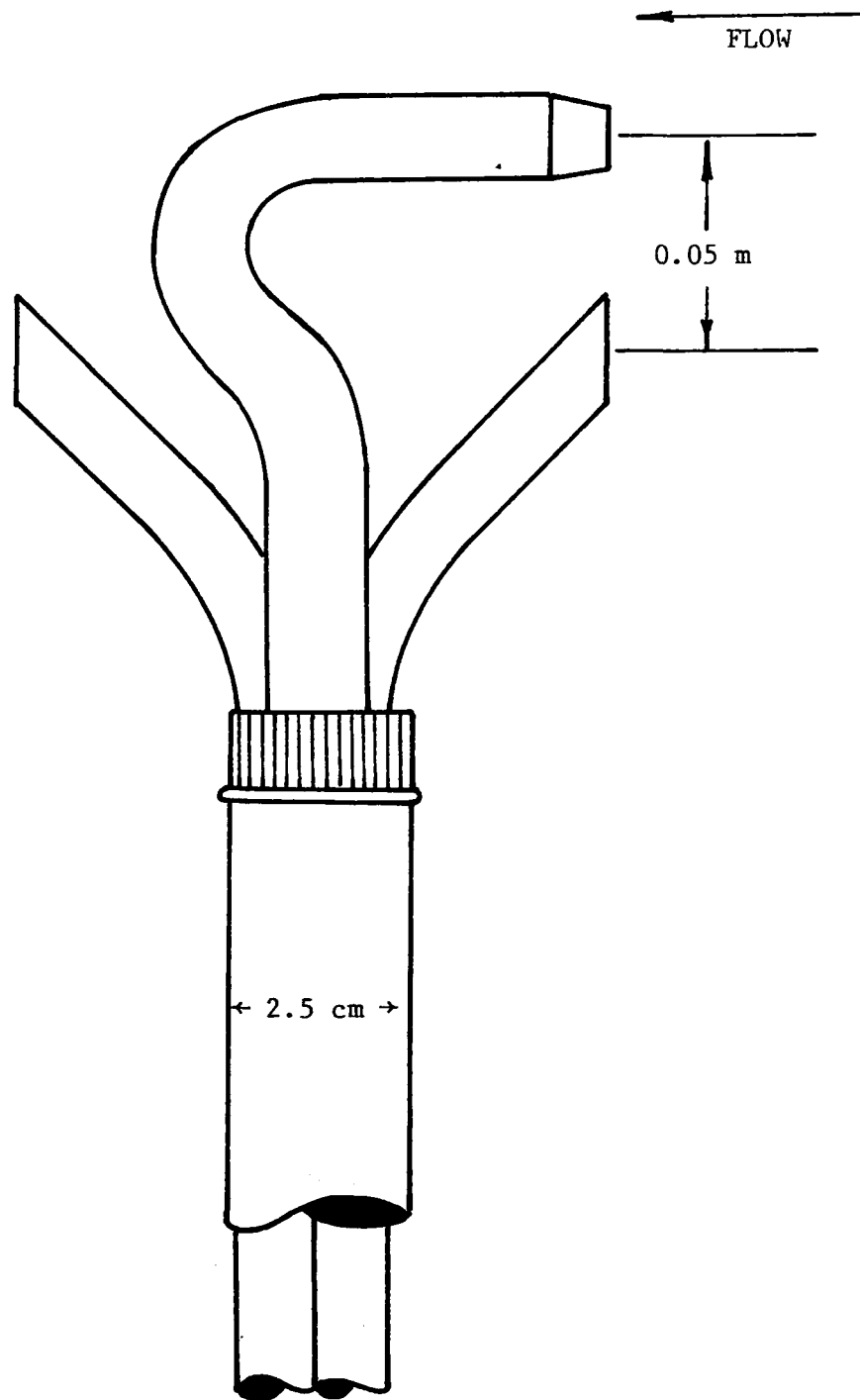


FIGURE 3a. Relative Positions of Sampling Probe and Pitot Tube with Sampling Probe 0.05 m Beyond the Pitot Tube.

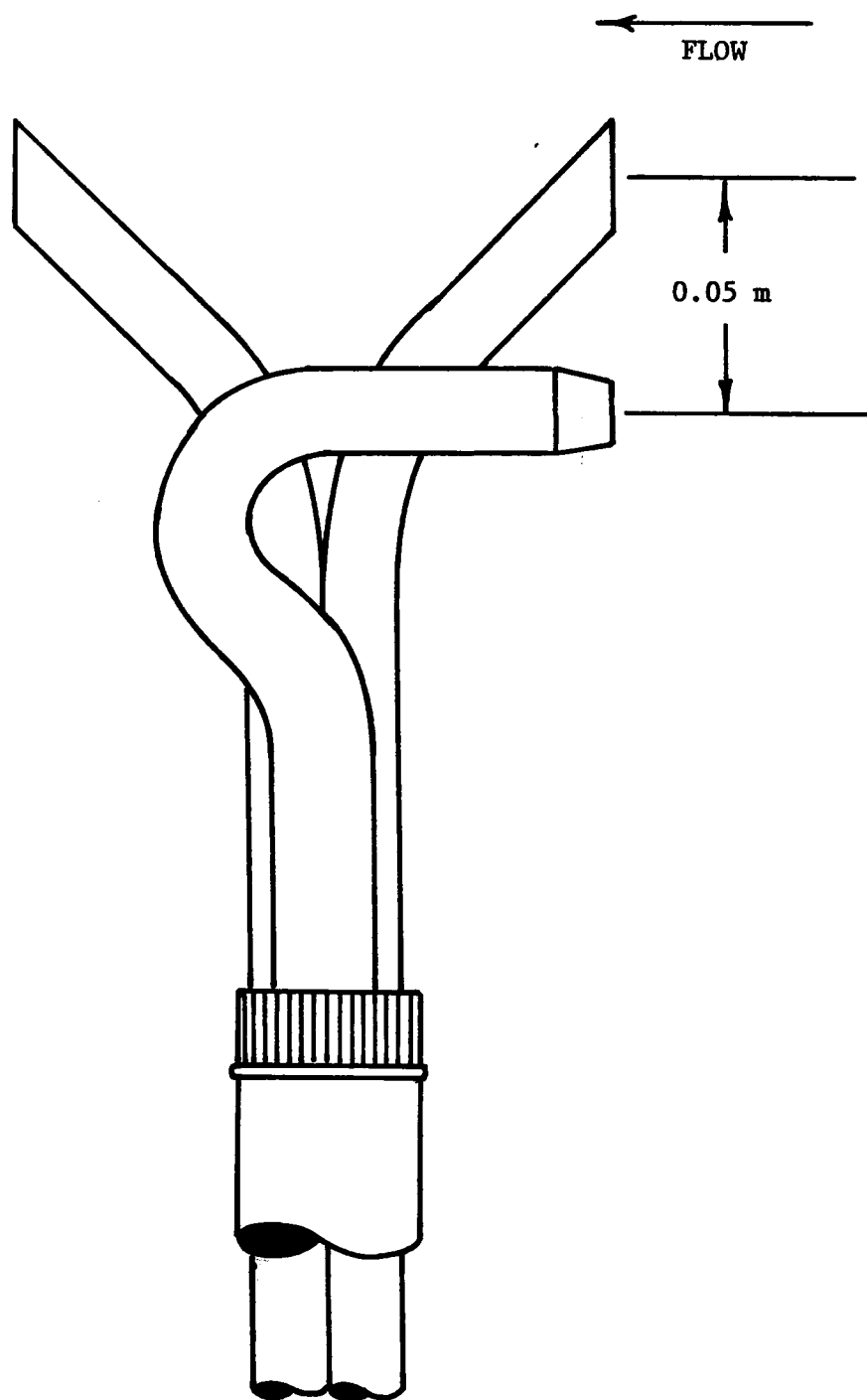


FIGURE 3b. Relative Positions of Sampling Probe and Pitot Tube with Sampling Probe 0.05 m Behind the Pitot Tube.

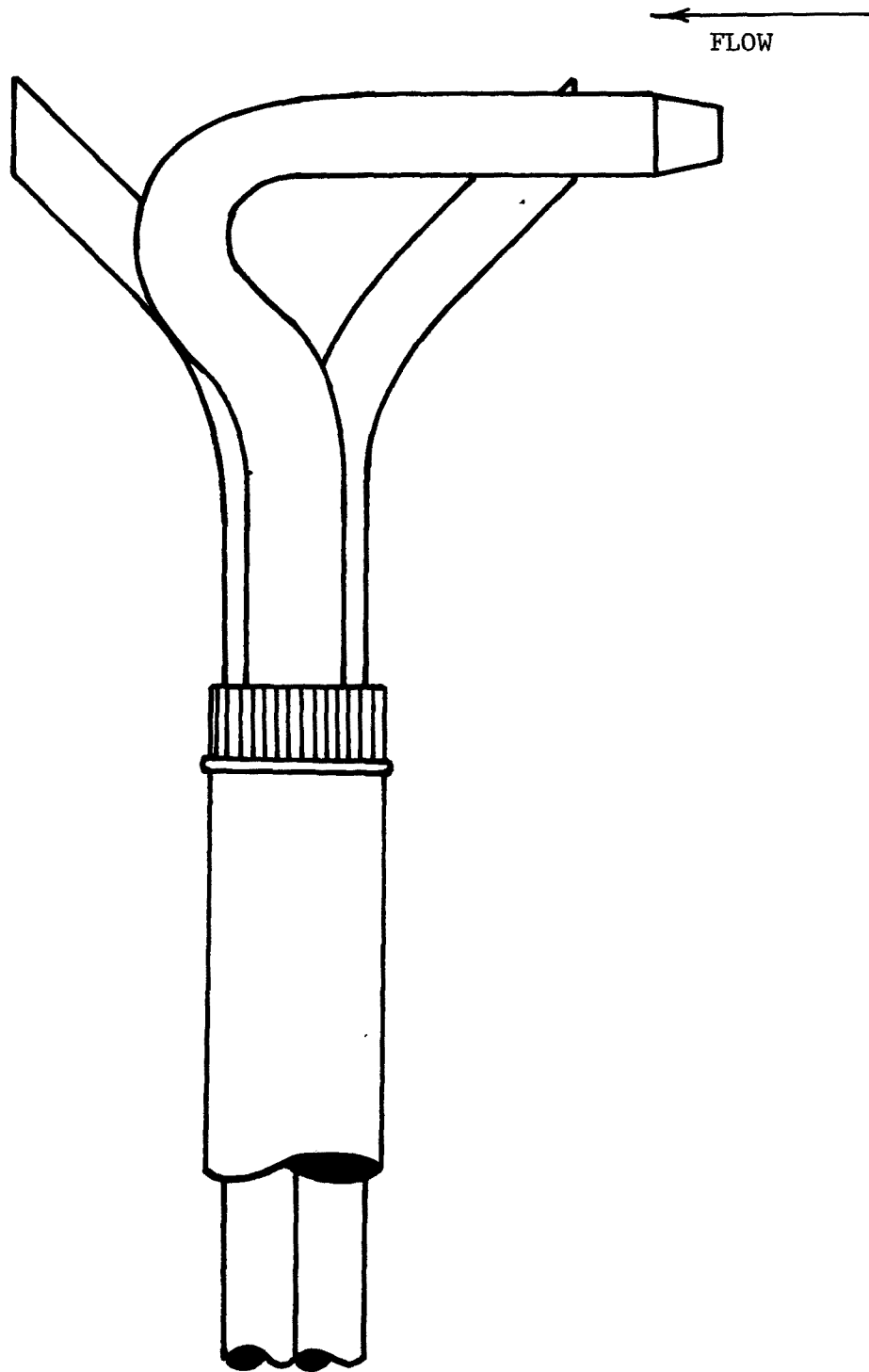


FIGURE 4. Relative Positions of Sampling Probe and Pitot Tube with Sampling Probe Port Slightly Upstream of the Upstream Port of Pitot Tube.

In the tests to determine the effects of pitch, the S-type pitot tube was inserted in the wind tunnel test section and the test section velocity was set at the desired (approximate) value. The pitch angle of the S-type tube was then set and the pressure difference between the fore and aft ports of the tube were measured. These measurements were made with the pitch angle varied from $+20^\circ$ to -20° in 5° increments. The pitching mechanism employed in the present tests was designed so that the center of rotation of the S-type pitot tube was at the forward port of the tube. The sign convention used here considers positive pitch to be the case where the probe is rotated so that the rear, or aft, port moves up (Figure 5). Thus, as the S-type pitot tube is pitched, the forward port of the tube remains at essentially the same location in the tunnel. This minimizes the effects of even small variations in flow velocity across the tunnel test section.

Once the S-type pitot tube had been tested at all the pitch angles noted above, the test section velocity was increased and the procedure outlined above was repeated. Pitch tests were conducted in the velocity range from approximately 6.096 m/s (20 ft/sec) to approximately 27.43 m/s (90 ft/sec) in increments of approximately 6.096 m/s (20 ft/sec). Pitch tests were conducted using pitot tubes 3-01, 3-04, and 4-10 (Figure 6).

Additional tests were conducted to measure the effect of pitch on the combination S-type pitot tube and sampling probe. To conduct these tests, the sampling probe was attached to the left side of the S-type pitot tube and the assembly pitched as a unit. In this configuration the distance between the centerline of the S-type tube and the sampling probe was 0.03175 m (1 1/4 in). Tests were conducted at sampling rates of 0.6 x isokinetic, 0.85 x isokinetic, 1 x isokinetic and 1.4 x isokinetic using pitot tube 4-10 and the appropriate nozzle size.

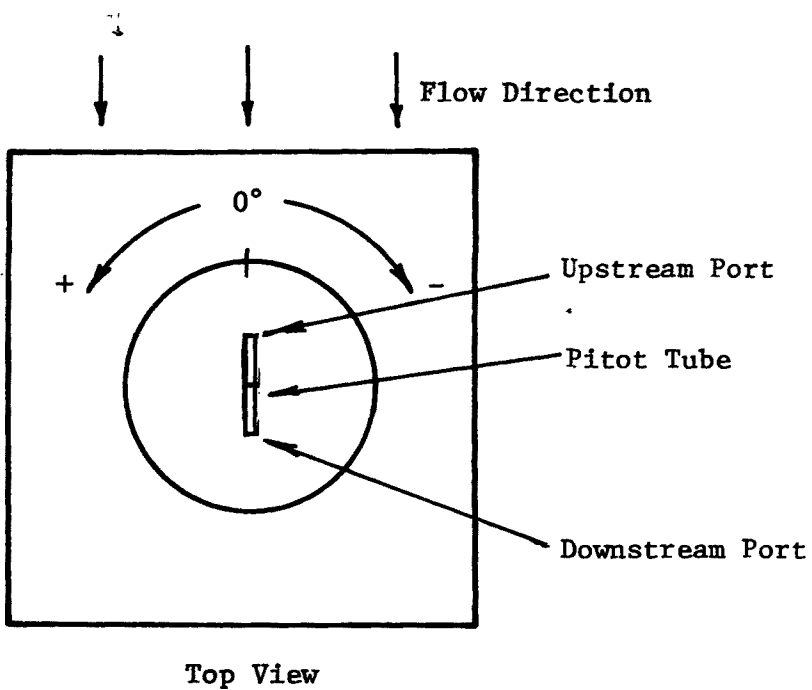
YAW TESTS

A series of tests were also conducted to determine the effects of yaw on the pitot coefficient for the S-type pitot tube. In conducting these tests, the S-type pitot tube was inserted in the wind tunnel and the test section speed was adjusted approximately to the desired value. The S-type pitot tube was then yawed to a prescribed value and the pressure difference between the fore and aft ports of the S-type pitot tube were measured. Tests were conducted, at a given tunnel speed, with the yaw angle varied from -30° to $+30^\circ$ in increments of 5° . Positive yaw angles correspond to counter clockwise rotation of the tube, as seen from the pressure sensing end of the tube (Figure 5).

Once measurements were made for all the yaw angles considered, the tunnel speed was increased to a new value and the yaw tests, outlined above, were repeated. In this manner, measurements were made over the velocity range from approximately 6.096 m/s (20 ft/sec) to approximately 27.43 m/s (90 ft/sec) in increments of approximately 6.096 m/s (20 ft/sec). Yaw tests were conducted using pitot tubes 3-01, 3-04, and 4-10.

Additional tests were conducted to measure the effects of yaw on a combined S-type pitot tube and sampling probe. For these tests the S-type pitot tube and sampling probe were clamped together and yawed in combination. In

Yaw



Pitch

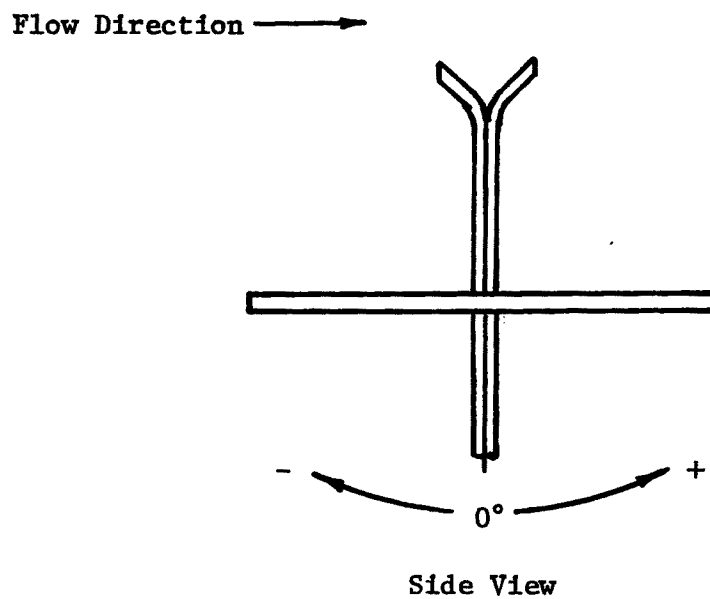


FIGURE 5. Sign Convention.

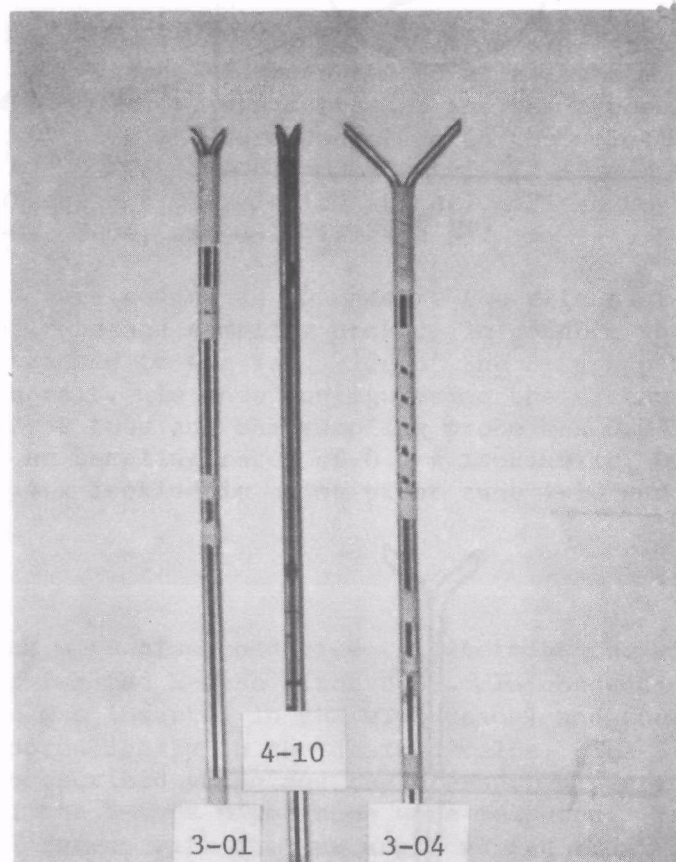


FIGURE 6. S-Type Pitot Tubes

this configuration the distance between the sampling probe centerline and the S-type pitot tube centerline was 0.03175 m (1 1/4 in). Tests were conducted with this combined probe at sampling rates of 0.6 x isokinetic, 0.85 x isokinetic, 1 x isokinetic and 1.4 x isokinetic using pitot tube 4-10 and the appropriate nozzle size.

SWIRL TESTS

A series of tests were conducted to determine the effect of swirl in the flow on the pitot coefficient of S-type pitot tubes. Swirl was produced in the wind tunnel by inserting a small wing section into the wind tunnel just upstream of the tunnel test section. The wing section was attached to the tunnel ceiling and had a length such that the tip of the wing section was located at the centerline of the tunnel. With this wing section positioned at an angle of attack, a wing-tip vortex is produced along the centerline of the tunnel. The existence of a swirling flow in the wind tunnel was verified by introducing a tuft grid into the test section and observing the movement of the tufts.

To determine the effect of swirl, the S-type pitot tube was first calibrated in the wind tunnel with the wing section removed from the tunnel. The same S-type pitot tube was again tested in the wind tunnel over the same speed range, but with the wing now mounted upstream of the test section. In the present tests, S-type pitot tubes 3-01, 3-04, and 4-10 were tested in this manner.

Additional details regarding the procedure used in each of the above tests are presented in References 2 and 3.

SECTION 5

DATA REDUCTION

The basic measurements in the bulk of the experiments reported herein consisted of the pressures (relative to atmospheric) measured individually at the pitot port and the static port of the standard elliptical nosed pitot-static tube and the pressures (relative to atmospheric) measured individually at the fore and aft ports of the S-type tube being tested. The wind tunnel test section velocity is determined from the measured pitot and static pressures on the elliptical nosed pitot static tube. Since this pitot-static tube has a pitot coefficient of unity the velocity is related to the measured pressures and the air density by:

$$V = \sqrt{\frac{2(p_t - p_\infty)}{\rho}} \quad (1)$$

The velocity, determined from the measured pressures on the fore and aft legs of the S-type pitot tube, is therefore given by:

$$V = C_p \sqrt{\frac{2(p_f - p_a)}{\rho}} \quad (2)$$

where C_p is the pitot coefficient for the probe, p_f is the pressure measured in the forward facing leg of the S-type pitot tube, p_a is the pressure measured in the aft facing leg of the S-type pitot tube, and ρ is the density of the gas (air in this case). Since the time between measurements made with the pitot-static tube in place and the measurements made with the S-type pitot tube in place is small, it is reasonable to assume that neither the velocity nor the density in the tunnel changes during the test. Therefore, combining Equations (1) and (2) yields:

$$C_p = \sqrt{\frac{(p_t - p_\infty)}{(p_f - p_a)}} \quad .$$

The velocity in the wind tunnel is obtained directly from Equation (1). The air density, ρ , is not measured directly but may be determined from the equation of state for the air in the wind tunnel, i.e.

$$\rho = p_\infty / RT \quad ,$$

where p_∞ is the barometric pressure (which is the same as the static pressure in the wind tunnel since the tunnel test section is vented) and T is the

temperature (absolute) of the gas (air) in the wind tunnel. The gas constant R is calculated quite accurately with corrections made for the moisture content in the air. Corrections were also made for the variation of the density of the manometer and barometer fluids (water and mercury, respectively) with temperature. These corrections, however, are quite small. Additional details regarding the methods of data reduction may be found in References 2 and 3.

SECTION 6

RESULTS AND DISCUSSION

EFFECT OF GEOMETRY ON S-TYPE PITOT TUBE CALIBRATION

The variation of the pitot coefficient versus the velocity for the S-type pitot tubes studied can be seen in Figures 7, 8, 9 and 10. One curve in each figure represents the results obtained with the "A" side facing into the flow stream, the other represents the results obtained with the "B" side facing into the flow stream. (The dashed line in each figure is the average coefficient for that tube for the velocity range above 4.57 m/s when inter-tube spacers were not used.) As can be seen in these figures, the pitot tubes gave readings at speeds greater than 6.09 m/s that proved the tubes to be symmetrical.

At wind tunnel speeds less than 3.05 m/s, the accuracy of the calculated pitot coefficient was found to be unacceptable since the pressure readings for the two ports of the S-type pitot tube are almost equal. The maximum difference in the two port readings was 0.005 inches of water, and the micromanometer is not sensitive enough to make the pressure readings reliable. There is a relatively large variation of the pitot coefficient in the range of 3.05 m/s to 6.09 m/s. However, above 6.09 m/s the pitot coefficient curves level out.

At speeds greater than approximately 15.25 m/s, small unsteady fluctuations were observed in the rearward facing port pressure readings although the test section air speed was held steady. These unsteady fluctuations are attributed to unstable turbulence patterns shedding from the forward facing port and passing over the rearward facing port. When unsteady fluctuations arose, a "mean" pressure reading was obtained by selecting the value in the center of the fluctuation range.

Since the four pitot tubes represented in Figures 7, 8, 9, and 10 belong to the family of pitot tubes where the inter-tube spacing is constant, but the port-to-port dimension varies from 3.18 cm (1.25 in) to 11.1 cm (4.38 in), it is possible to estimate the effect of port-to-port spacing on the pitot coefficient for a family of pitot tubes. An inspection of Figures 7, 8, 9, and 10 shows that as the port-to-port distance increases the average coefficient increases slightly.

To determine the effect of inter-tube spacing on the pitot coefficient, several spacers were placed between the two legs of the S-type pitot tubes being tested. The inter-tube spacers used were 0.25 cm, 1.5 cm, and 3.01 cm. The results of these studies showed that the average pitot coefficients of

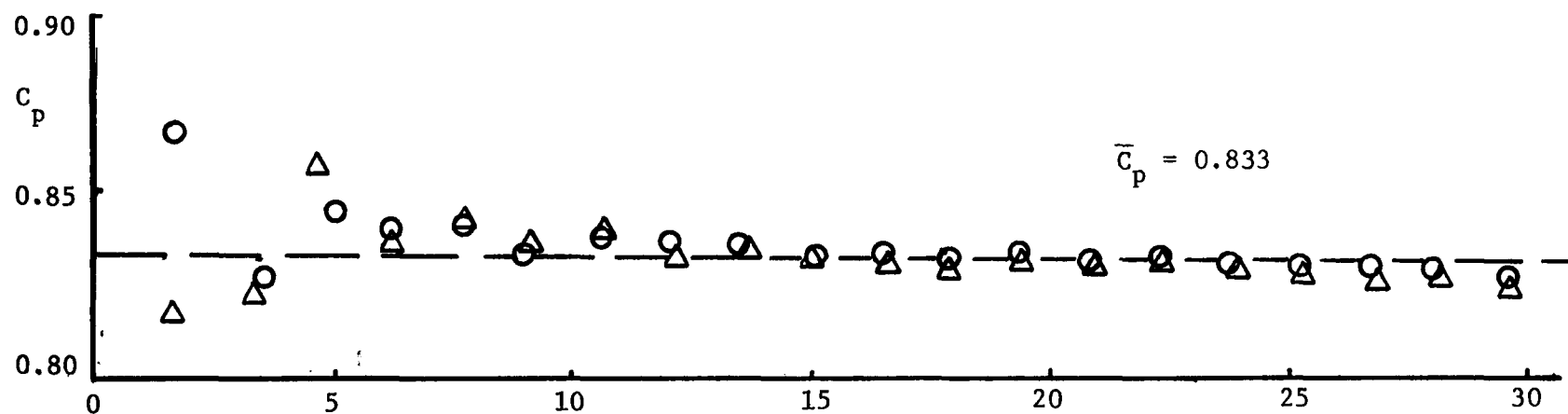


FIGURE 7. Pitot Coefficient Versus Velocity for S-Type Pitot Number 3-01

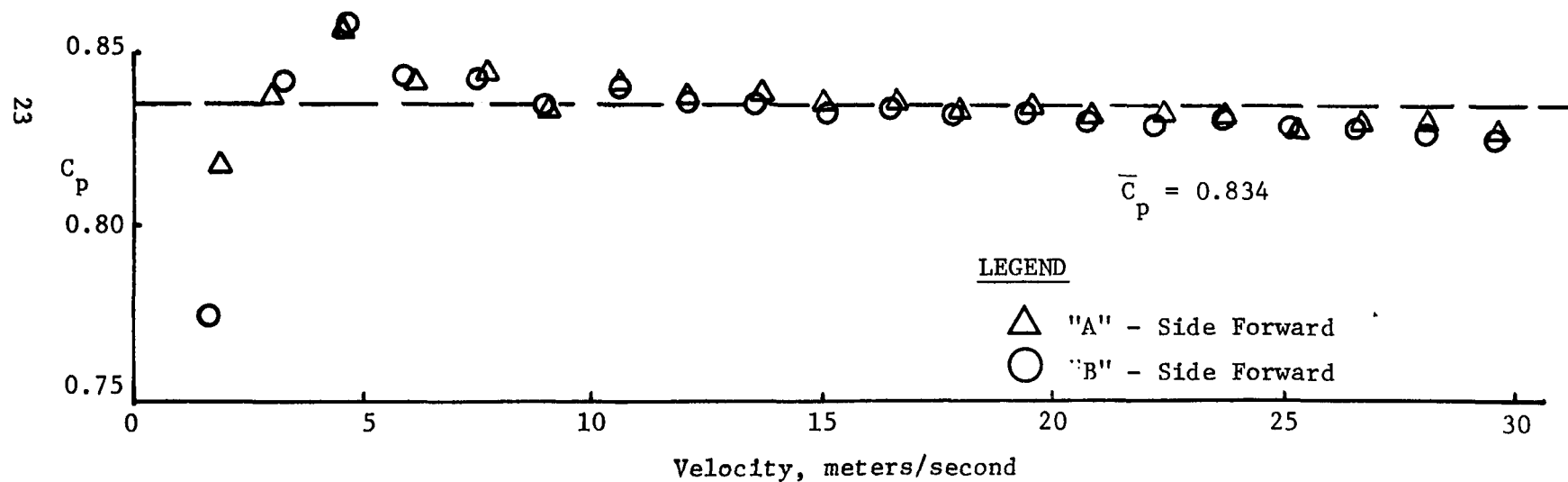


FIGURE 8. Pitot Coefficient Versus Velocity for S-Type Pitot Number 3-02

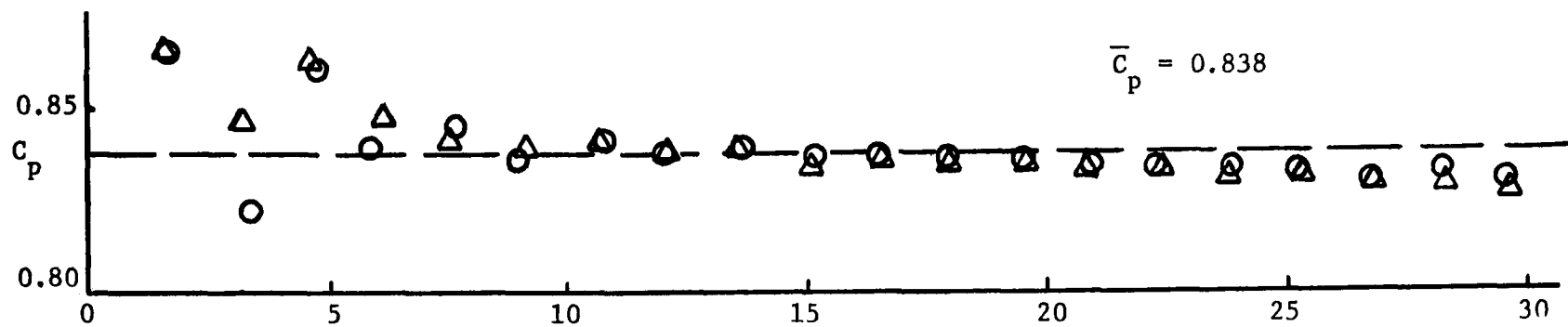


FIGURE 9. Pitot Coefficient Versus Velocity for S-Type Pitot Number 3-03

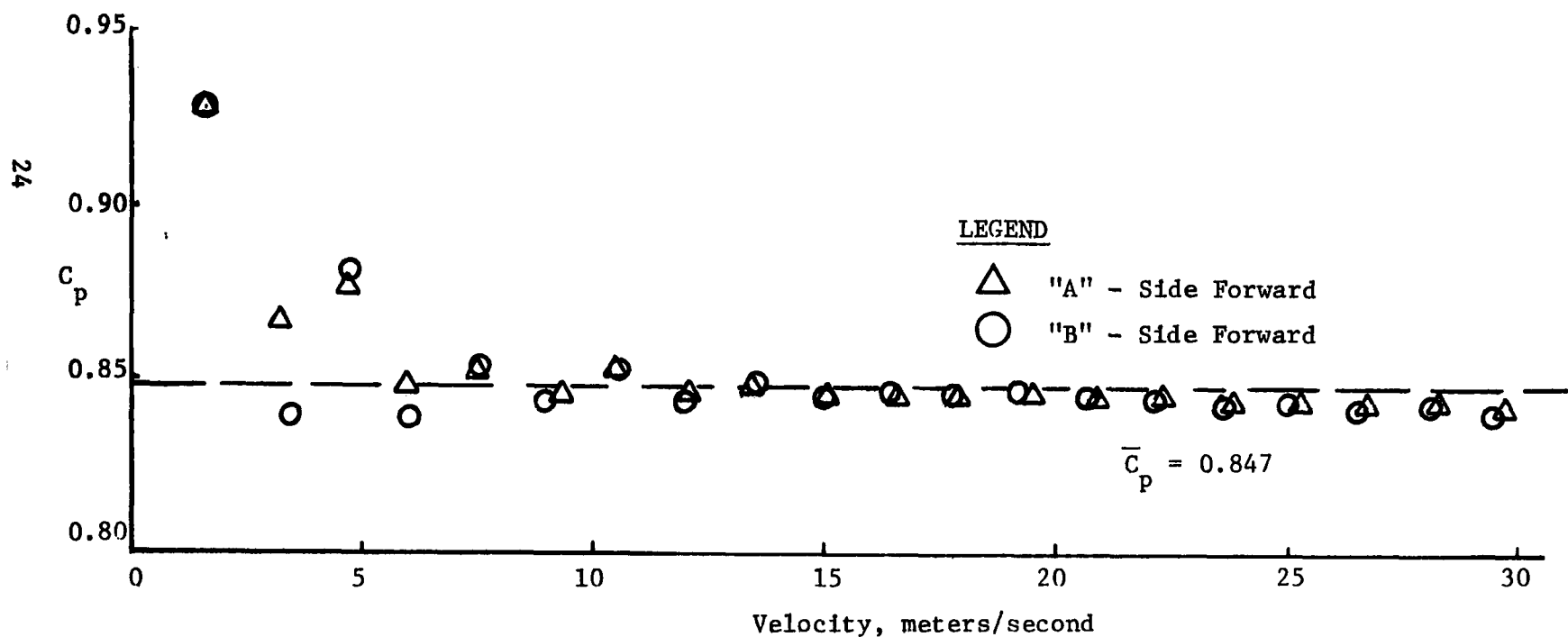


FIGURE 10. Pitot Coefficient Versus Velocity for S-Type Pitot Number 3-04

S-type pitot tubes with spacers were slightly lower than those for tubes that had an identical port-to-port dimension but did not have a spacer.

Also, it was found that filling the gap produced by the spacers placed between the two legs of the tubes being tested did affect the average pitot coefficient. That is, when the gap region was filled by taping the two legs of the tubes together the taped pitot gave an average pitot coefficient higher than that for the same pitot without tape. However, the pitot coefficients for the taped tubes were found to be approximately equal to those for S-type pitot tubes having the same port-to-port dimension and no inter-tube spacing.

It is possible to determine the overall effect of changes in geometry by comparing the average pitot coefficients for the 14 tubes tested. The average pitot coefficient \bar{C}_p for the tubes tested, is presented in Figure 11 as a function of the nondimensional port-to-port spacing $(P-P)/W$ where W is the outside diameter of the pitot legs. The nondimensional inter-tube spacing S/W for each test is denoted by the symbol used. (The two flagged symbols in Figure 11 represent the results of special tests in which the gap between the legs of the S-type pitot tube was enclosed by wrapping tape around the legs of the tubes.) From Figure 11 it is clear that there is no discernible trend of the average pitot coefficient with variation of either port-to-port spacing or inter-tube spacing. Any variation due to changes in these dimensions is so small that it is masked by the data scatter. The data scatter is remarkably small, being no more than 2.5 percent. One is forced to conclude that for the range of port-to-port spacings and inter-tube spacings tested, the average pitot coefficient is essentially independent of either of these geometric dimensions.

INTERFERENCE EFFECTS - ZERO SAMPLING RATE

A number of tests were conducted to determine the effect on the S-type pitot tube of locating a sampling probe with nozzle close to the S-type pitot tube. These tests were conducted using tube 3-01. Figures 12, 13, and 14 show the variation of the average pitot coefficient with the centerline to centerline distance between the S-type pitot tube and the sampling probe with no flow through the sampling probe (zero sampling rate). In these and subsequent figures, the average pitot coefficient has been normalized by the average pitot coefficient for the S-type pitot tube alone, $\bar{C}_{p\infty}$, and the centerline to centerline distance, C-C, has been normalized by the diameter of the legs in the S-type pitot tube, W .

Figure 12 shows the effects with three different sampling probe nozzle diameters of centerline to centerline spacing on the average pitot coefficient, for the case where the inter-tube spacing is zero. In general, for the two smaller nozzles the average pitot coefficient for small centerline to centerline distances is below the average pitot coefficient for the S-type tube alone, $\bar{C}_{p\infty}$. As the centerline to centerline distance was increased (by moving the sampling probe), the average pitot coefficient increased to some one to two percent larger than the average coefficient for the S-type pitot tube alone, $\bar{C}_{p\infty}$ (at centerline to centerline distances greater than ten tube diameters). For the largest sampling probe nozzle inside diameter (0.0127 m [0.5 in]) the average pitot coefficient at all centerline to centerline

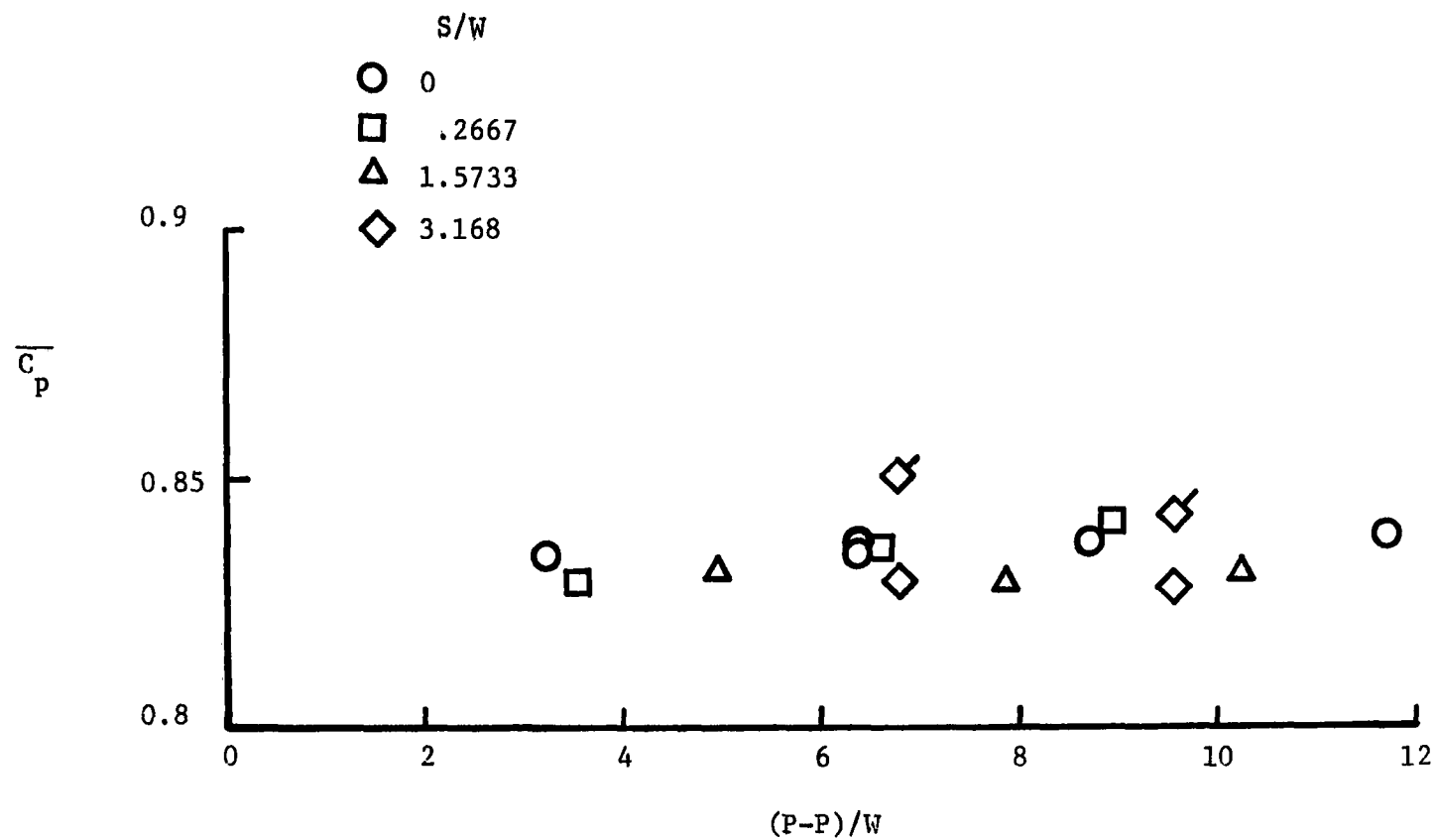


FIGURE 11. Effects of Port-to-Port Spacing and Inter-Tube Spacing on the Average Pitot Coefficient.

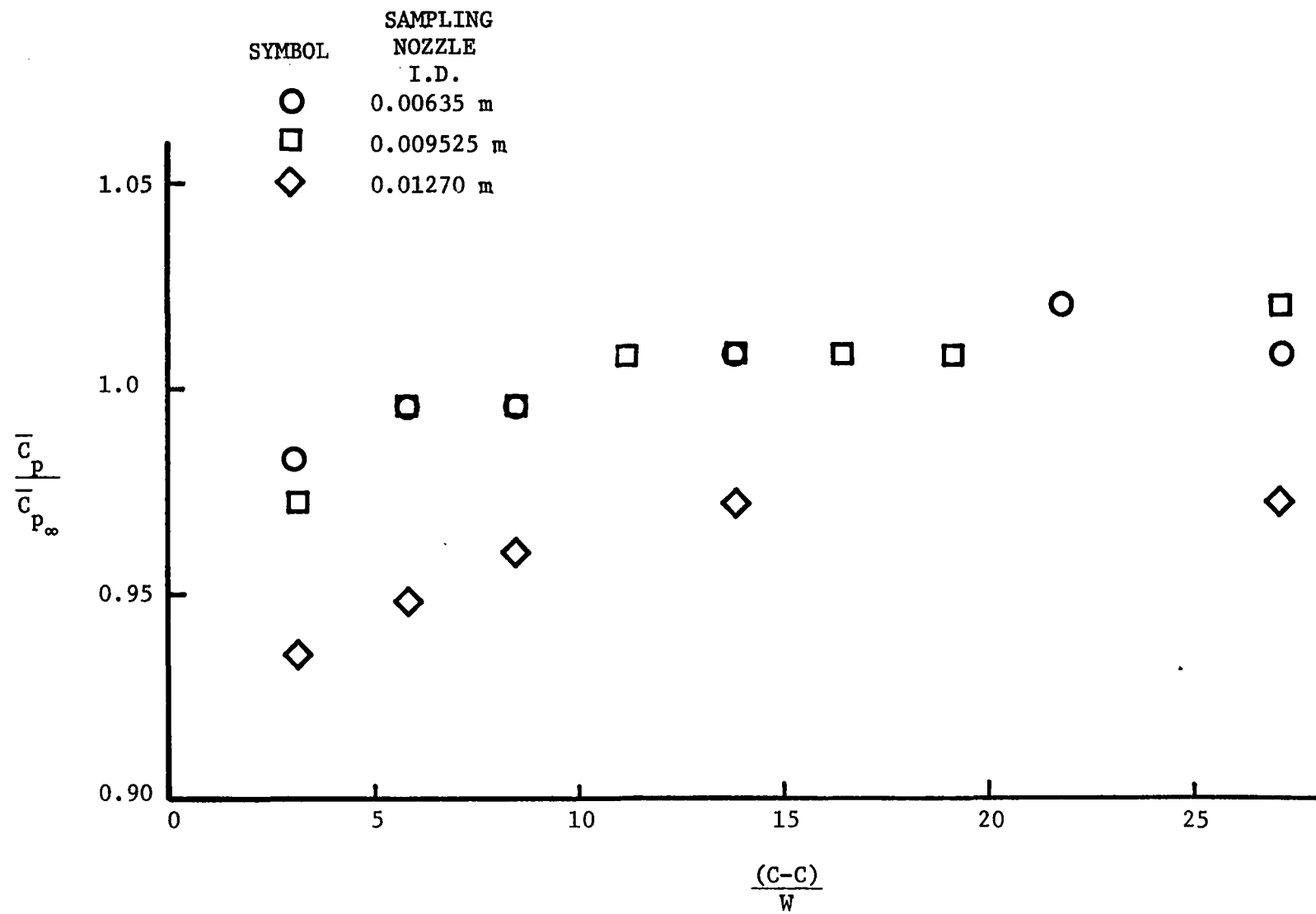


FIGURE 12. Interference Effects on an S-Type Pitot Tube, Sampling Rate = 0, Inter-tube Spacing = 0.

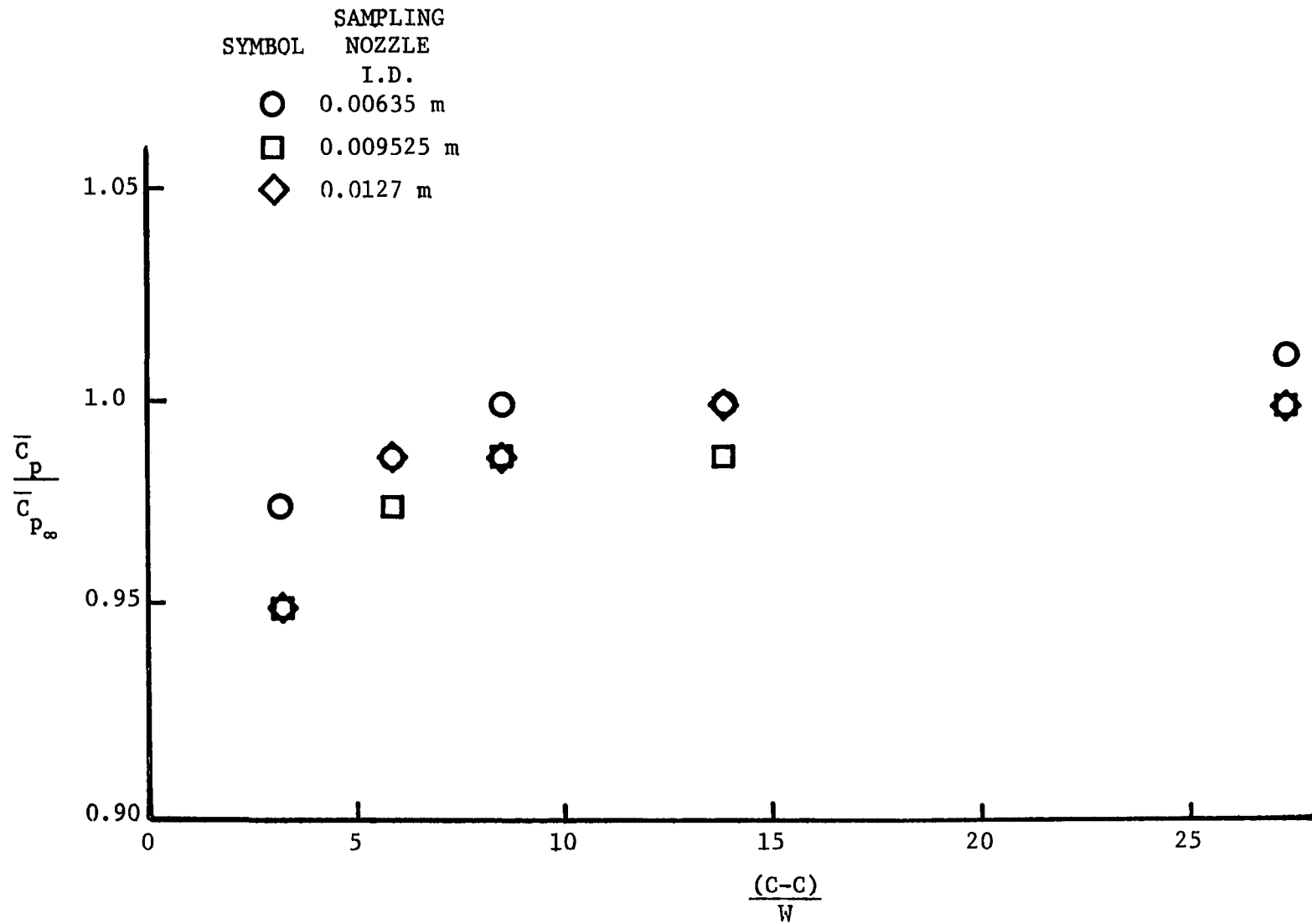


FIGURE 13. Interference Effects on an S-Type Pitot Tube, Sampling Rate = 0, Inter-tube Spacing = 0.01499 m.

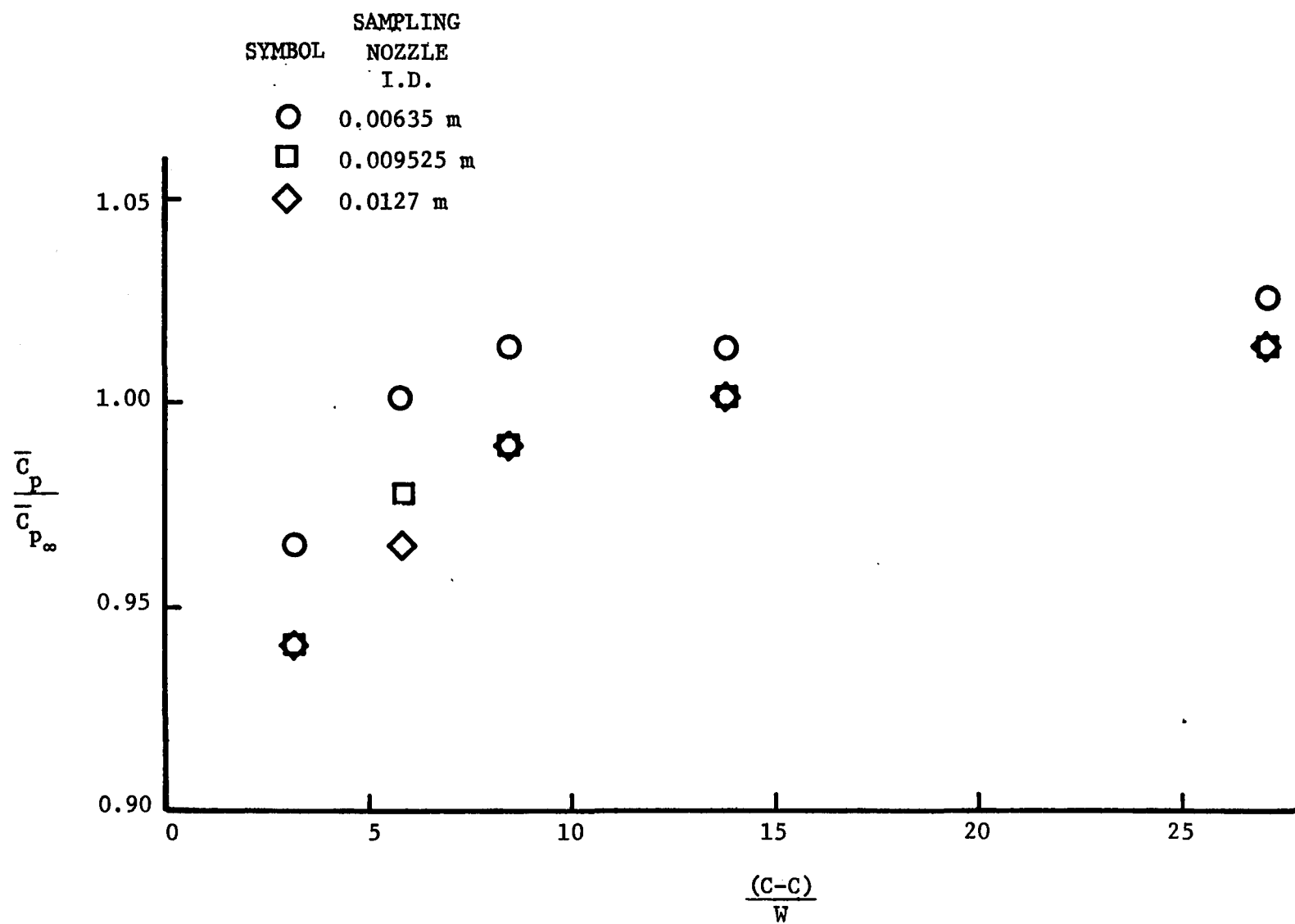


FIGURE 14. Interference Effects on an S-Type Pitot Tube, Sampling Rate = 0, Inter-tube Spacing = 0.03018 m.

distances is less than the average pitot coefficient for the S-type pitot tube alone.

A comparison of Figures 12, 13, and 14 shows the effect of inter-tube spacing on interference. For an inter-tube spacing of 0.01499 m (0.59 in) the interference effects seem to be minimized, but for a larger inter-tube spacing 0.03018 m (1.188 inches) the effects seem to be of the same order as those for zero inter-tube spacing. It is difficult to reach any definite conclusion regarding the effect of inter-tube spacing since the effects seem to be small and of the same order as the data scatter, particularly for large centerline-to-centerline distance. It is clear, however, that for centerline-to-centerline distances of less than ten diameters of the pitot tube leg, the average pitot coefficient is less than the average pitot coefficient for the S-type pitot tube alone. Further, this effect is largest for the larger sampling probe diameters.

INTERFERENCE EFFECTS - SAMPLING AT 0.85 x ISOKINETIC AND ISOKINETIC RATES

Figures 15 and 16 show the interference effects obtained while sampling at a rate of 0.85 x isokinetic and Figure 17 shows the interference effects obtained while sampling at the isokinetic flow rate. Again these tests were conducted using S-type pitot tube 3-01. Comparison of Figures 12 through 17 shows the total effect of sampling at various flow rates on the interference between the sampling probe and the S-type pitot tube. It is apparent that sampling tends to reduce the interference effects and that this reduction in interference appears most drastic when sampling at a rate of 0.85 x isokinetic with an S-type pitot tube with zero inter-tube spacing (Figure 15). However, the effects in all cases seem quite small, on the order of three or four percent.

INTERFERENCE EFFECTS - MISALIGNMENT OF S-TYPE PITOT TUBE, SAMPLING PROBE COMBINATION

A few additional tests were conducted to determine the magnitude of the interference when the S-type pitot tube and the sampling probe were not inserted the same distance into the wind tunnel. These tests were conducted using S-type pitot tubes 3-01 and 3-02. Typical results for three positions of the sampling probe relative to pitot tube 3-01 are shown in Figure 18 for the variation of the ratio $\bar{C}_p/\bar{C}_{p\infty}$ with $(C-C)/W$. In all three positions the nose of the sampling nozzle (1.27 cm I.D.) was in the same plane as the nose of the S-type pitot tube. The circular symbols represent the case where the sampling probe is inserted into the wind tunnel the same distance as the S-type pitot tube. The square symbols represent the case where the sampling probe is inserted into the wind tunnel 0.0508 m (2 in) behind the S-type pitot tube and the diamond symbols represent the case where the S-type pitot tube is inserted into the wind tunnel 0.0508 m (2 in) beyond the sampling probe. Clearly the interference effects are smaller when the sampling probe is inserted into the air stream less than the S-type probe. Additional studies were conducted using pitot tube 3-01 with 0.635 cm and 0.953 cm I.D. nozzles. The results from this additional study and from analogous studies using pitot 3-02 were similar to those shown in Figure 18. These additional studies on pitot/nozzle misalignment are reported in Reference 2.

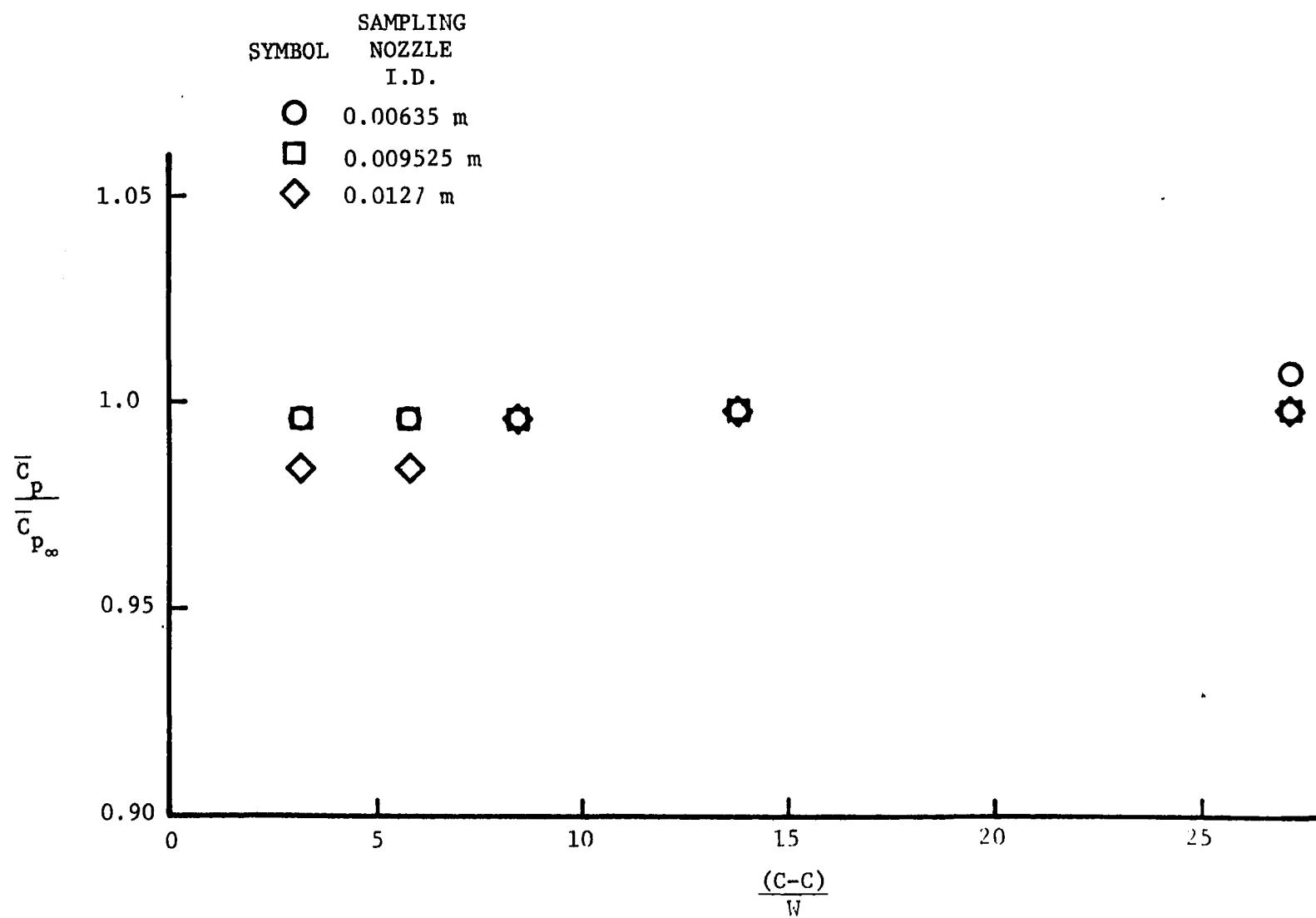


FIGURE 15. Interference Effects on an S-Type Pitot Tube, Sampling Rate = 0.85 x Isokinetic, Inter-tube Spacing = 0.

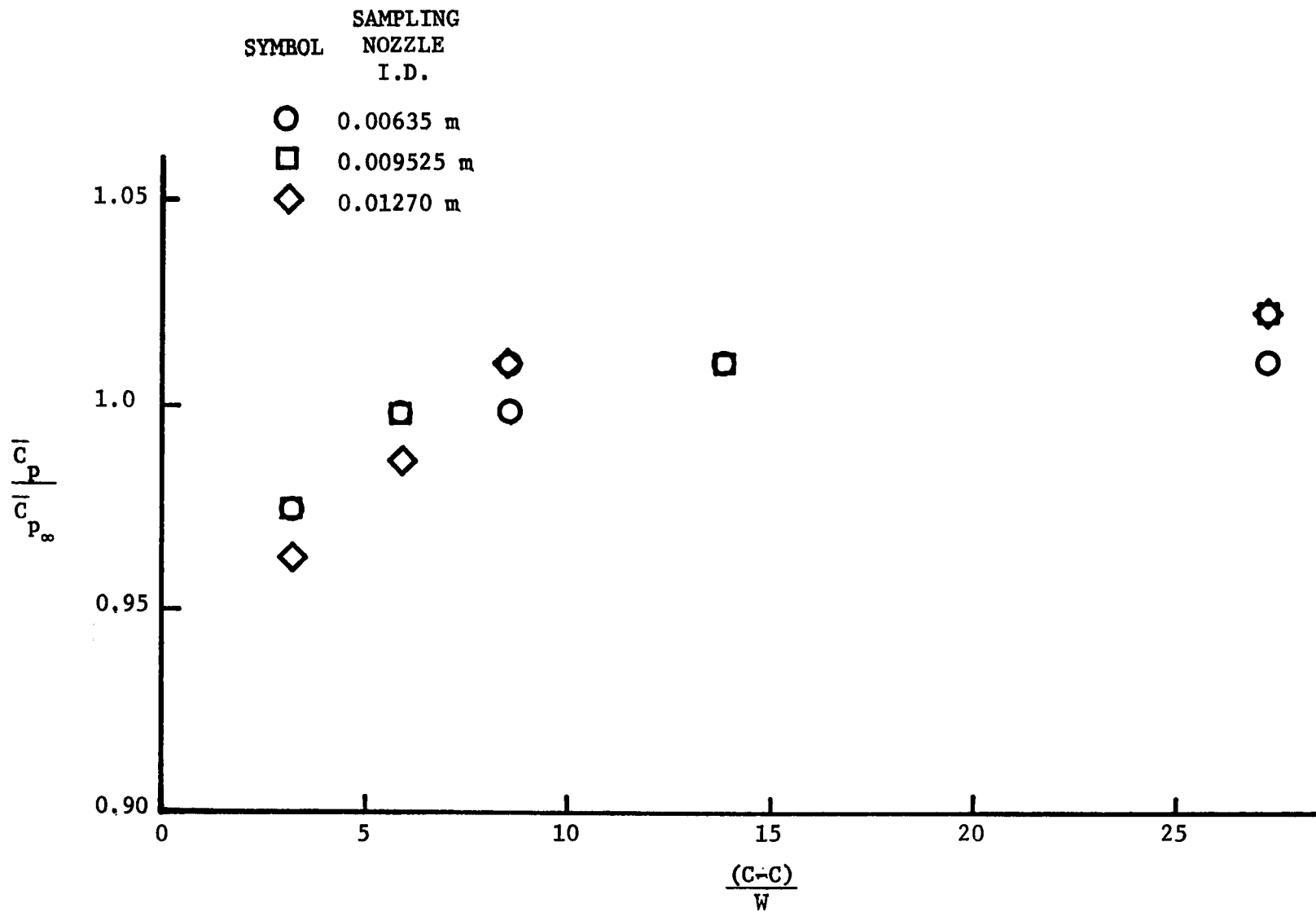


FIGURE 16. Interference Effects on an S-Type Pitot Tube, Sampling Rate = 0.85 x Isokinetic, Inter-tube Spacing = 0.01499 m.

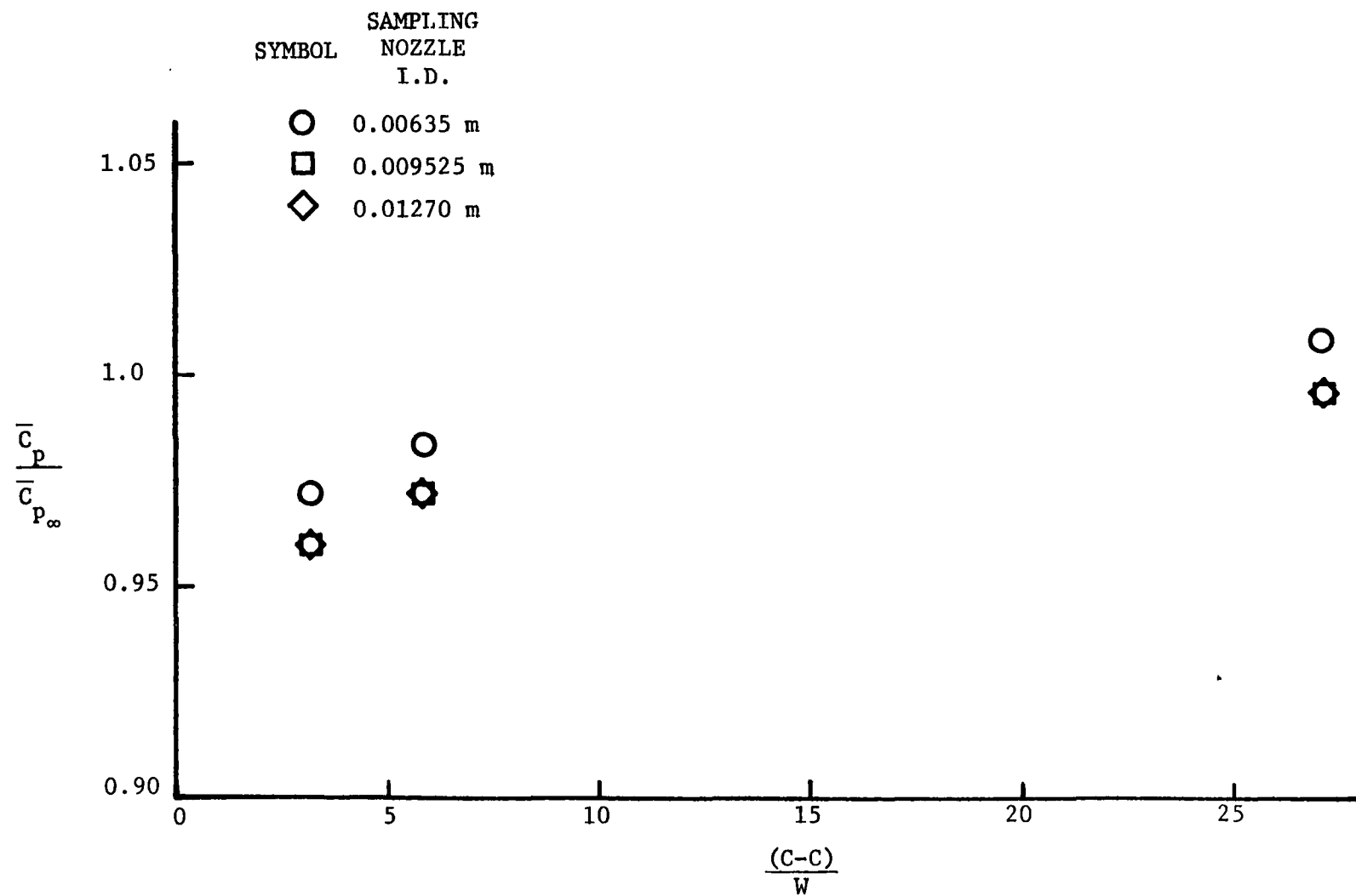


FIGURE 17. Interference Effects on an S-Type Pitot Tube, Sampling Rate = Isokinetic, Inter-tube Spacing = 0.

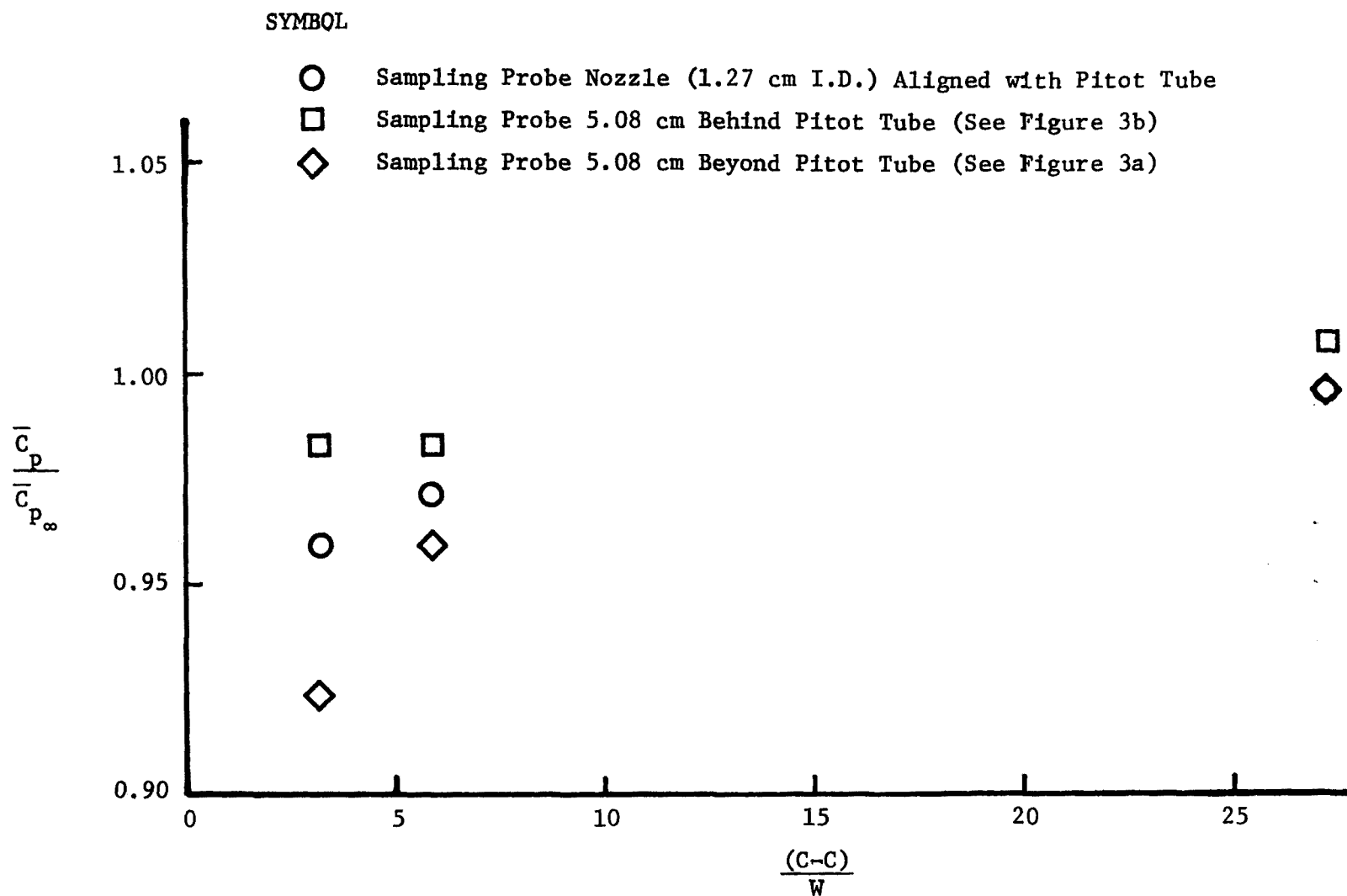


FIGURE 18. Effects of Misalignment of S-Type Pitot Tube (3-01 - Sampling Probe Combination, Sampling Rate = Isokinetic, Inter-tube Spacing = 0.

EFFECT OF YAW AND PITCH IN THE ABSENCE OF A SAMPLING NOZZLE

The results of the yaw tests without interference are presented in Figures 19, 20, and 21. These figures show the relationship between pitot coefficient and the angle of yaw for each particular S-type pitot tube tested. An analysis of the figures show that, for each pitot tube, tunnel speed has no significant affect on this relationship. This means that the four figures for each pitot tube may be averaged together. The result is a single curve that is representative of all the curves for that tube. The averaged curves for the three different S-type pitot tubes are presented in Figure 22.

For S-type pitot tube 4-10, the pitot coefficient has a maximum value of 0.855 in the 0° yaw position. This is a difference of 0.6 percent from the accepted value of 0.85. On the other hand, one finds that for S-type pitot tube 3-04, C_p is at its minimum value (0.846) in the 0° yaw position. The averaged curve for S-type pitot tube 3-01 is somewhat erratic and notably lacking in symmetry, possibly due to dents and nicks caused by handling. It is observed that C_p reaches a maximum value at a yaw angle of about 5° while its value in the 0° yaw position is 0.829.

From these figures it is seen that the necessary range of yaw angles needed to insure that C_p lie within five percent of 0.85 depends on the particular S-type pitot tube. For pitot tube 4-10 this range extends from -9° to 9° . Figure 22 shows that S-type pitot tube 3-04 is relatively insensitive to yaw. From this figure it is found that S-type pitot tube 3-04 can undergo a full $\pm 30^\circ$ yaw and still easily maintain C_p within five percent of 0.85. More specifically, C_p never differs from 0.85 by more than 3.88 percent. With S-type pitot tube 3-01, the acceptable yaw range is from -25° to 25° .

Figures 23, 24, and 25 represent the results of the pitch tests with no interference. As in the case of yaw without interference, an analysis of the data reveals that the performance of any specific pitot tube is nearly independent of the tunnel velocity. Consequently the curves can be averaged together, allowing each S-type pitot to be represented by only one performance curve. For purposes of comparison, these averaged graphs are all presented together in Figure 26.

The basic shape of the curve representing pitot tube 4-10 is that of a "check mark" with its vertex (the minimum point) occurring at about 6° pitch. The value of C_p at 0° pitch is of particular interest. From Figure 26 it is found that this value, 0.852, is within 0.24 percent of the assumed value of 0.85. It is also seen that within five percent accuracy, the pitot tube may be pitched from -6° to 20° .

The characteristic curve for S-type pitot tube 3-04 shows that the pitot coefficient is nearly insensitive to pitch angles from -10° to 20° . Also, the pitot coefficient does not exceed the five percent tolerance from -20° to 20° .

Unlike the averaged curves for S-type pitot tubes 4-10 and 3-04, the characteristic curve for S-type pitot tube 3-01 cannot be represented by two straight line segments. In order to keep the pitot coefficient within a five percent tolerance, this pitot tube can only be pitched in a range going from

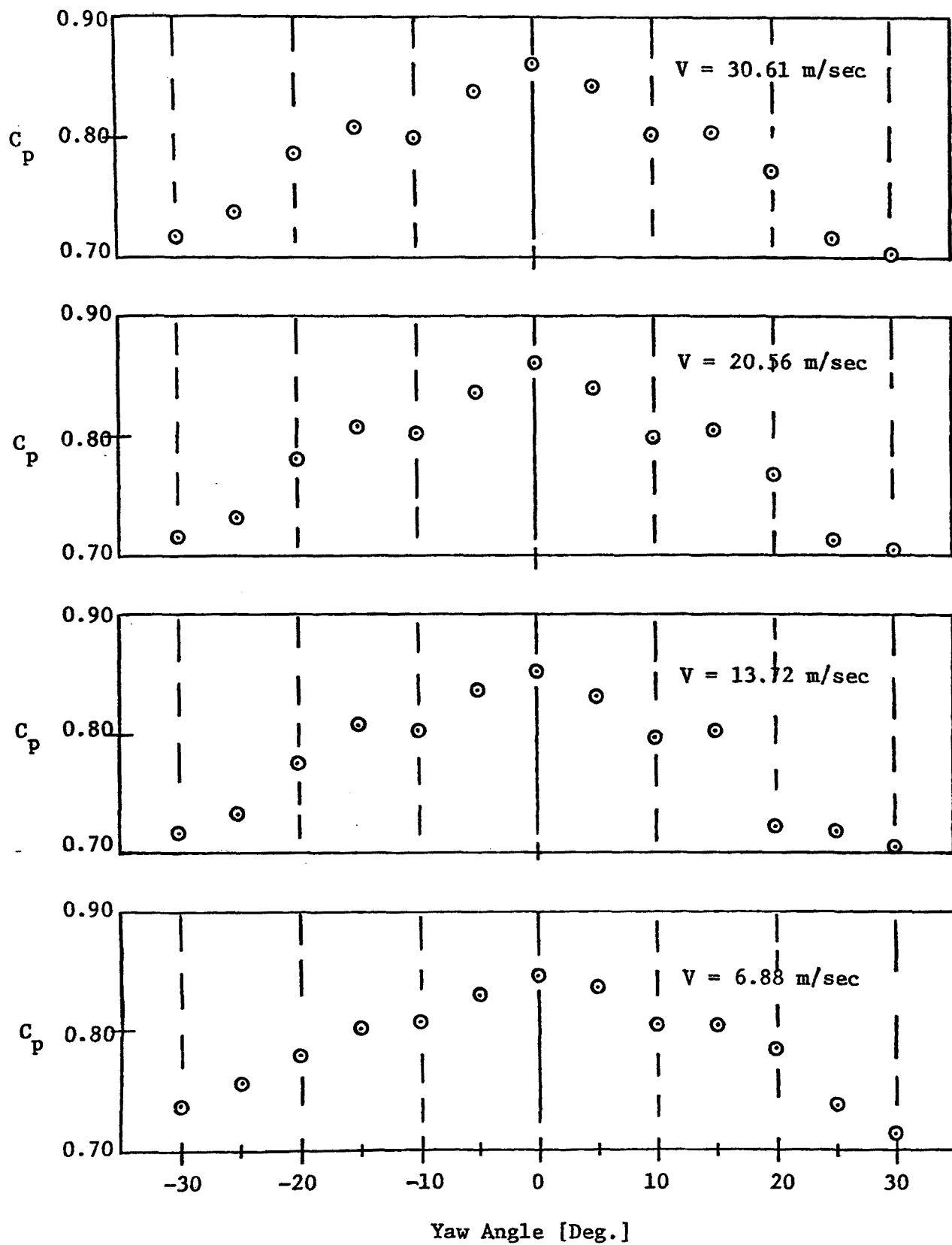


FIGURE 19. Effect of Yaw on S-Tube 4-10

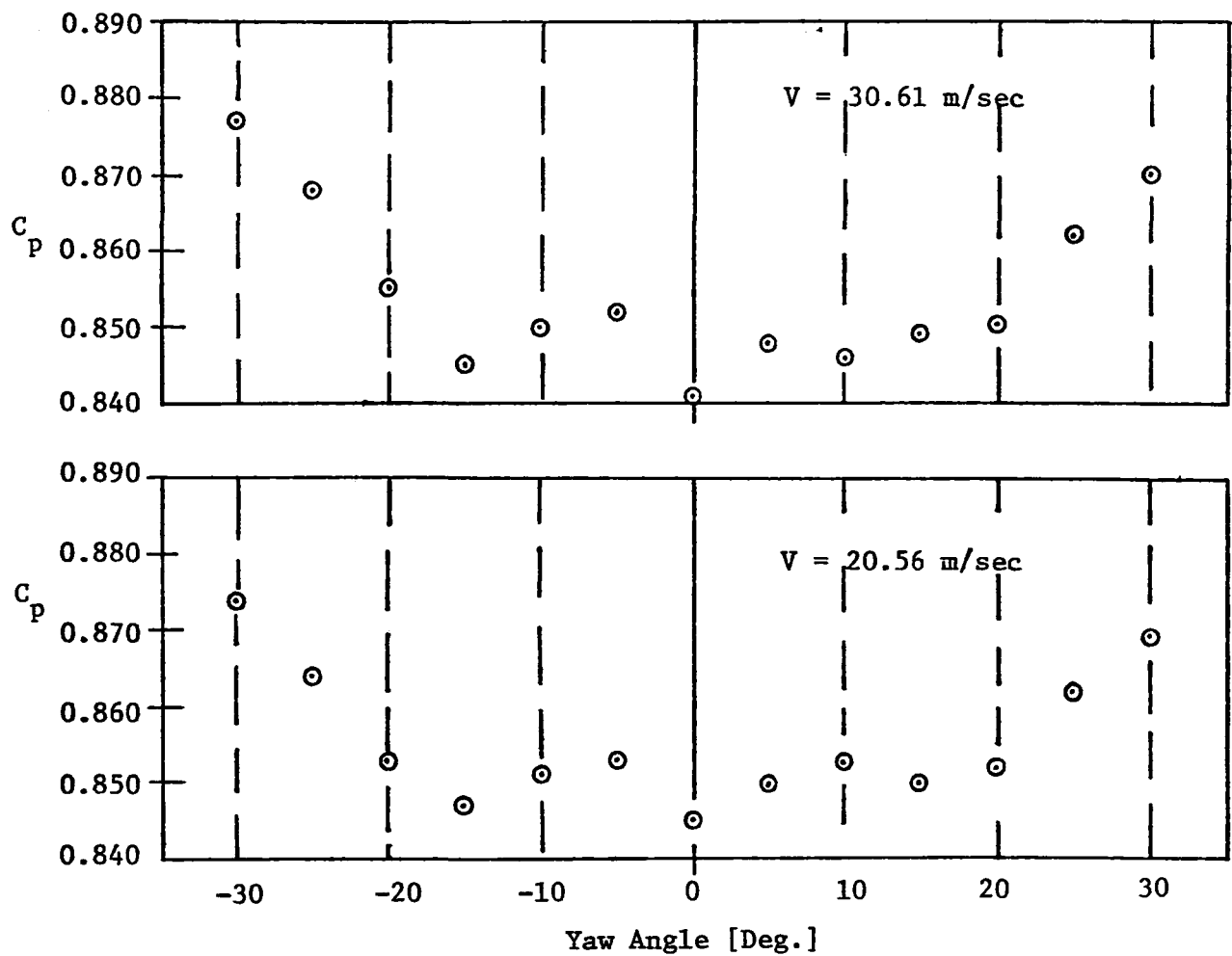


FIGURE 20. Effect of Yaw on S-Tube 3-04

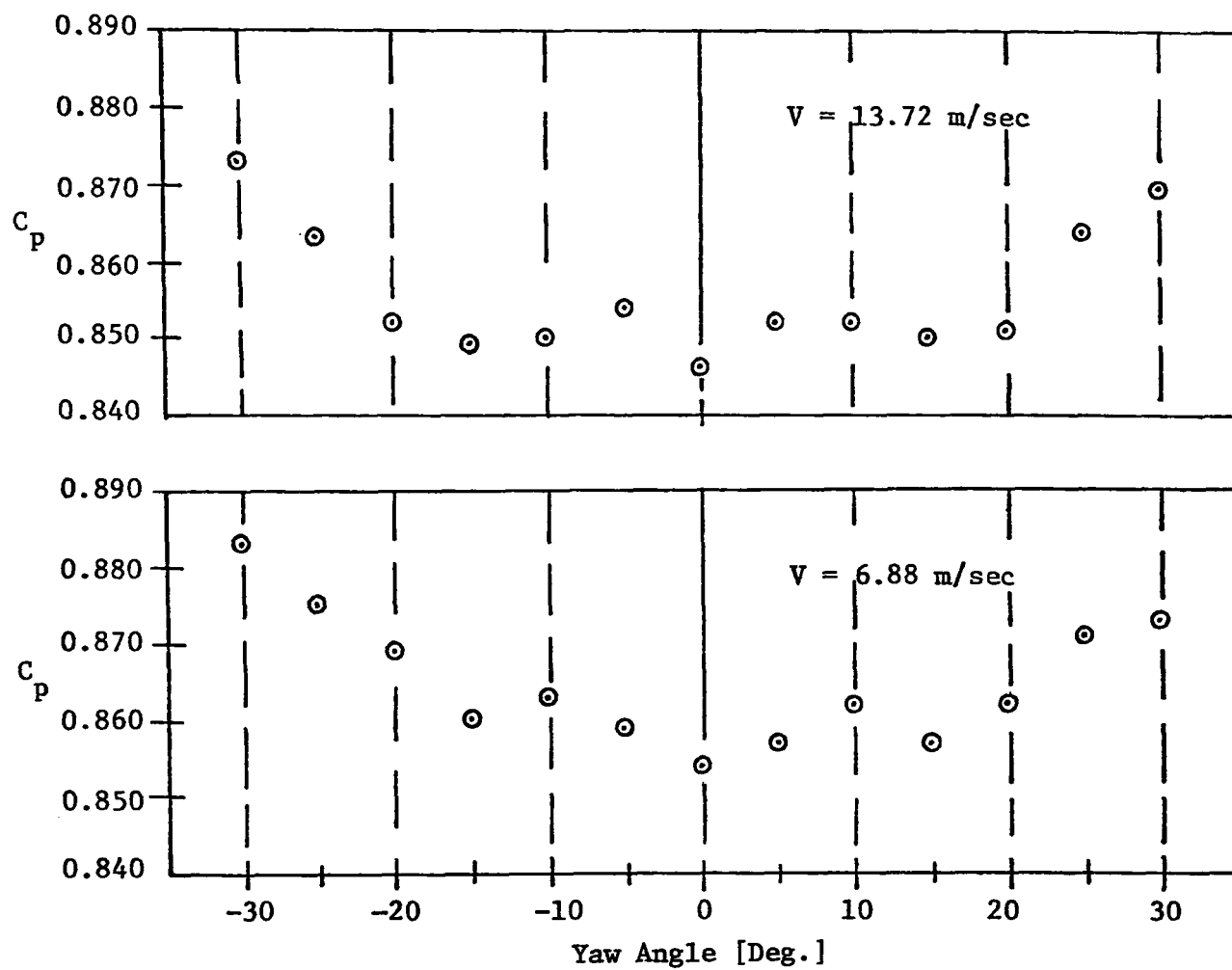


FIGURE 20. Continued

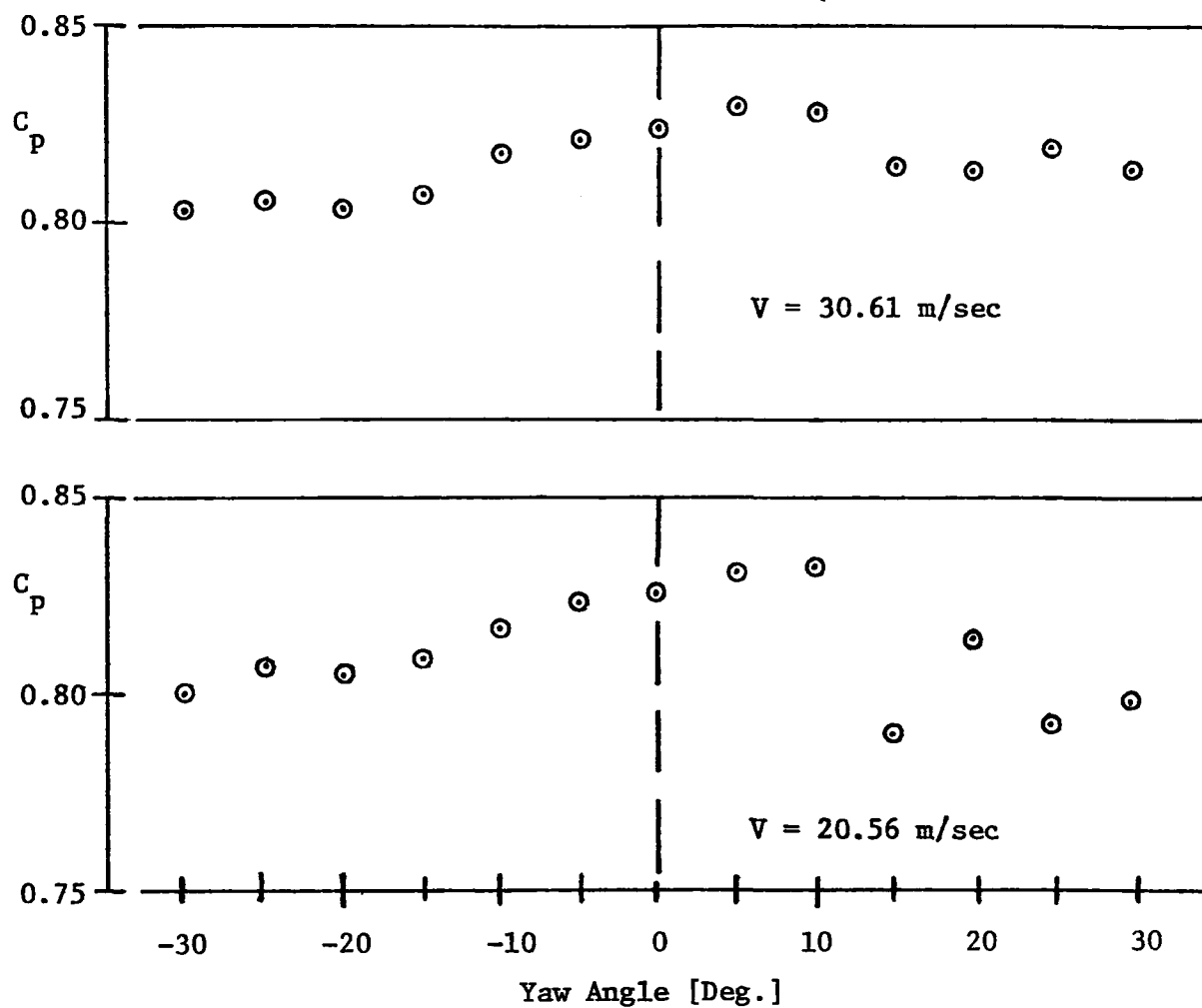


FIGURE 21. Effect of Yaw on S-Tube 3-01

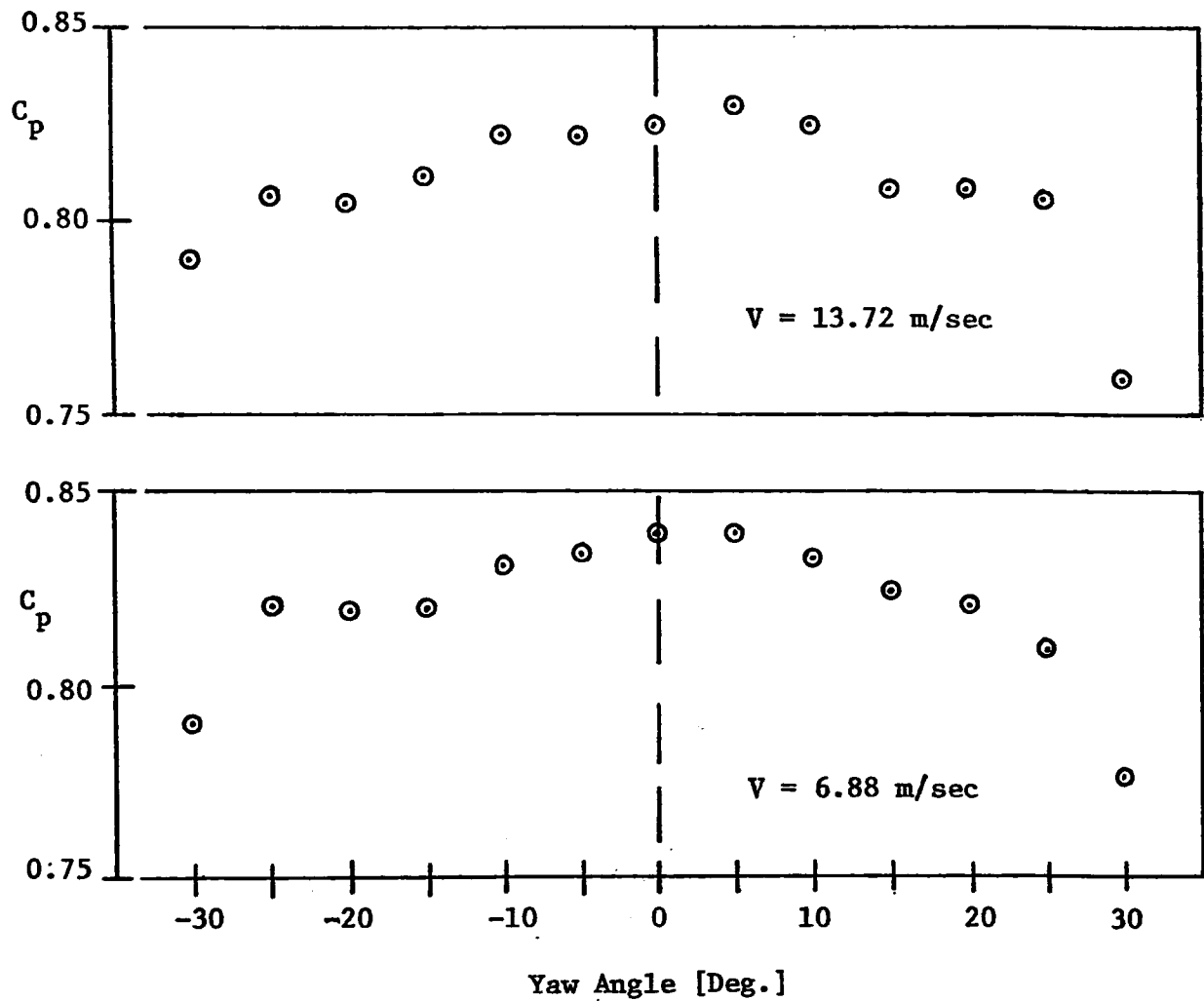


FIGURE 21. Continued

LEGEND

○ S-tube 4-10

□ S-tube 3-04

△ S-tube 3-01

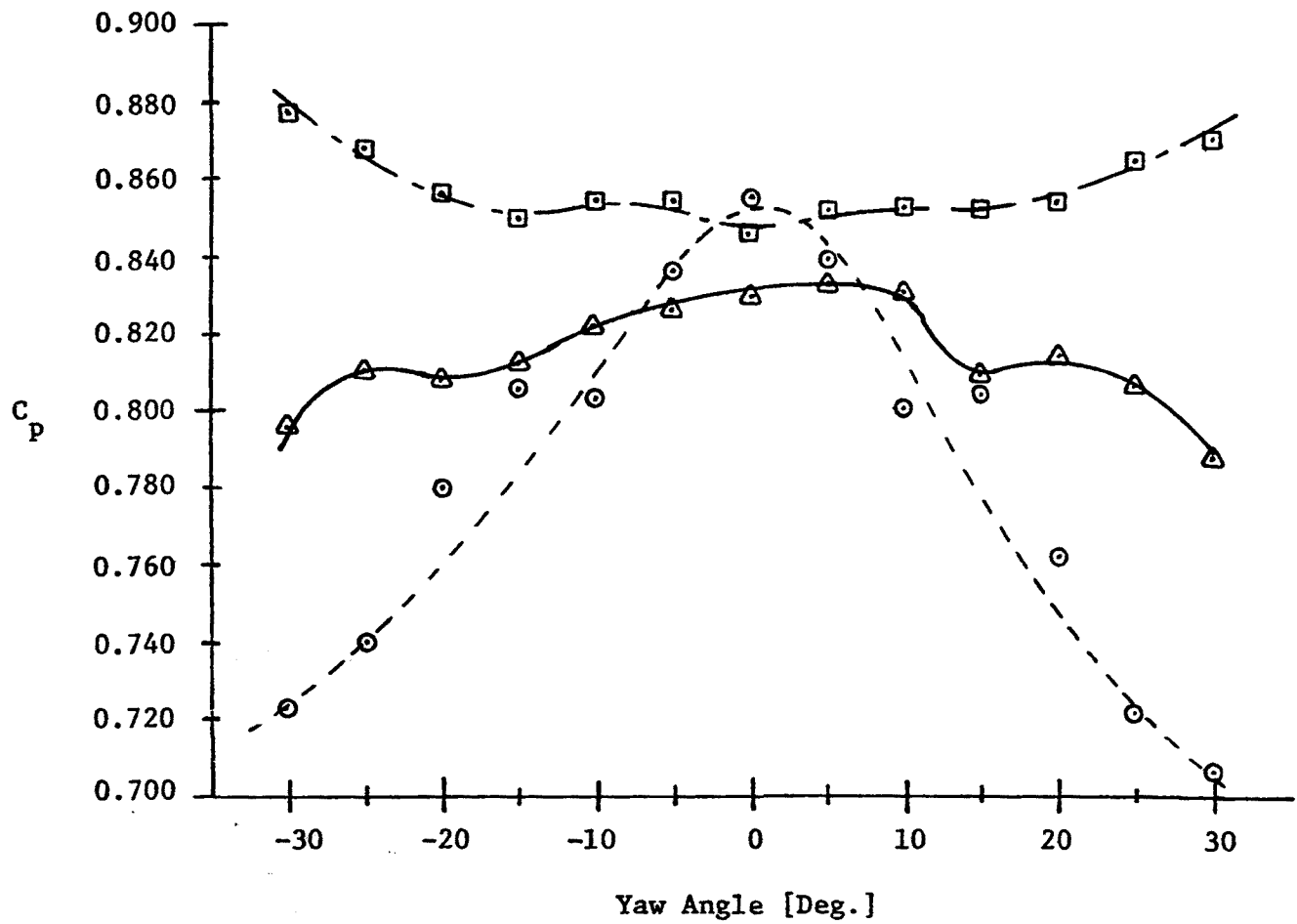


FIGURE 22. Averaged Effect of Yaw

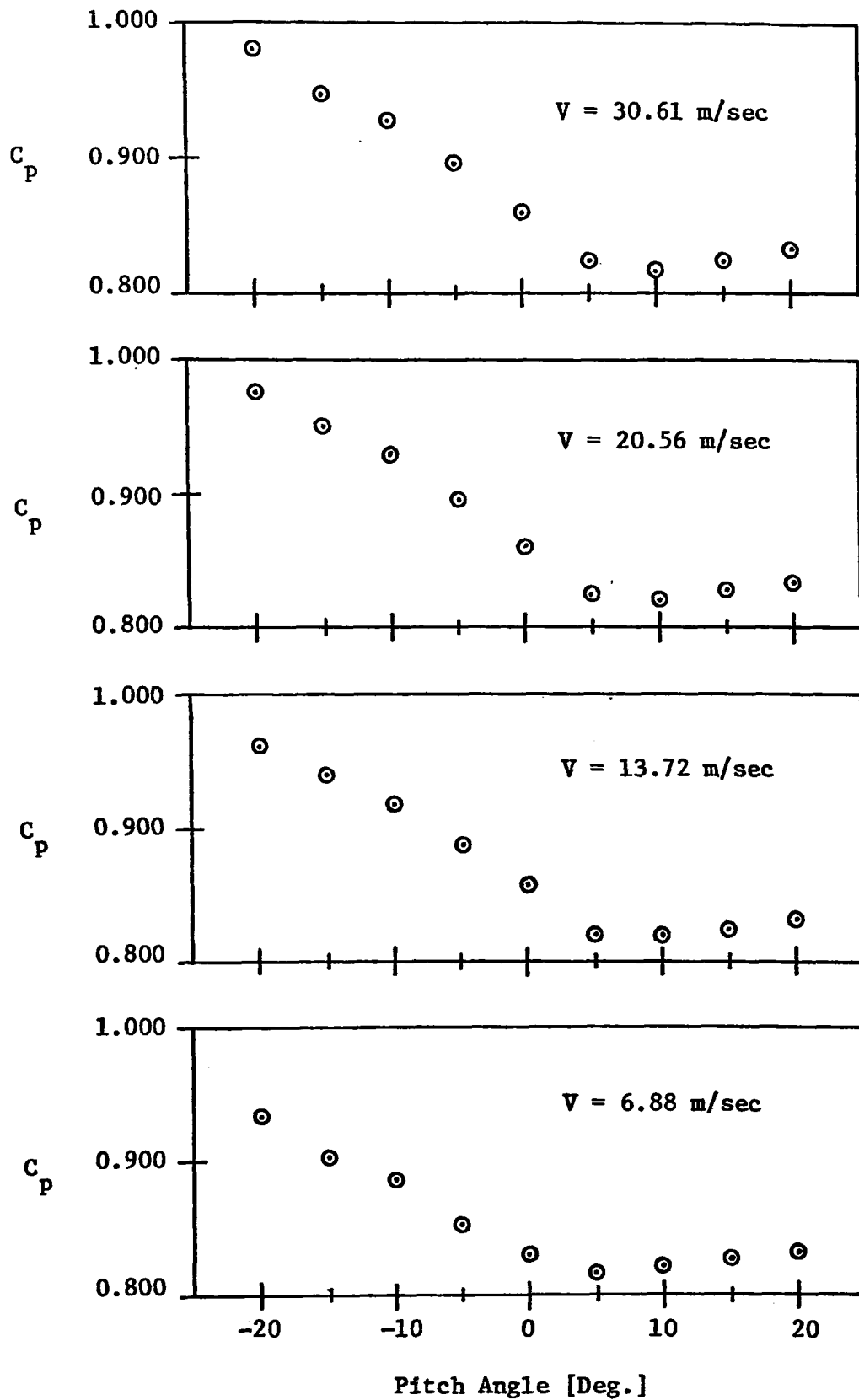


FIGURE 23. Effect of Pitch on S-Tube 4-10

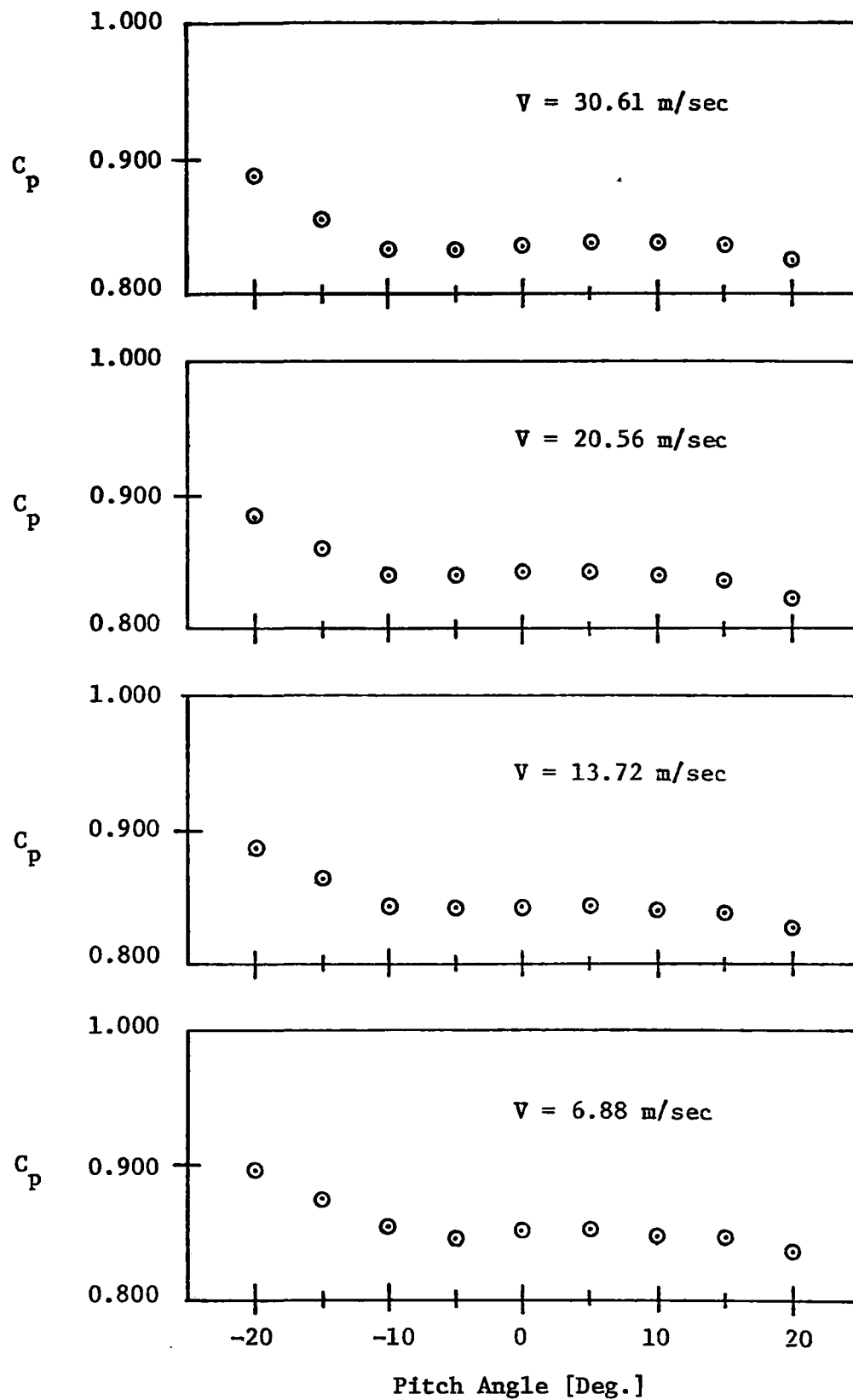


FIGURE 24. Effect of Pitch on S-Tube 3-04

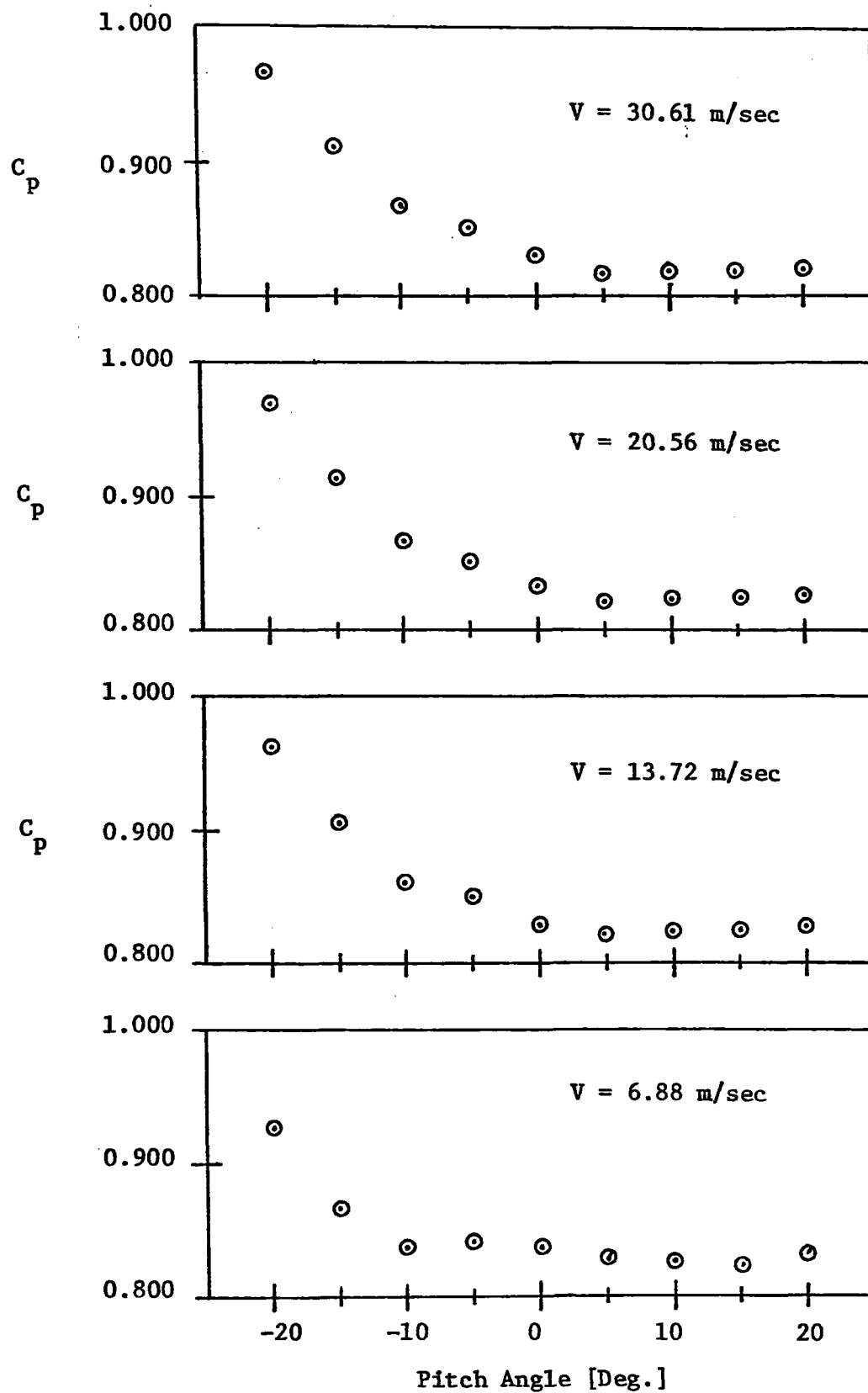


FIGURE 25. Effect of Pitch on S-Tube 3-01

L E G E N D

○ S-tube 4-10

□ S-tube 3-04

△ S-tube 3-01

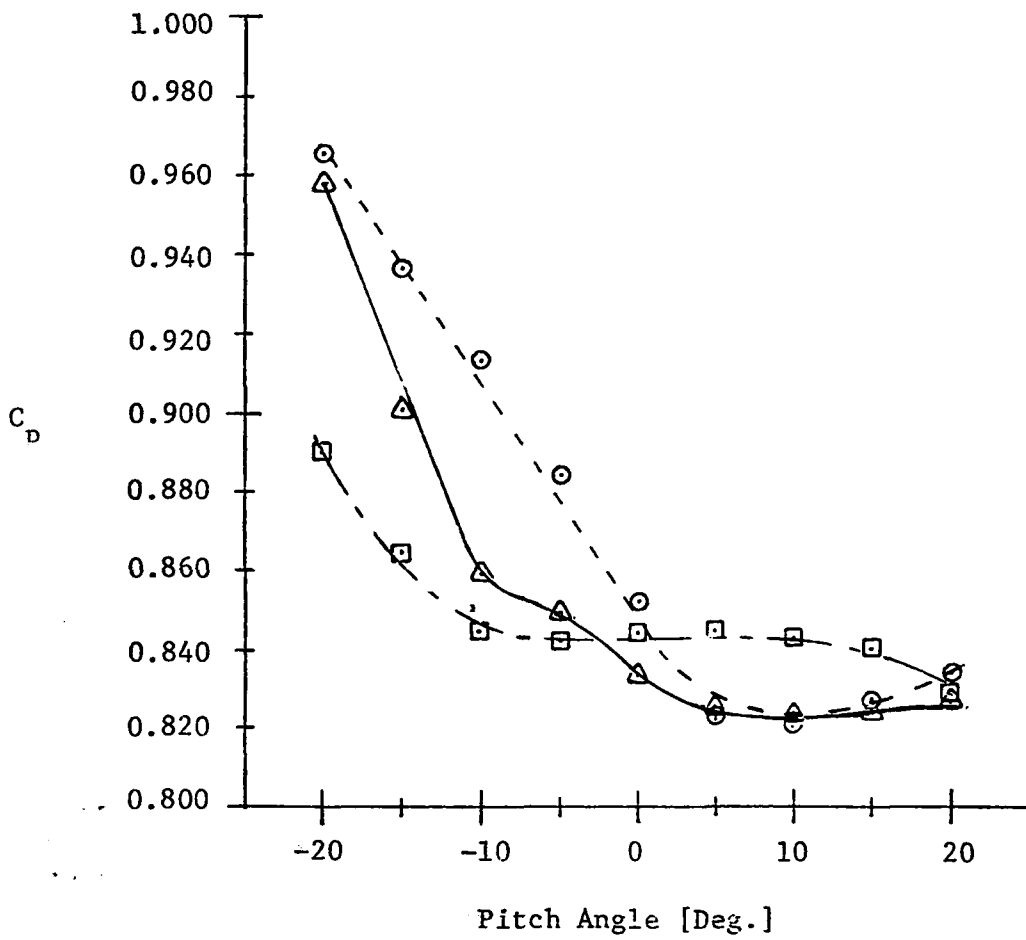


FIGURE 26. Averaged Effect of Pitch

-14° to 20°. As mentioned earlier, this pitot tube was damaged slightly which could account for the difference from the other pitot tubes.

EFFECT OF YAW WITH INTERFERENCE

Figures 27, 28, 29, and 30 show the relationship between pitot coefficient and angle of yaw for the various speeds and flow rates tested. A comparative analysis shows that for any given flow rate, the tunnel velocity has very little effect on the performance of the S-type pitot tube. (That is, for a specific flow rate, changes in the tunnel velocity do not significantly alter the relationship between C_p and the angle of yaw.) A similar analysis also reveals that the functional relationship between pitot coefficient and yaw angle is insensitive to changes in the sampling probe flow rate. This means, in effect, that the 14 individual curves in Figures 27, 28, 29, and 30 are essentially one and the same. Hence, an averaging process can be applied to these curves to obtain a single curve that is representative of the entire set. For purposes of comparison, this single curve is presented along with the averaged curve for yaw without interference in Figure 31.

From Figure 31 it is observed that interference affects the yaw performance of S-type pitot tube 4-10 in an unsymmetrical fashion. Also, it is observed that the value for the pitot coefficient corresponding to 0° yaw is not within five percent of the desired value of 0.85. More importantly, however, the figures show that for the entire yawing range of $\pm 30^\circ$, C_p varies up to 12 percent of the 0.85 value. In the neighborhood of $\pm 20^\circ$, the presence of the sampling probe serves to diminish the value of the pitot coefficient, whereas at the higher yaw angles this condition is reversed.

EFFECT OF PITCH WITH INTERFERENCE

As in the case of yaw with interference, interference of the sampling probe also had to be considered in the pitch study. Figures 32 through 38 portray the relationship between pitot coefficient and angle of pitch for S-type pitot tube 4-10 at various tunnel speeds and sampling probe flow rates. An analysis of these figures shows that with respect to pitch the performance of this pitot tube is nearly independent of tunnel speed and sampling probe flow rate. Consequently, all the figures may be averaged to produce a single graph which describes the dependence of pitot coefficient on pitch angle. This graph is given in Figure 39 together with the averaged graph for pitch without interference.

Figure 39 shows that for pitch angles between -15° and 2°, the pitot coefficient is within five percent of the accepted value of 0.85. It is also observed that the pitot coefficient reaches a minimum value of 0.783 at the 10° pitch angle position. Hence, it is possible to pitch the pitot tube between -15° and 20° and never experience errors larger than 7.9 percent. For the entire range tested ($\pm 20^\circ$), the error is within 9.7 percent for S-type tube 4-10.

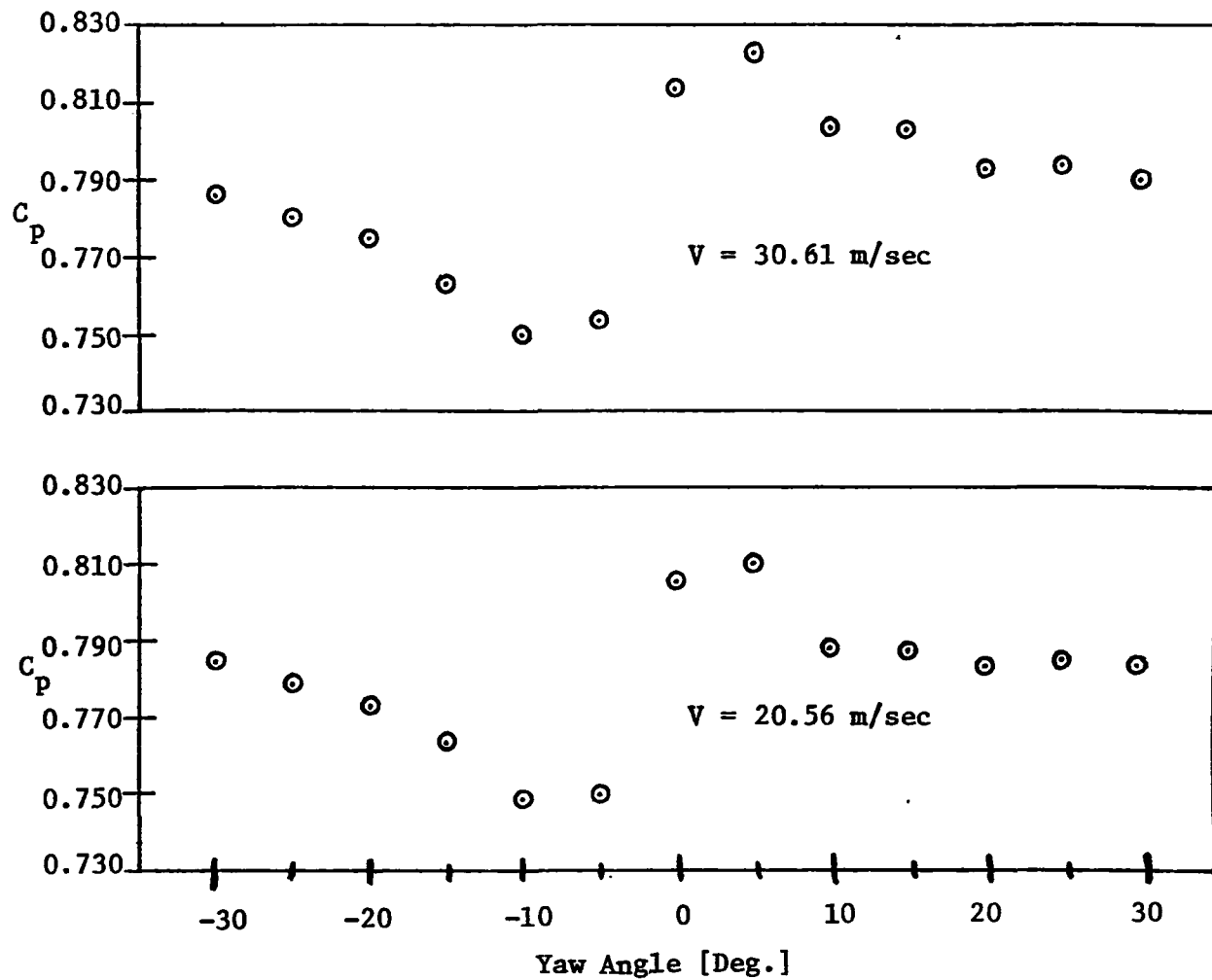


FIGURE 27. Effect of Yaw with Interference; Sampling Rate: $0.60 \times$ Isokinetic Flow Rate

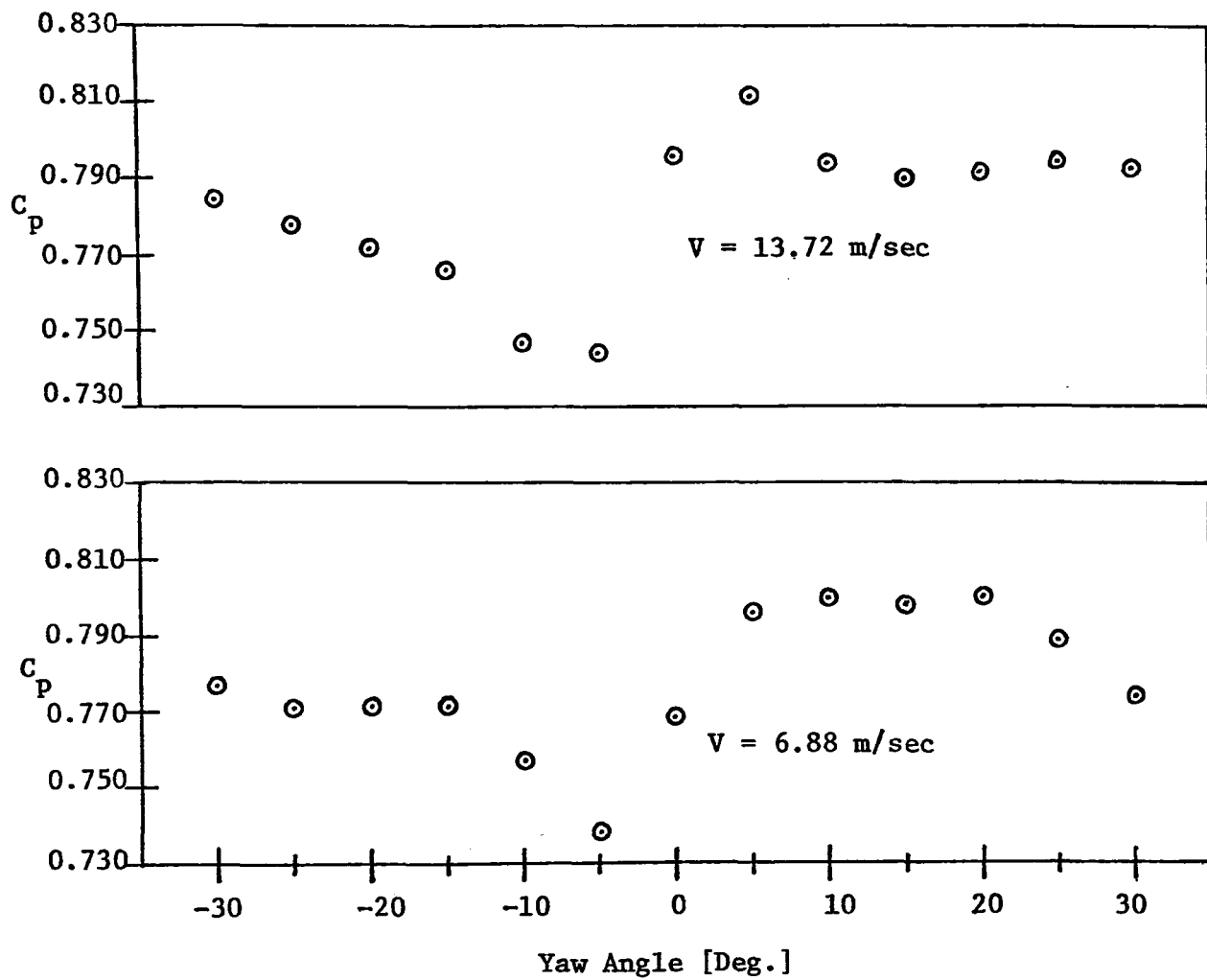


FIGURE 27. Continued

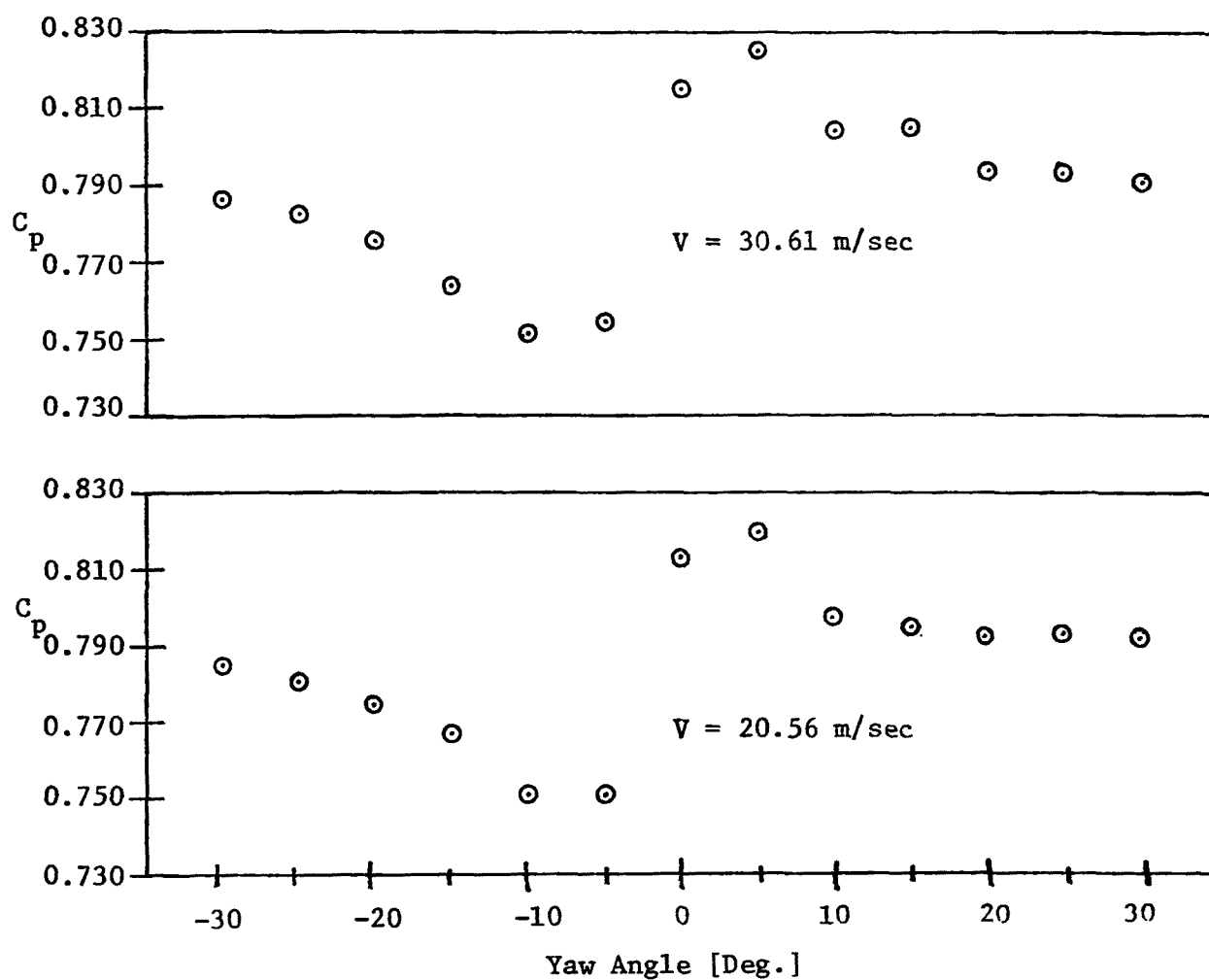


FIGURE 28. Effect of Yaw with Interference; Sampling Rate: $0.85 \times$ Isokinetic Flow Rate

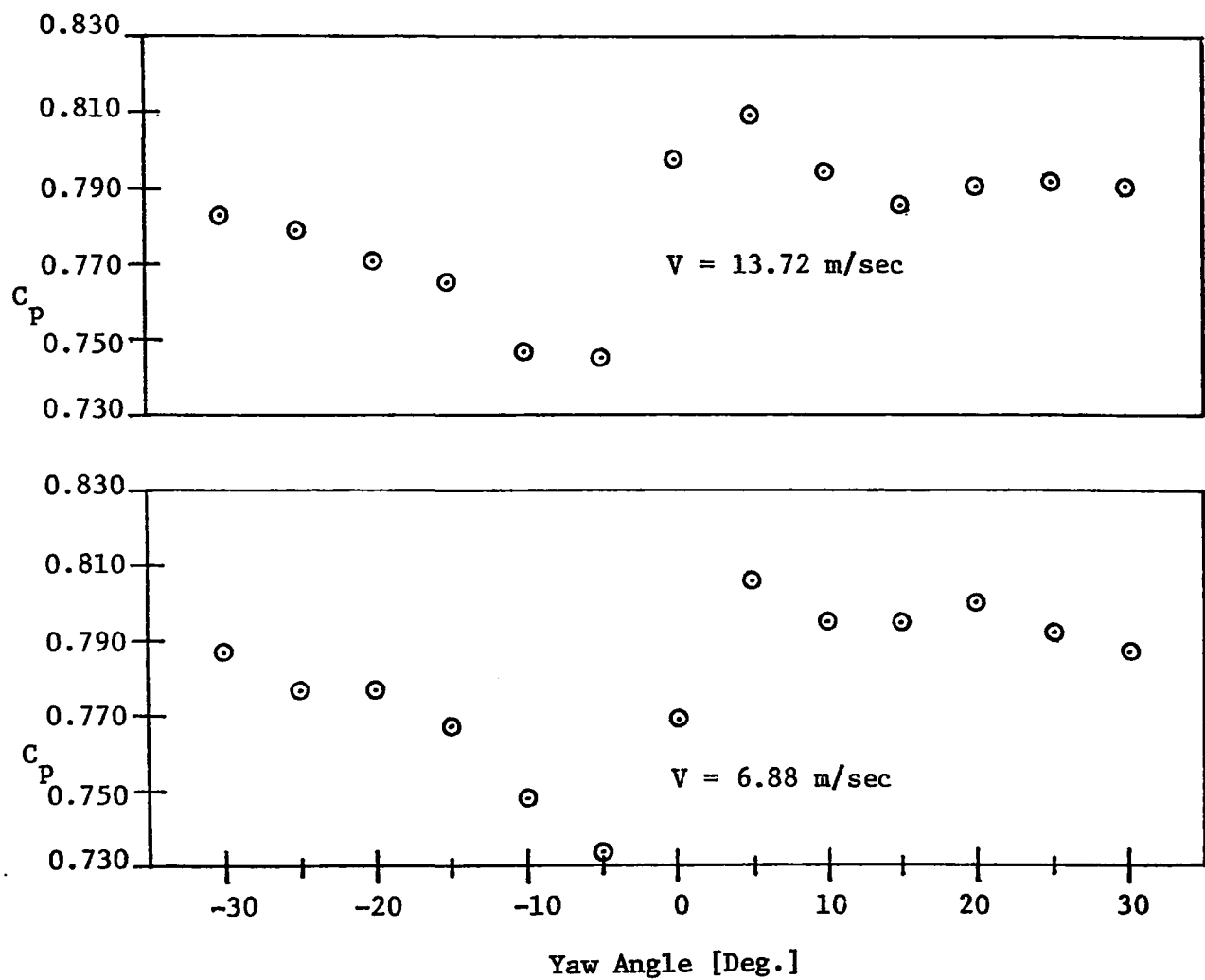


FIGURE 28. Continued

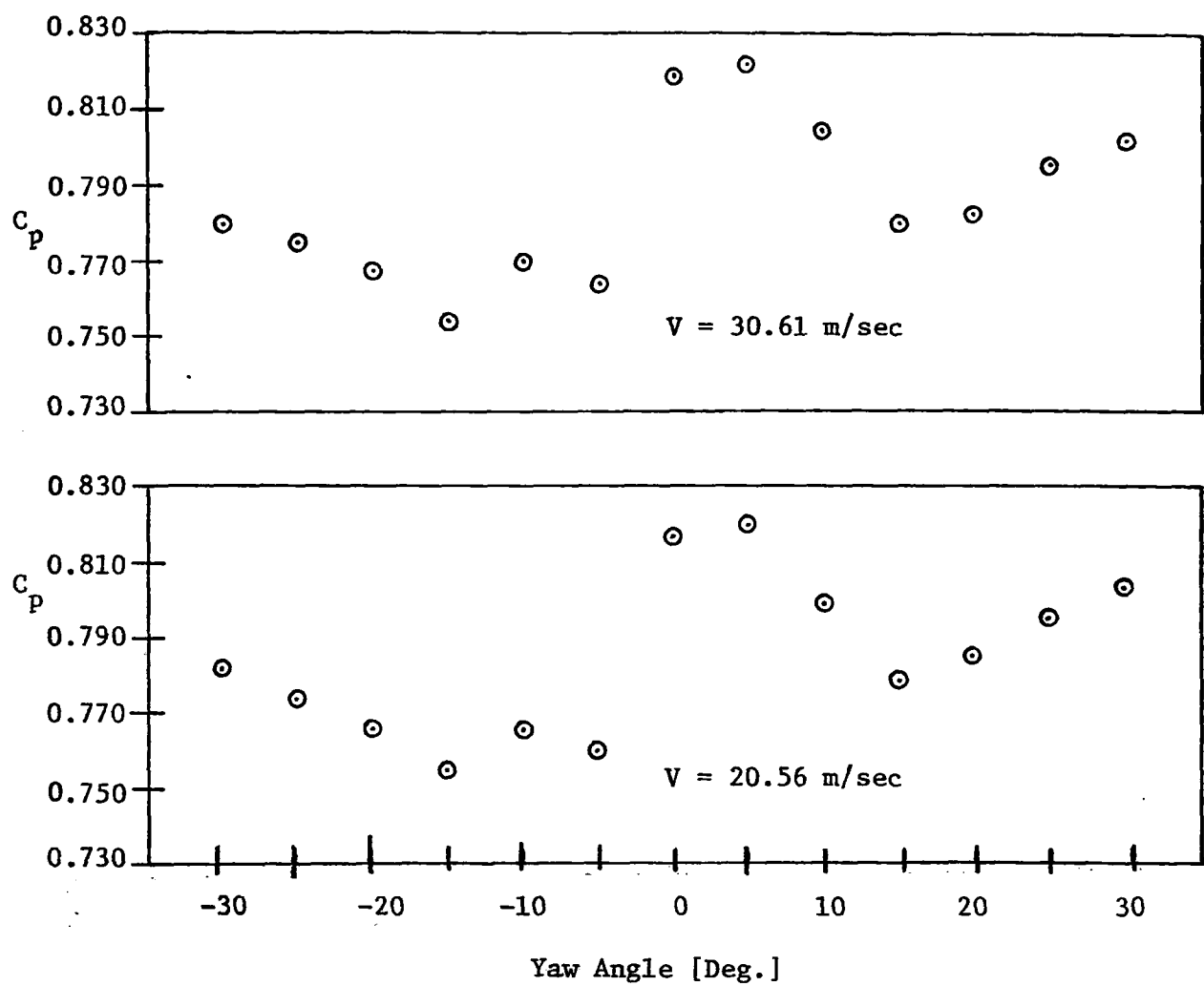


FIGURE 29. Effect of Yaw with Interference; Sampling Rate: 1.00 x Iso-kinetic Flow Rate

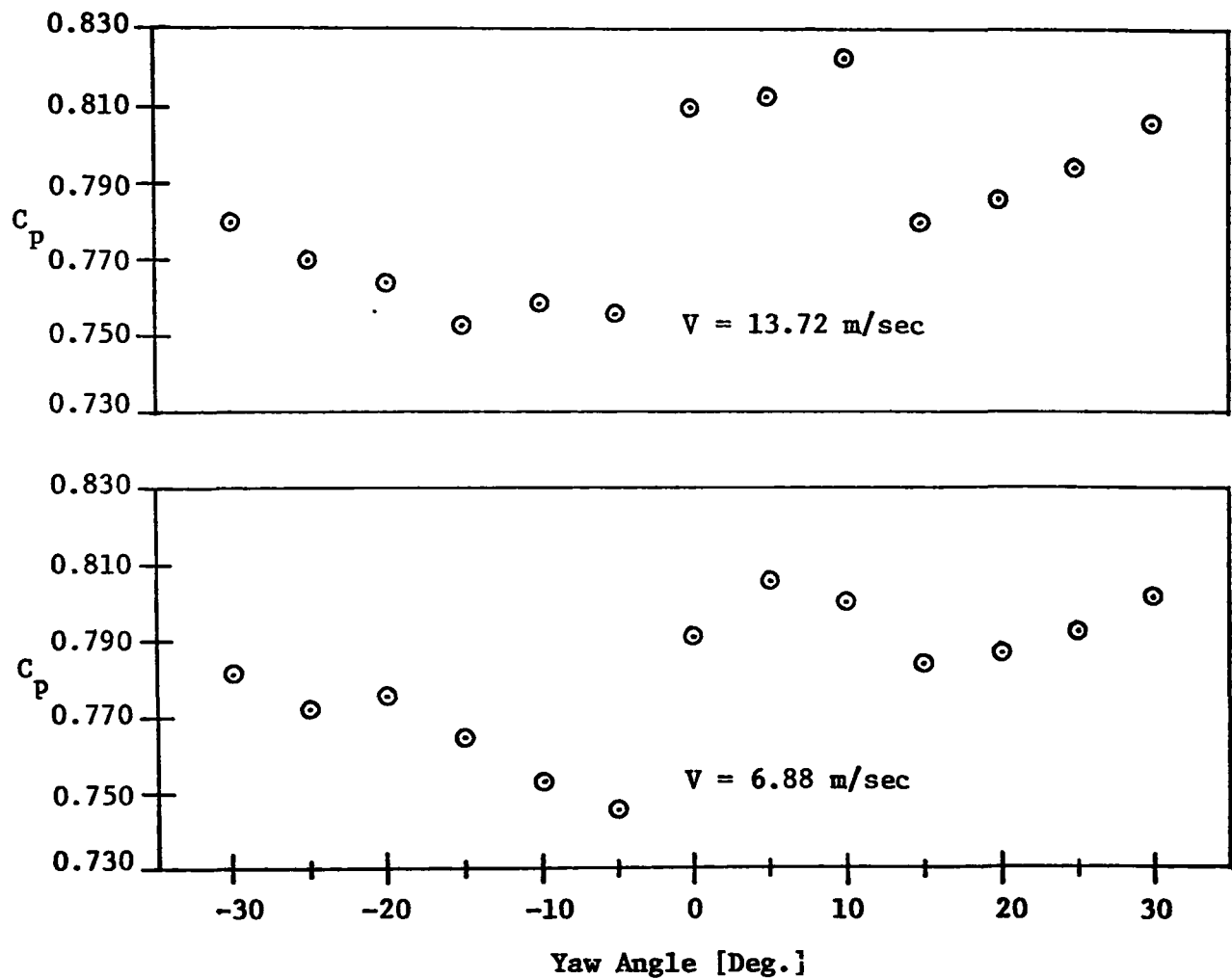


FIGURE 29. Continued

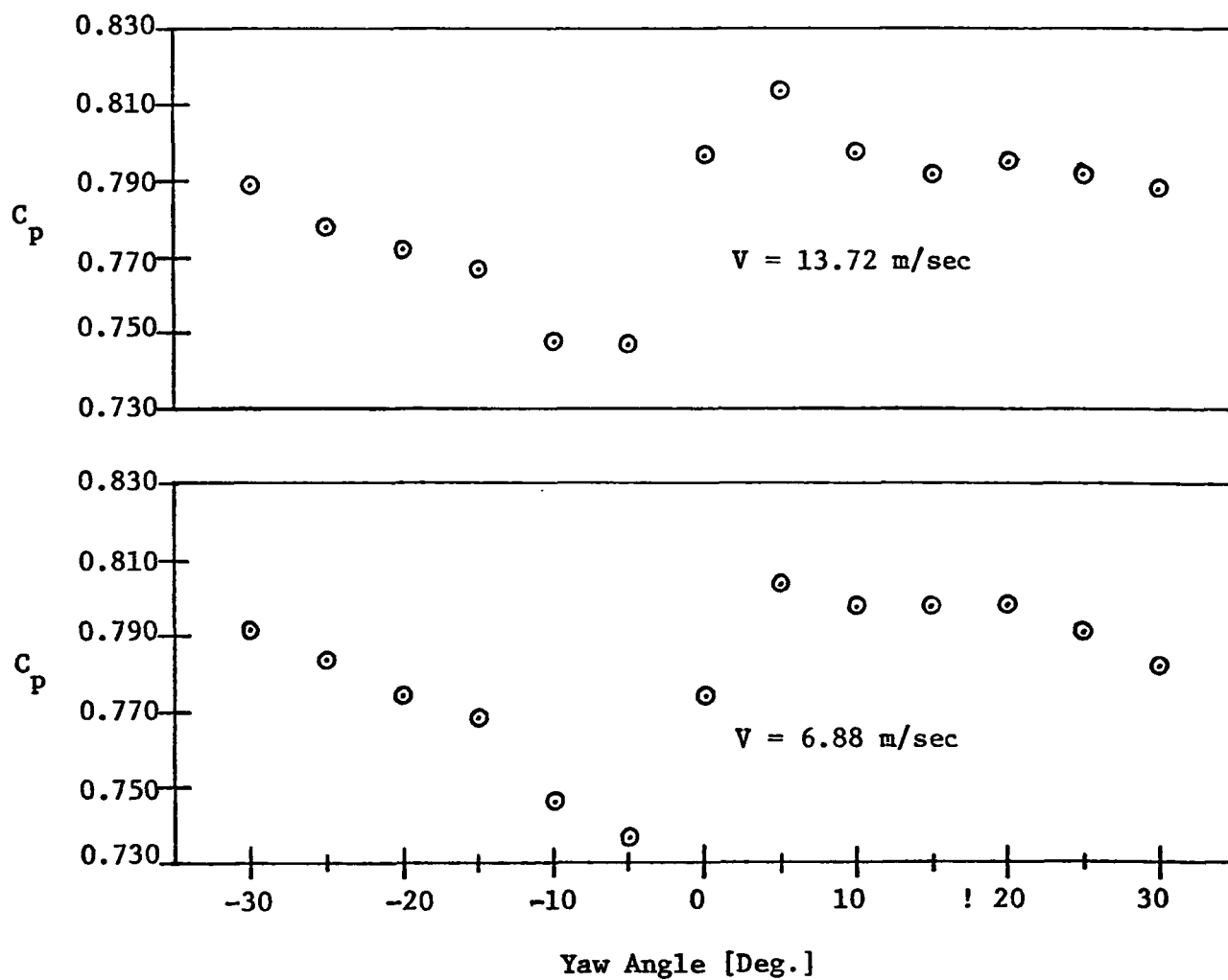


FIGURE 30. Effect of Yaw with Interference; Sampling Rate: $1.4 \times$ Iso-kinetic Flow Rate

LEGEND

○ Yaw

□ Yaw with Interference

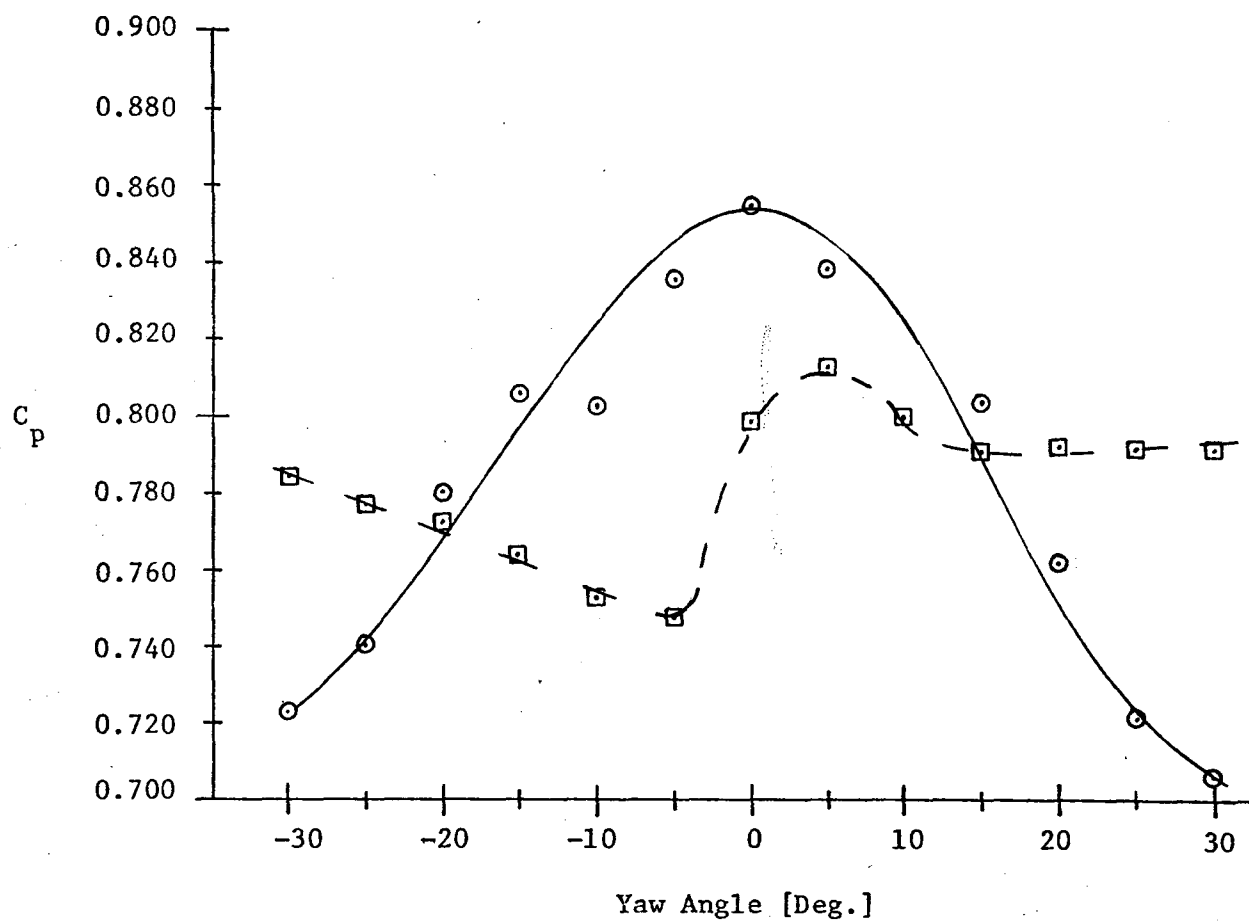


FIGURE 31. Averaged Effect of Yaw with Interference on S-Tube 4-10

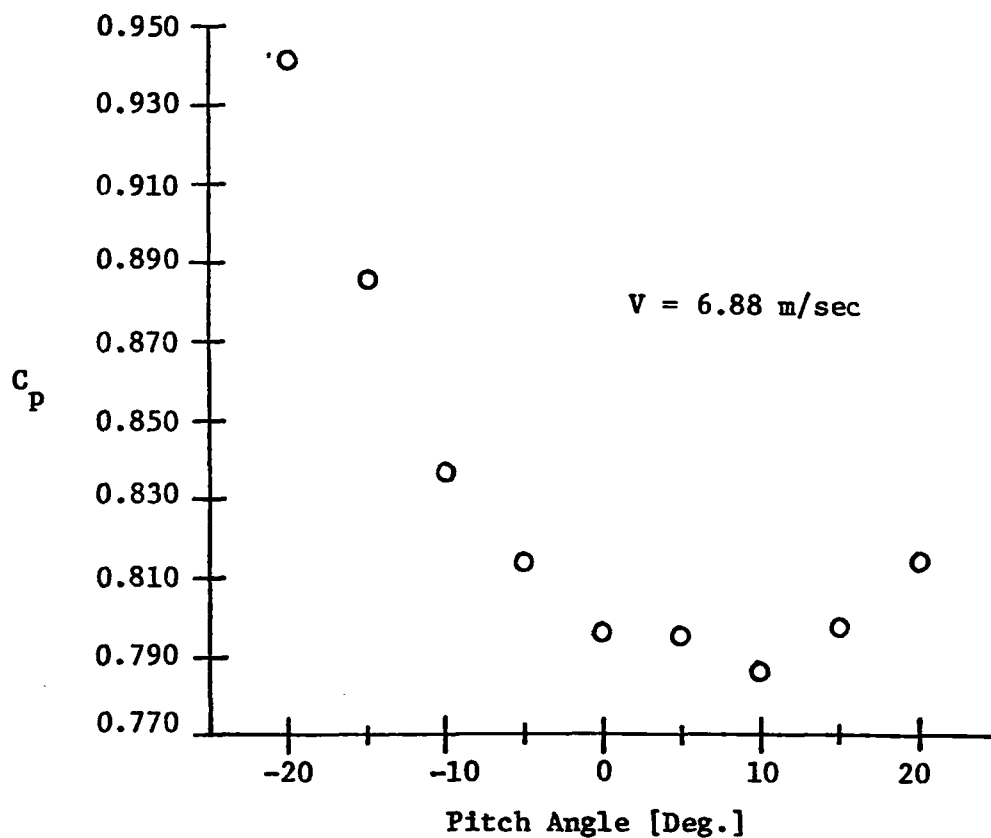
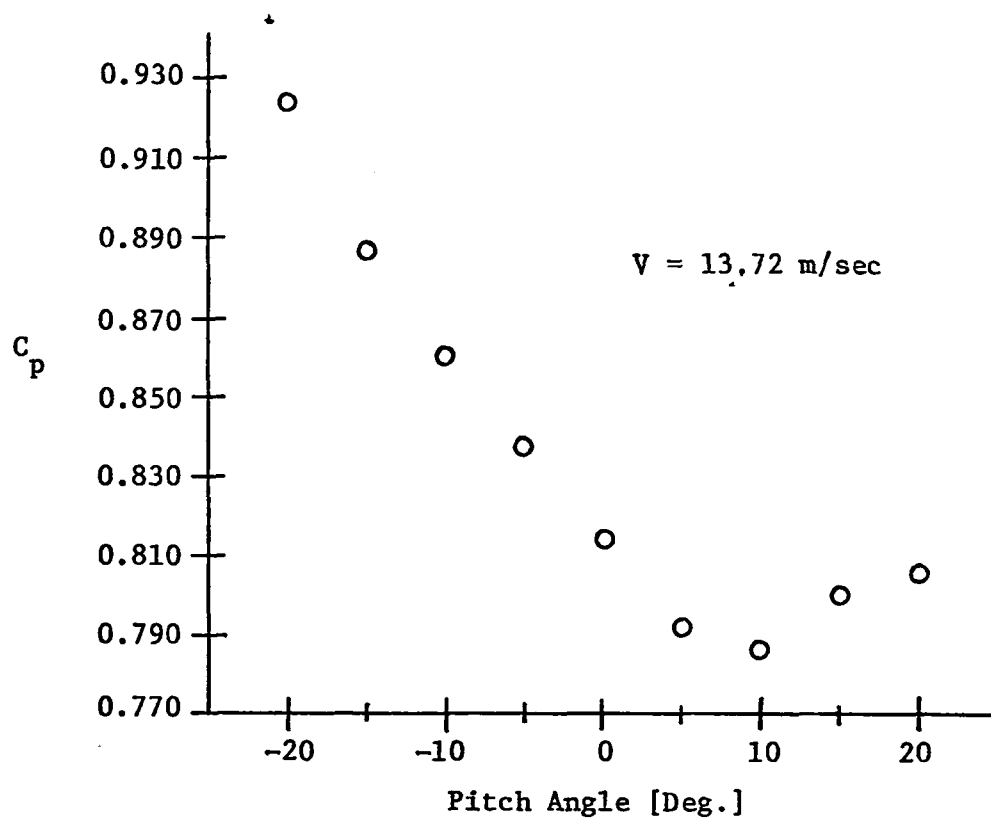


FIGURE 32. Effect of Pitch with Interference; Sampling Rate: $0.60 \times$ Isokinetic Flow Rate

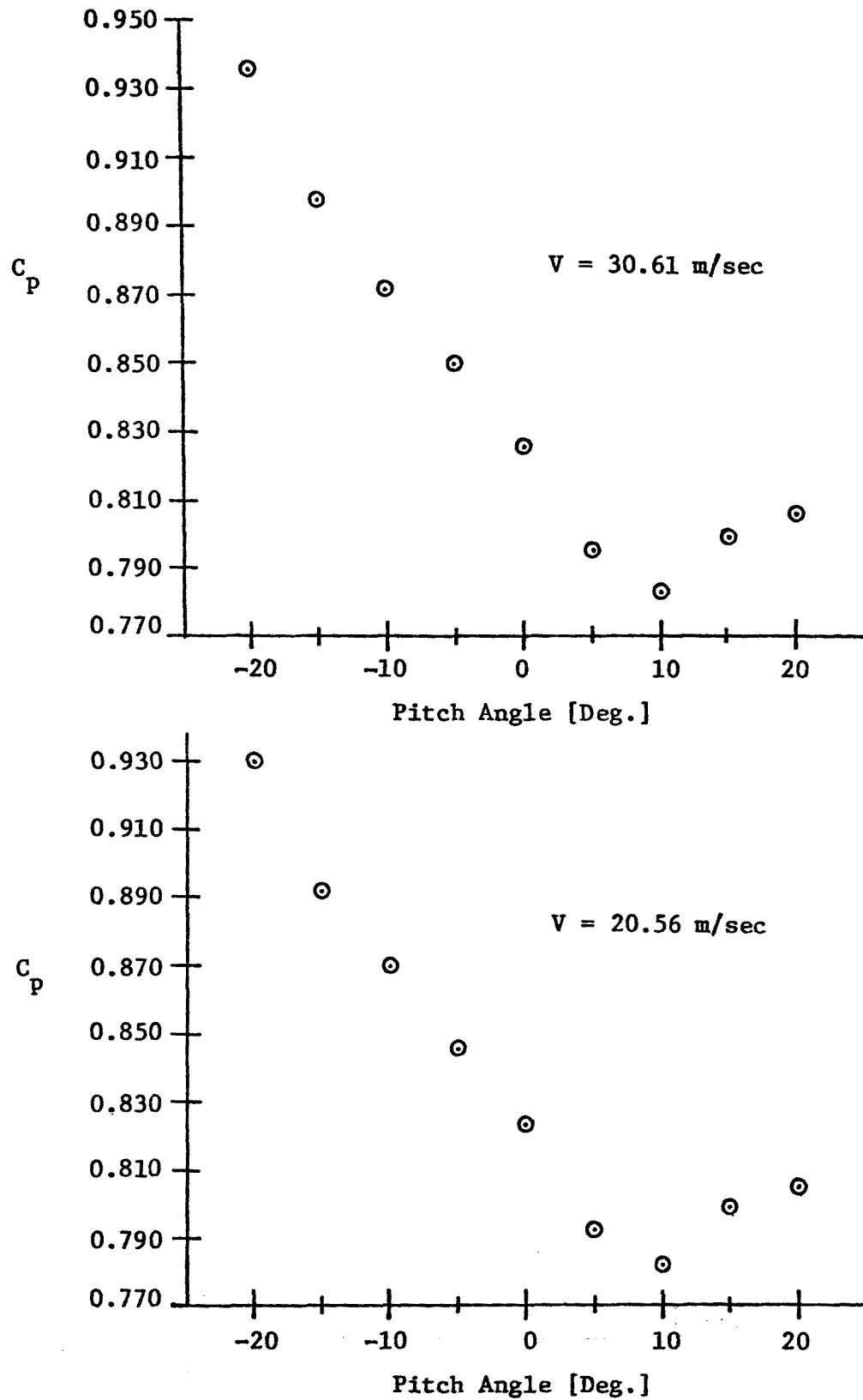


FIGURE 33. Effect of Pitch with Interference; Sampling Rate: 0.60 x Isokinetic Flow Rate

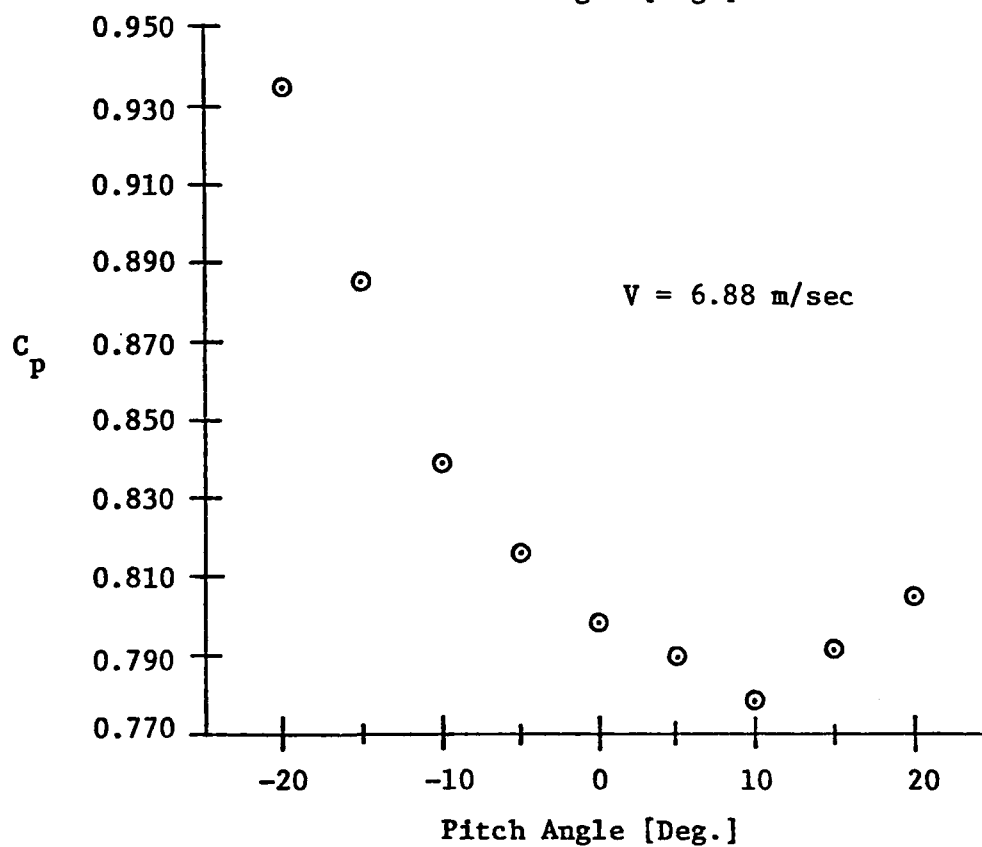
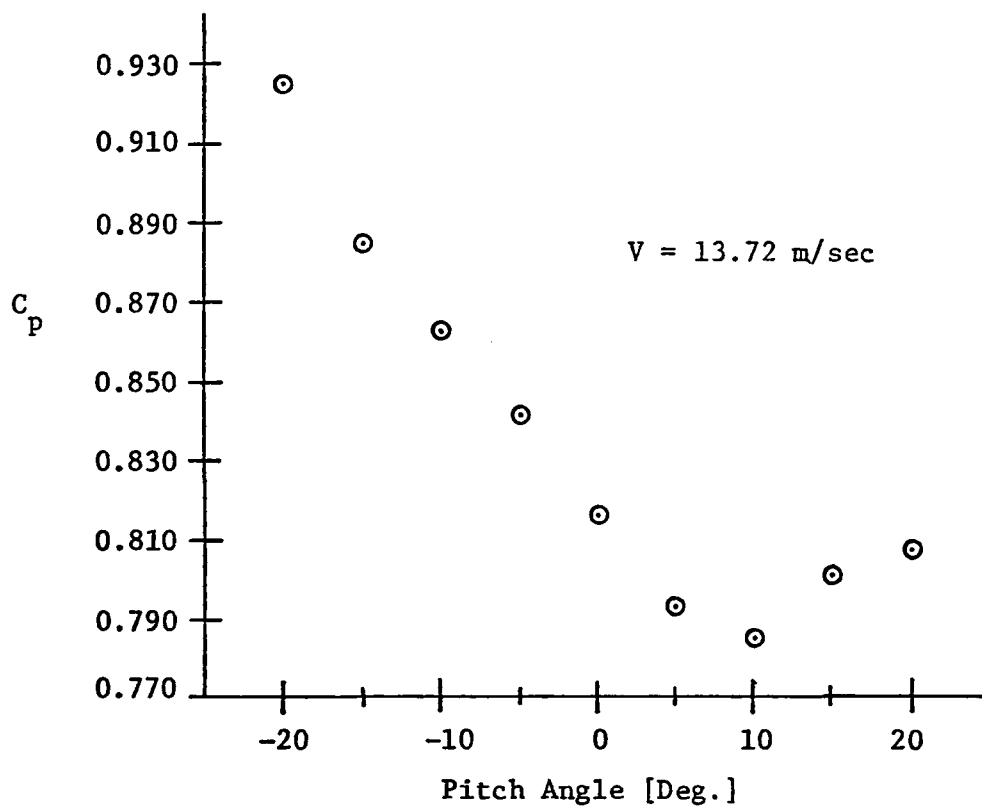


FIGURE 34. Effect of Pitch with Interference; Sampling Rate: 0.85 x Isokinetic Flow Rate

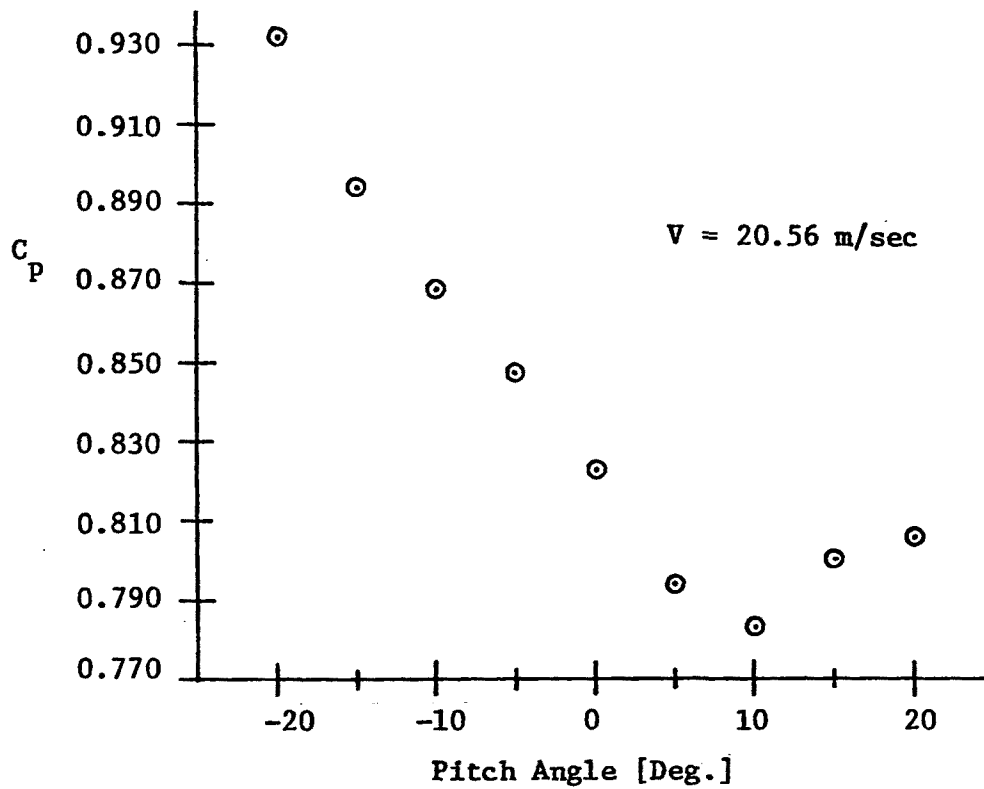
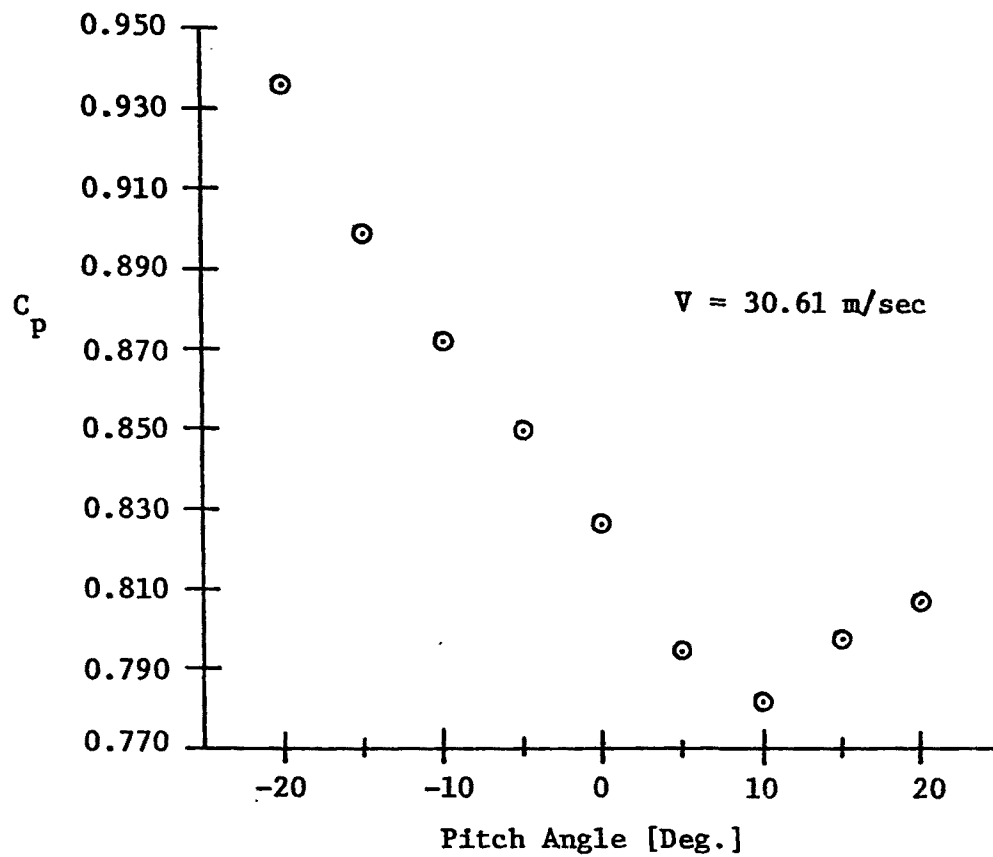


FIGURE 35. Effect of Pitch with Interference; Sampling Rate:
0.85 x Isokinetic Flow Rate

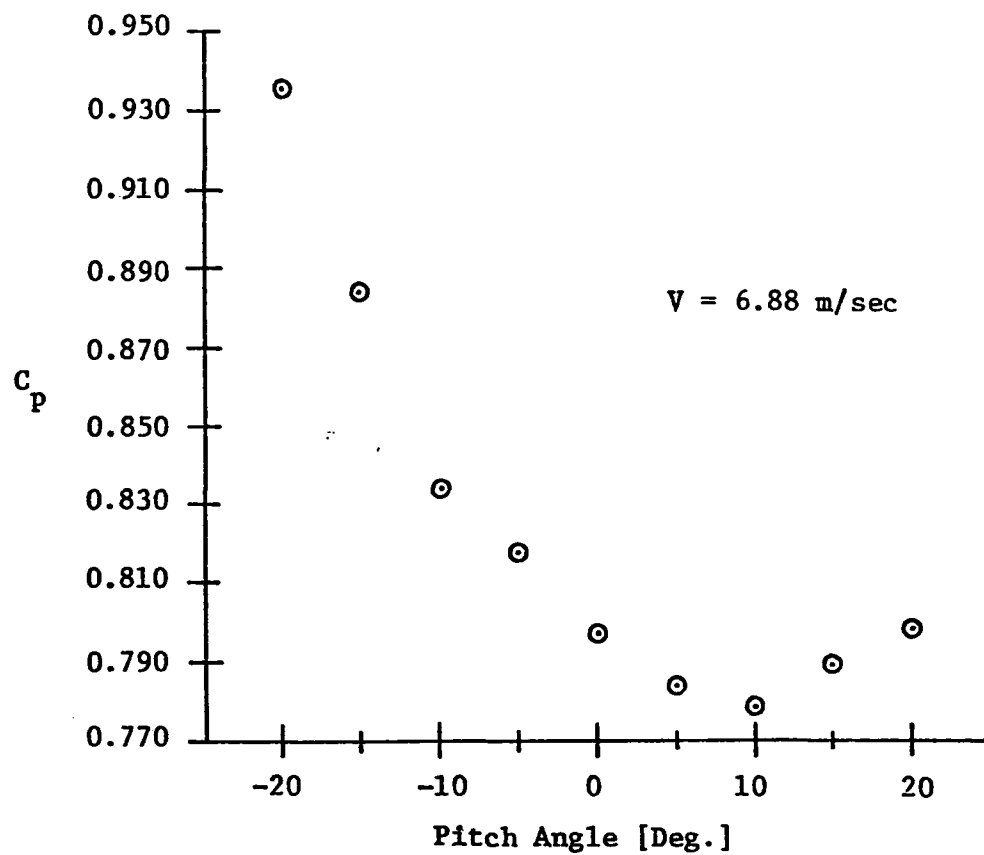
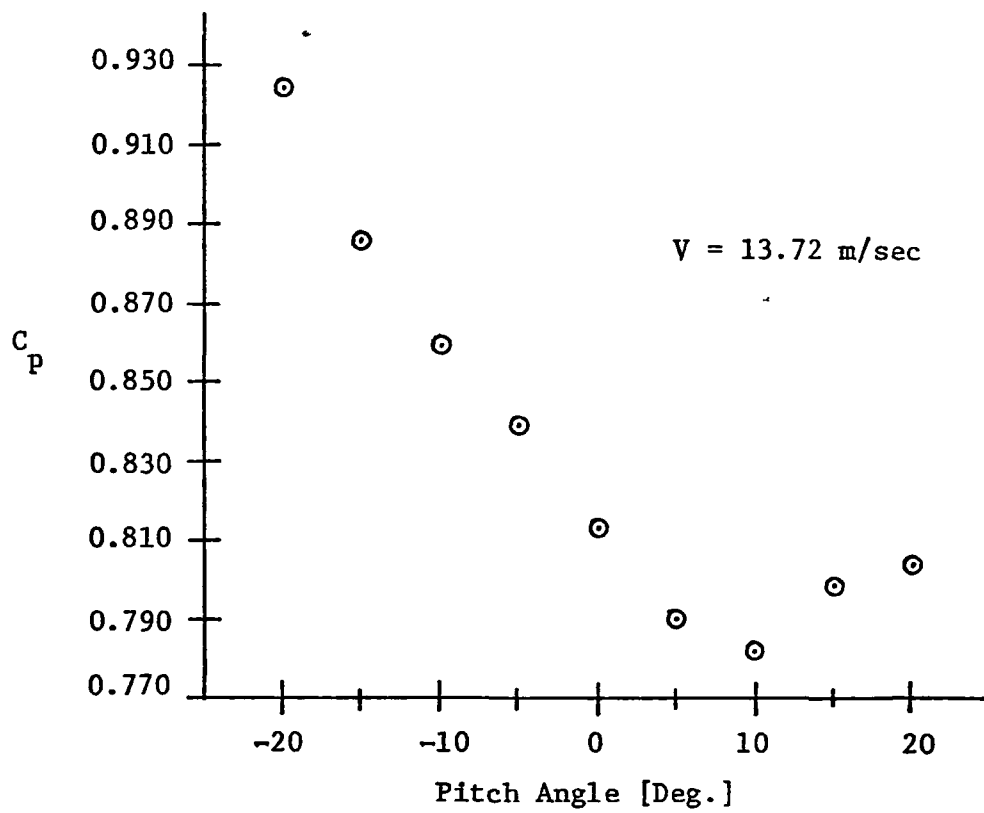


FIGURE 36. Effect of Pitch with Interference; Sampling Rate:
1.00 x Isokinetic Flow Rate

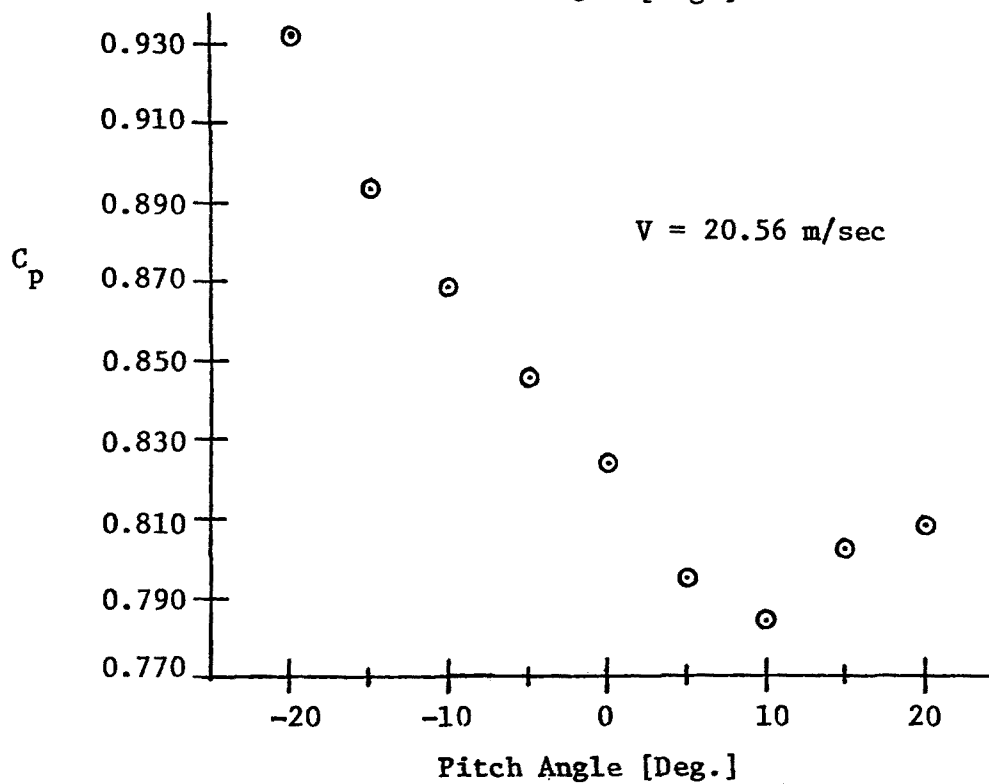
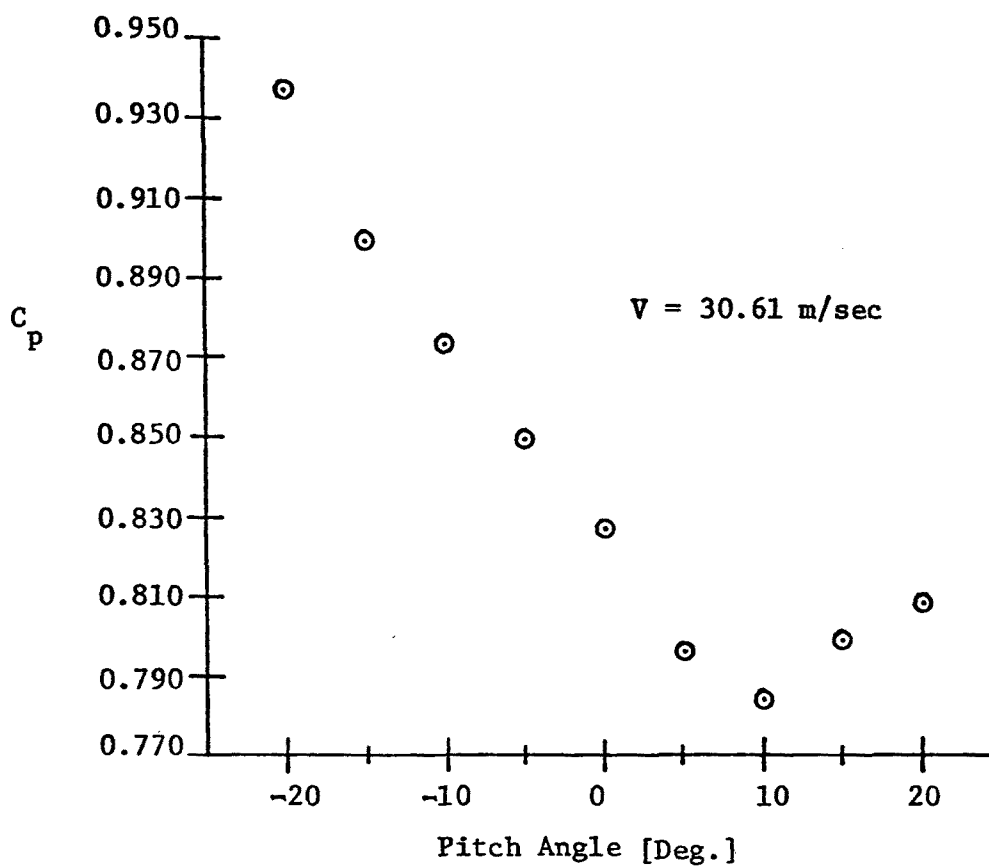


FIGURE 37. Effect of Pitch with Interference; Sampling Rate: 1.00 x Isokinetic Flow Rate

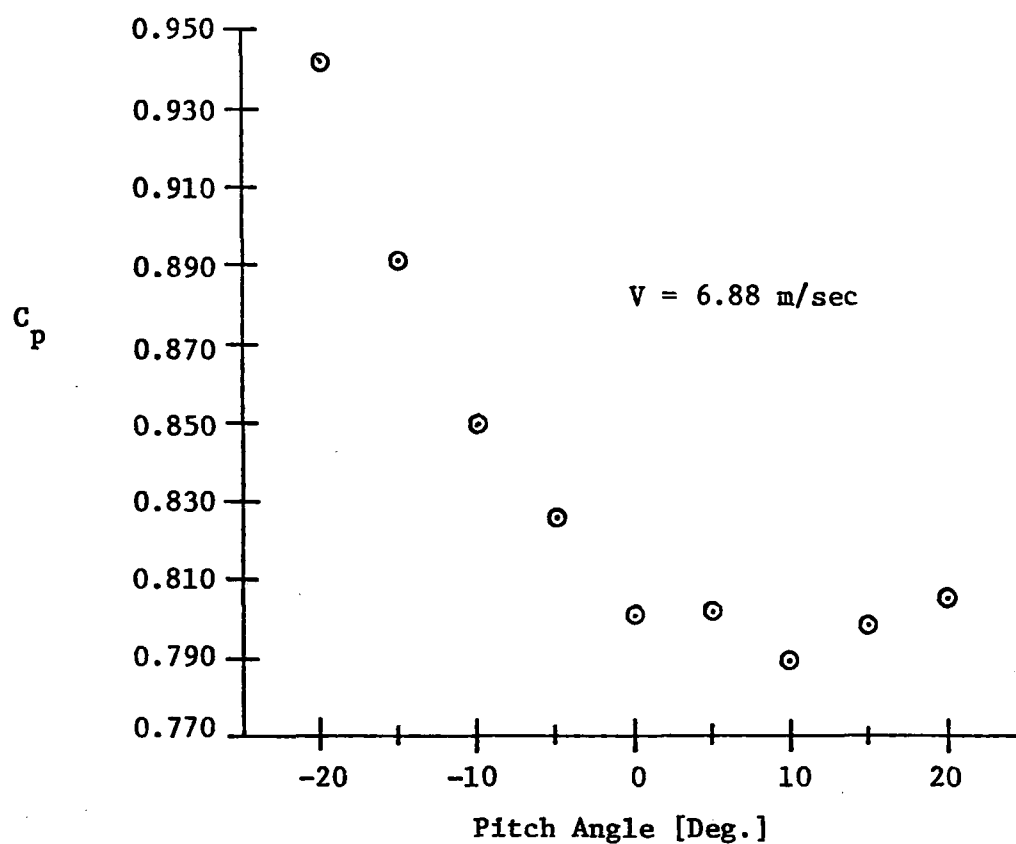
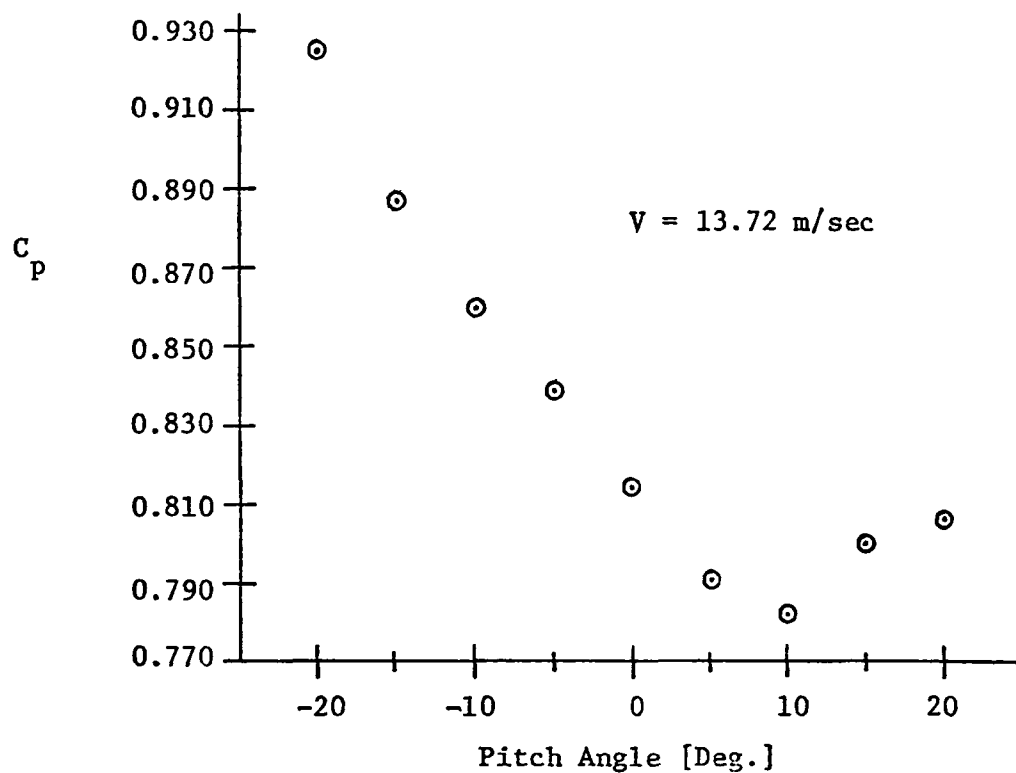


FIGURE 38. Effect of Pitch Interference; Sampling Rate: $1.40 \times$ Isokinetic Flow Rate

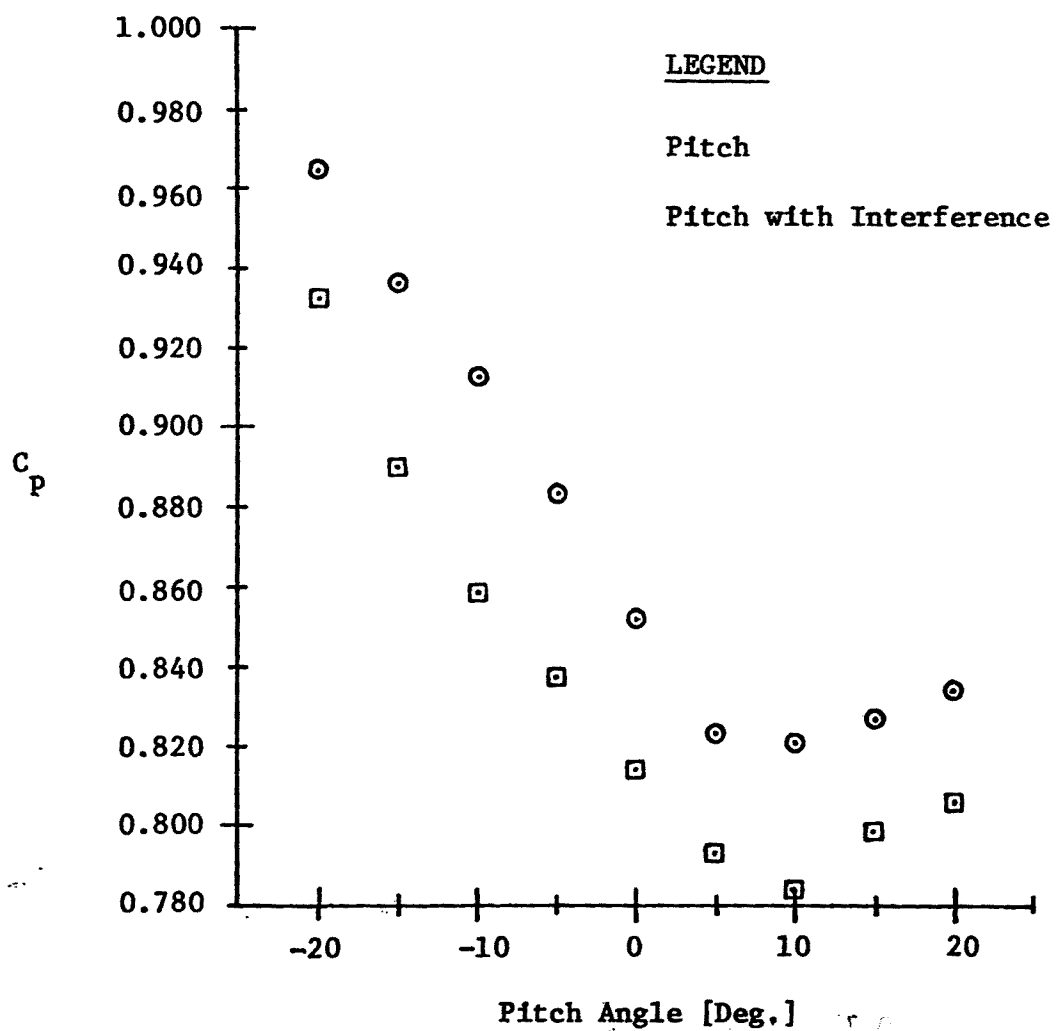


FIGURE 39. Averaged Effect of Pitch with Interference on S-Tube 4-10

EFFECT OF SWIRL

The results of the swirl tests are presented in Figures 40, 41, and 42. In comparing the curves for swirling flow with the curves for unobstructed or no swirl flow it is evident that the average value of the pitot coefficient for any given pitot tube is higher in the presence of swirl (See Table 2 below).

S-Tube	C_p		% Diff.
	UNOBSTRUCTED	SWIRL	
4-10	0.857	0.889	3.7
3-04	0.848	0.871	2.7
3-01	0.830	0.868	4.6

TABLE 2. Effect of Swirl on Average Pitot Coefficient for Several S-type Pitot Tubes.

Since swirling flow is intended to simulate actual flow conditions in the stacks while the unobstructed flow represents ideal flow conditions, the above table indicates how the behavior of an S-type pitot tube may change in an actual stack from its behavior under ideal laboratory conditions. Hence, the pitot tube whose overall percent difference is the smallest would be preferred. From Table 2, this would be S-tube 3-04.

Considering only the curves that represent swirling flow (Figures 40, 41, and 42), it is apparent that the degree of variation in pitot coefficients varies from tube to tube. For example, the coefficient of pitot tube 4-10, C_p does not change by more than 1.3 percent and the coefficient of pitot tube 3-04 does not change by more than 2.8 percent. In contrast, the coefficient for tube 3-01 varies by as much as 4.7 percent. Similar comparisons in the case of unobstructed flow show that pitot tube 4-10 allows changes in C_p as large as 4.6 percent. S-type pitot tube 3-04 gives changes not larger than 1.4 percent and pitot tube 3-01 keeps C_p within a range of 0.85 percent. Thus, the behavior of pitot tube 4-10 is quite insensitive to speed in swirling flow, but very sensitive to speed in unswirled flow. The behavior of tube 3-01 is opposite to that of 4-10. However, the behavior of pitot 3-04 is insensitive to speed under both flow conditions.

Another useful means for judging the effects of swirl on the pitot coefficient is simply to compute the difference between C_p in swirling flow and the C_p for unswirled flow for each of the speeds considered. This will show the velocity dependence that is characteristic of a particular pitot tube. For instance, with pitot tube 4-10 it is found that at the lower speeds (around 6 m/s) the difference is as much as 6.39 percent. While at the higher speeds (around 12 m/s and higher) it diminishes to around three percent. In the case of pitot tube 3-04 this difference never exceeds 4.5 percent. Finally for

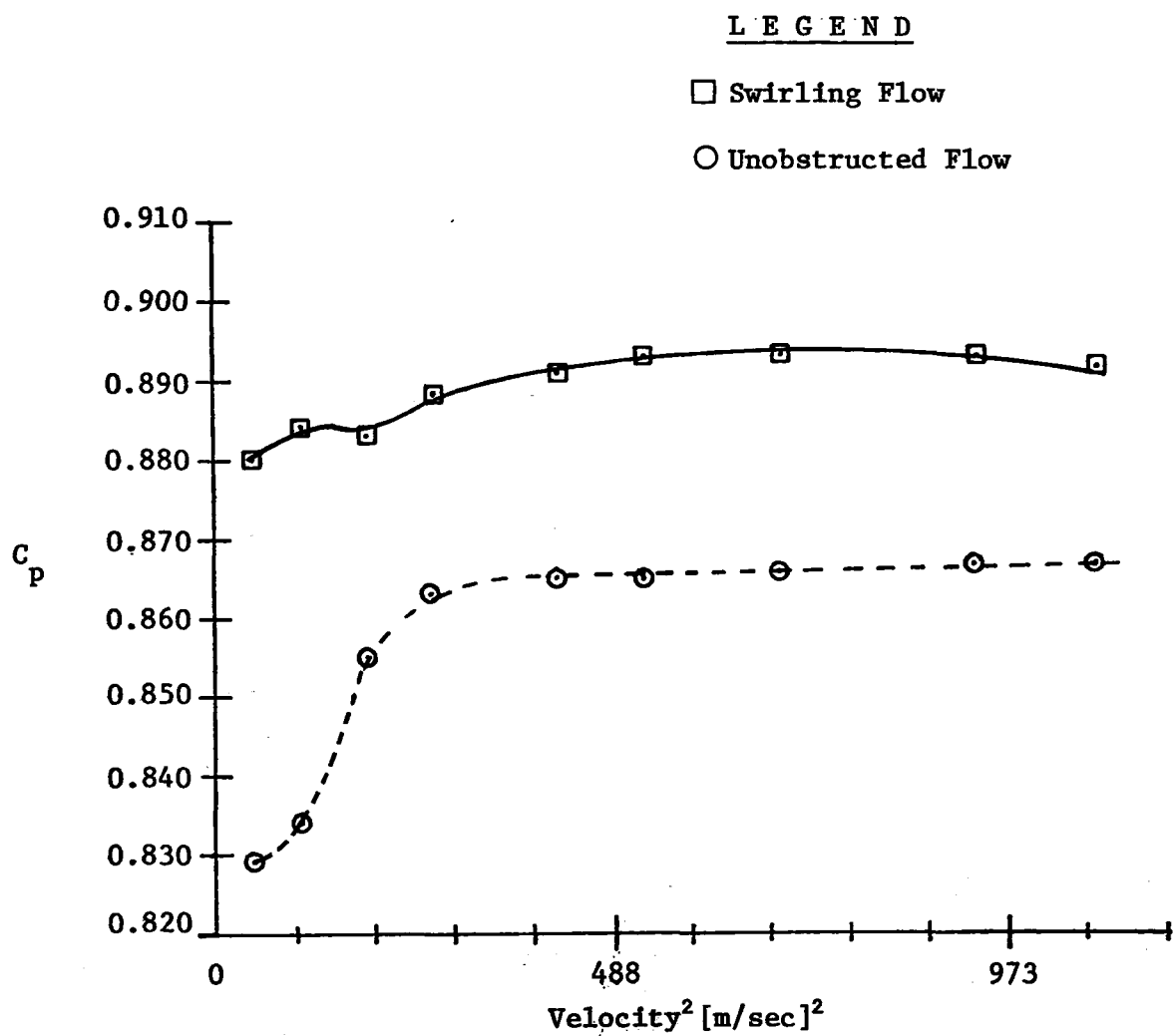


FIGURE 40. Effects of Swirl on S-Tube 4-10

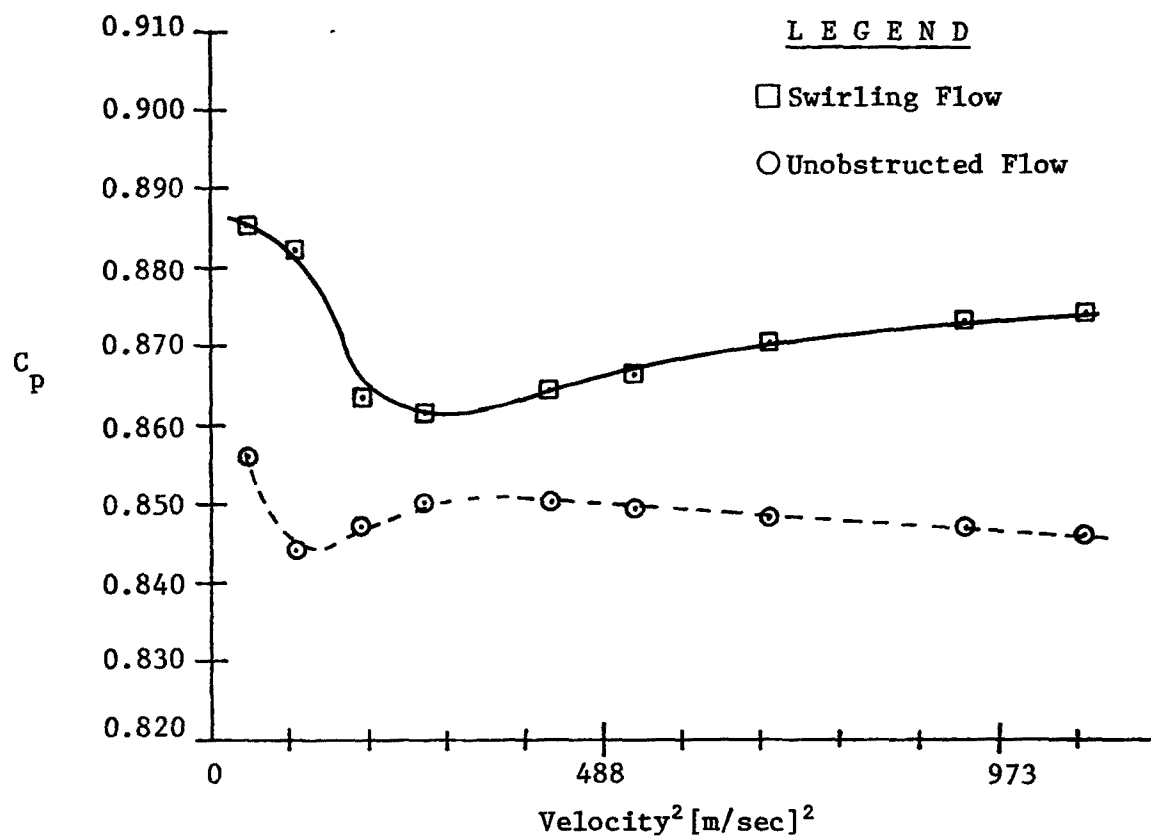


FIGURE 41. Effects of Swirl on S-Tube 3-04

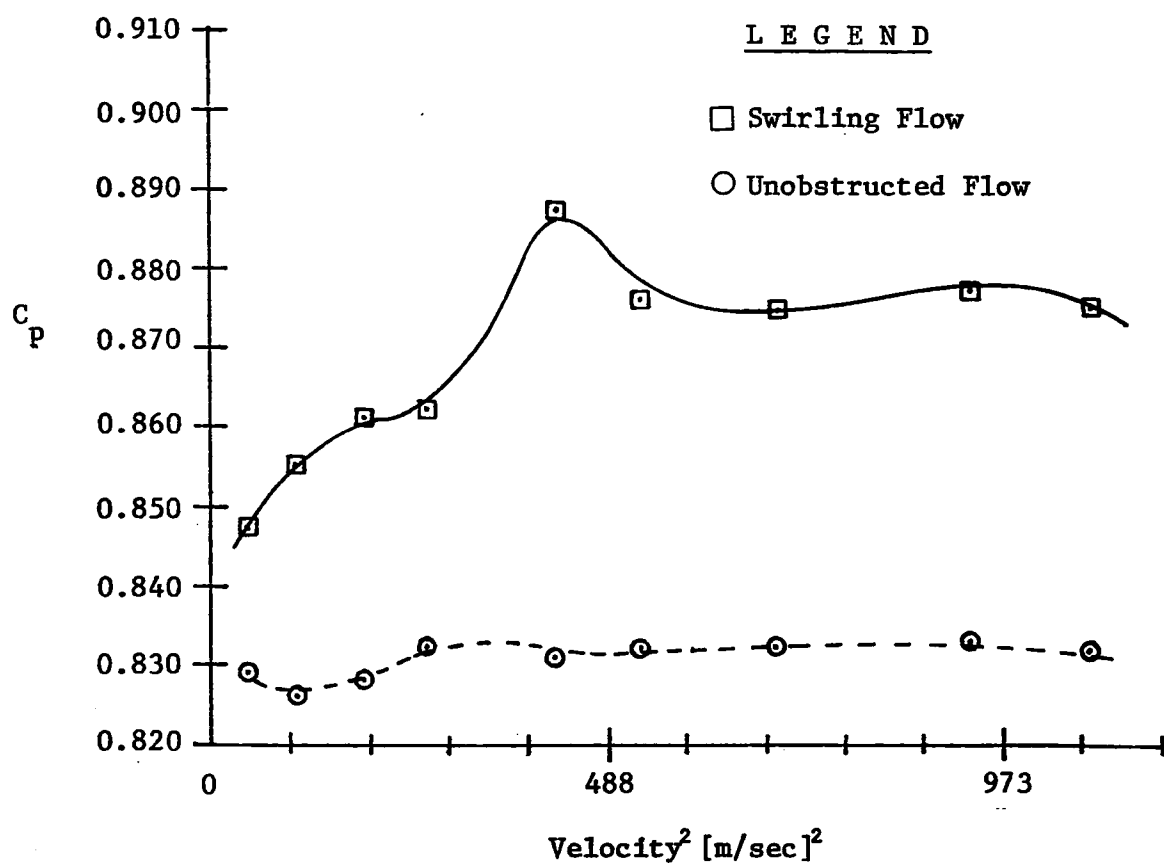


FIGURE 42. Effects of Swirl on S-Tube 3-01

pitot tube 3-01, unlike tube 4-10, this marginal difference increases with tunnel speed. For speeds of 18.3 m/s (60 ft/sec) and greater, the difference is on the order of 5.4 percent. Thus, once again, S-type pitot tube 3-04 displays better characteristics in swirl than the others.

REFERENCES

1. Gnyp, A. W., St. Pierre, C. C., Smith, D. S., Mozzon, D., and Steiner, J. An Experimental Investigation of the Effect of Pitot Tube-Sampling Probe Configurations on the Magnitude of the S-Type Pitot Tube Coefficient for Commercially Available Source Sampling Probe. University of Windsor, Canada, February 1975.
2. Terry, E. W. Calibration of Stauscheibe (S-Type) Pitot Tubes and The Effects of Geometry and Interference on Their Accuracy. M.S. Thesis, North Carolina State University, Raleigh, North Carolina, 1977.
3. Willis, B. F. The Effects of Yaw, Pitch, Interference and Swirl on the Accuracy of Stauscheibe (S-Type) Pitot Tubes. M.S. Thesis, North Carolina State University, Raleigh, North Carolina, 1977.

APPENDIX A

VELOCITY PROFILE OF WIND TUNNEL TEST SECTION

A dynamic pressure survey of the North Carolina State University Subsonic Wind Tunnel was conducted to determine the variation of the dynamic pressure (which is related to the velocity) across the width of the test section. This survey was performed at the same vertical and longitudinal positions as those used to test the S-type pitot tubes. Tests were performed for three different speeds at the center of the test section: 6 m/s (20 ft/sec), 17 m/s (55 ft/sec), and 27.5 m/s (90 ft/sec). The results are shown in Figure A1, and this figure shows that the velocity changes less than two percent for distances within 0.15 m (6 in) of the centerline.

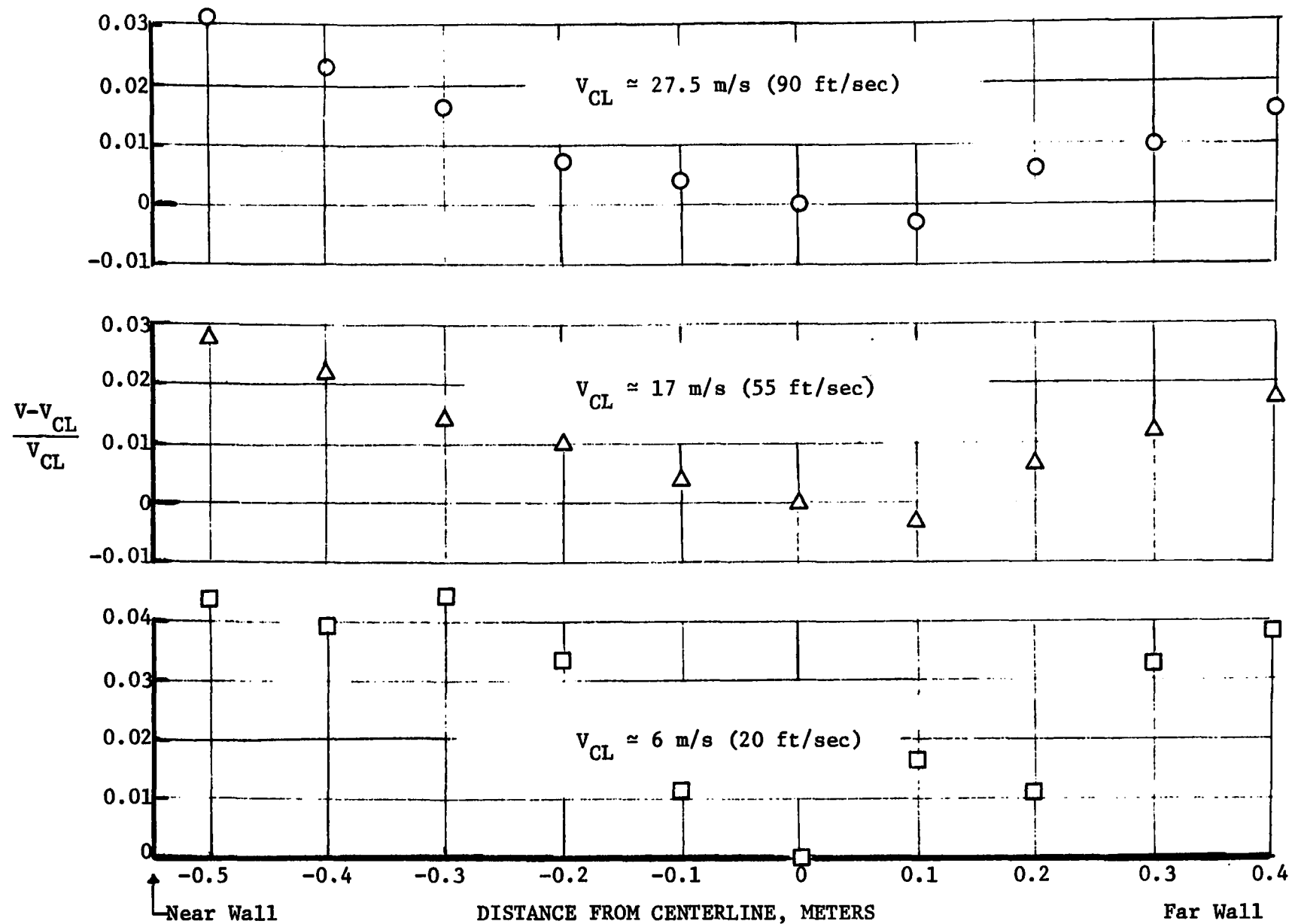


FIGURE A1. Velocity Profile Across Test Section of NCSU Wind Tunnel

TECHNICAL REPORT DATA <i>(Please read Instructions on the reverse before completing)</i>		
1. REPORT NO.	2.	3. RECIPIENT'S ACCESSION NO.
4. TITLE AND SUBTITLE A Study on the Accuracy of Type S Pitot Tube		5. REPORT DATE
		6. PERFORMING ORGANIZATION CODE
7. AUTHOR(S) F. C. Williams, F. R. DeJarnette		8. PERFORMING ORGANIZATION REPORT NO.
9. PERFORMING ORGANIZATION NAME AND ADDRESS Mechanical and Aerospace Engineering Department North Carolina State University Raleigh, North Carolina 27607		10. PROGRAM ELEMENT NO. 1HA327
		11. CONTRACT/GRANT NO. R 803168
12. SPONSORING AGENCY NAME AND ADDRESS Environmental Monitoring and Support Laboratory Office of Research and Development U. S. Environmental Protection Agency Research Triangle Park, N.C. 27711		13. TYPE OF REPORT AND PERIOD COVERED Final
		14. SPONSORING AGENCY CODE EPA 600/08
15. SUPPLEMENTARY NOTES		
16. ABSTRACT A study was done to identify and quantify the design parameters that affect the performance of type S pitot tubes in field use. Fourteen different pitot tubes were studied. In addition the effect of the sampling probe on the performance of several of these pitot tubes was determined as a function of distance, pitch, yaw and swirl. The results showed that the coefficient of the type S pitot tube under non-ideal flow conditions was very sensitive to the distance between the static and wake pressureports of the pitot tube. Increasing the spacing between the two ports decreased the sensitivity of the coefficient to yaw, pitch and swirl. Inserting the pitot tube 5 cm. further into the stack than the sampling probe also seemed to reduce the effects of non-ideal flow on the pitot coefficient.		
17. KEY WORDS AND DOCUMENT ANALYSIS		
a. DESCRIPTORS	b. IDENTIFIERS/OPEN ENDED TERMS	c. COSATI Field/Group
Pitot tube, Velocity measurement		13B
18. DISTRIBUTION STATEMENT Release to public	19. SECURITY CLASS (This Report) Unclassified	21. NO. OF PAGES
	20. SECURITY CLASS (This page) Unclassified	22. PRICE